

# Ruthenium-Based Heterocyclic Carbene-Coordinated Olefin Metathesis Catalysts<sup>†</sup>

Georgios C. Vougioukalakis<sup>‡</sup> and Robert H. Grubbs<sup>\*,§</sup>

Institute of Physical Chemistry, National Centre of Scientific Research “Demokritos”, 15310 Agia Paraskevi, Greece, and Division of Chemistry and Chemical Engineering, California Institute of Technology, Pasadena, California 91125

Received July 6, 2009

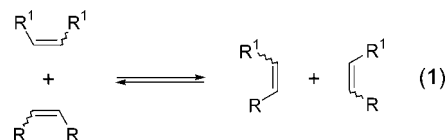
## Contents

1. Brief Introduction to Olefin Metathesis	1746
2. Introduction to the Use of Heterocyclic Carbenes as Ancillary Ligands in Ruthenium-Based Metathesis Catalysts	1748
3. Heterocyclic Carbene Frameworks Used in Ruthenium-Based Metathesis Catalysts	1749
3.1. Symmetrical Imidazol- and Imidazolin-2-ylidenes	1749
3.2. Unsymmetrical Imidazol- and Imidazolin-2-ylidenes	1754
3.3. Chiral Monodentate <i>N</i> -Heterocyclic Carbenes	1756
3.4. Chiral Bidentate <i>N</i> -Heterocyclic Carbenes	1757
3.5. Four- and Six-Membered Ring <i>N</i> -Heterocyclic Carbenes	1758
3.6. 1,2,4-Triazol-5-ylidenes, Cyclic (Alkyl)(amino) Carbenes, Thiazol-2-ylidenes, and Other Heterocyclic Carbene Ligands	1759
3.7. Carbene Biscoordination	1760
4. Phosphine-free Heterocyclic Carbene-Coordinated Ruthenium Catalysts	1761
4.1. Chelating Alkoxybenzylidene Ligands	1761
4.2. Chelating Thioether and Chelating Sulfoxide Benzylidene Ligands	1764
4.3. Mono- and Bis(pyridine)-Coordinated Catalysts	1765
4.4. Chelating Quinolin- and Quinoxalin-ylidenes	1767
4.5. Bidentate Alkylidenes Chelated through Imine Donors	1768
4.6. 14-Electron Phosphonium Alkylidenes	1768
5. Ruthenium Alkylidene Variation: Fischer-Type Carbenes, Indenylidenes, Vinylidenes, Cyclic Ruthenium Alkylidenes, and Other Alkylidene Ligands	1769
6. Variation of the Phosphine Ligand	1771
7. Anionic Ligand(s) Variation	1772
7.1. Halides	1772
7.2. Monodentate and Bidentate Aryloxides	1772
7.3. <i>N,O</i> -, <i>P,O</i> -, and <i>O,O</i> -Bidentate Ligands	1772
7.4. Carboxylates and (Alkyl)sulfonates	1773
7.5. Nitrile- and Isonitrile-Coordinated Alkylidene-Free Ruthenium Catalysts	1774
8. <i>N</i> -Heterocyclic Carbene-Coordinated ( $\eta^6$ -Arene)ruthenium Metathesis Catalysts	1775
9. <i>N</i> -Heterocyclic Carbene-Coordinated Ruthenium Catalysts Designed for Homogeneous Metathesis in Water and Protic Solvents	1777

10. Removal of Ruthenium Impurities from Metathesis Products and Ruthenium Recycling Strategies	1778
11. Decomposition Studies	1780
12. Conclusions and Perspectives	1783
13. Acknowledgments	1783
14. References	1783

## 1. Brief Introduction to Olefin Metathesis

The fascinating story of olefin (or alkene) metathesis (eq 1) began almost five decades ago, when Anderson and Merckling reported the first carbon–carbon double-bond rearrangement reaction in the titanium-catalyzed polymerization of norbornene.<sup>1</sup> Nine years later, Banks and Bailey reported “a new disproportionation reaction . . . in which olefins are converted to homologues of shorter and longer carbon chains . . .”.<sup>2</sup> In 1967, Calderon and co-workers named this metal-catalyzed redistribution of carbon–carbon double bonds olefin metathesis, from the Greek word “μετάθεση”, which means change of position.<sup>3</sup> These contributions have since served as the foundation for an amazing research field, and olefin metathesis currently represents a powerful transformation in chemical synthesis, attracting a vast amount of interest both in industry and academia.<sup>4–6</sup>



The generally accepted mechanism for olefin metathesis was originally proposed by Chauvin and Hérisson in 1970.<sup>7</sup> According to this mechanism, olefin metathesis proceeds through metallacyclobutane intermediates, generated by the coordination of the olefin(s) to a metal alkylidene, via a series of alternating [2 + 2]-cycloadditions and cycloreversions (Scheme 1).<sup>8</sup> Because of the reversibility of all individual steps in the catalytic cycle, an equilibrium mixture of olefins is obtained. For the metathesis to be productive and useful, it is necessary to shift the equilibrium in one direction. These inceptive mechanistic explorations, followed by highly sophisticated attempts to synthesize metal alkylidenes and metallacyclobutanes, eventually led to the synthesis of the first well-defined olefin metathesis catalysts. However, as will be also discussed in the following sections, there are many details of the olefin metathesis mechanism that still remain unclear.

The most important olefin metathesis subtypes are presented in Scheme 2. The ring-opening metathesis polymer-

\* Corresponding author.

<sup>†</sup> This article is part of the Carbenes special issue.

<sup>‡</sup> National Centre of Scientific Research “Demokritos”.

<sup>§</sup> California Institute of Technology.



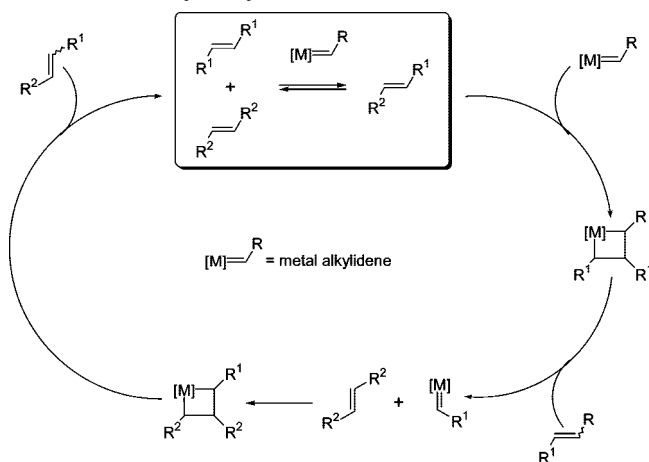
Georgios C. Vougioukalakis was born on Crete, Greece, in 1976. He received his B.Sc. from the University of Crete and his Ph.D. from the same university under the direction of Michael Orfanopoulos. He then moved to the California Institute of Technology where he worked for two years with Robert H. Grubbs. After another postdoctoral year with Nikos Hadjichristidis at the University of Athens, he joined the National Centre of Scientific Research "Demokritos". His research interests include organic and organometallic chemistry and photochemistry, homogeneous catalysis and photocatalysis, and the development of polymeric structures and nanostructures mostly related to energy issues and nanotechnology.



Robert H. Grubbs was born near Possum Trot, KY, in 1942. He received his B.A. and M.Sc. degrees from the University of Florida working with Merle Battiste and his Ph.D. from Columbia University for work with Ron Breslow. After a postdoctoral year with Jim Collman at Stanford University, he joined the faculty at Michigan State University. In 1978, he moved to the California Institute of Technology, where he is now the Victor and Elizabeth Atkins Professor of Chemistry. His research interests include polymer chemistry, organometallic catalysis, and development of new synthetic organic methodology.

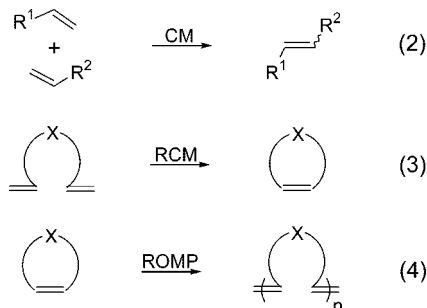
ization (ROMP) of monomers containing strained, unsaturated rings was one of the earliest commercial applications of olefin metathesis.<sup>4,5,9</sup> The driving force for ROMP is the ring-strain release,<sup>10</sup> upon going to the polymerized products. The ring-strain release also determines the irreversible nature of ROMP, as the pathway back to the cyclic compound(s) has to overcome a significant thermodynamic barrier. Ring-closing metathesis (RCM) is widely used in organic synthesis. The driving force for RCM is primarily entropic, because one substrate molecule affords two molecules of product; furthermore, since the small molecules released from this reaction are volatile (if not gaseous), RCM is practically irreversible and can proceed to completion. On the other hand, cross metathesis (CM) is more challenging than both RCM and ROMP, as it lacks the entropic driving force of RCM and the ring-strain release of ROMP, which can lead to relatively low yields of the desired cross-product.<sup>5</sup> For

### Scheme 1. Catalytic Cycle of Olefin Metathesis



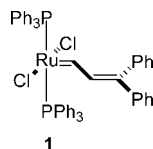
these reasons, CM has been an underutilized metathesis transformation. Other types of olefin metathesis reactions include acyclic diene metathesis polymerization (ADMET), ring-opening cross-metathesis (ROCM), ring-rearrangement metathesis (RRM), and ethenolysis (ethenolysis is the cross-metathesis of ethylene with an internal olefin).<sup>4,5</sup>

### Scheme 2. Most Common Types of Olefin Metathesis Reactions

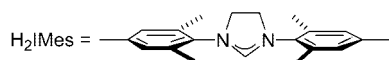
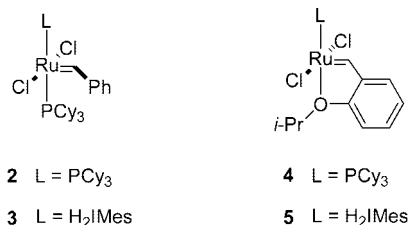


Early metathesis catalysts were multicomponent systems formed in situ from transition-metal halides and main-group metal alkyl cocatalysts. Some representative examples include  $\text{WCl}_6/\text{EtAlCl}_2$ ,  $\text{WCl}_6/\text{BuSn}_4$ , and  $\text{MoO}_3/\text{SiO}_2$ .<sup>4,5</sup> Occasionally, a third component had to be added to the catalytic system as an activator, e.g., the Calderon catalyst ( $\text{WCl}_6/\text{EtAlCl}_2/\text{EtOH}$ ).<sup>3a</sup> However, these catalytic systems were of limited use in organic synthetic applications, mainly because of the harsh reaction conditions they require and their prolonged initiation periods. Additionally, the propagating species were neither quantitatively nor uniformly formed, resulting in lack of reaction control. The first single-component metathesis catalysts were based upon titanium,<sup>11</sup> tantalum,<sup>12</sup> and tungsten,<sup>13</sup> with the synthesis of the first members of these catalytic families reported in the late 1970s. Later on, well-defined molybdenum-based catalysts were also synthesized.<sup>14</sup> Unfortunately though, despite the high catalytic activity of these early transition-metal catalysts, their somewhat limited functional group tolerance and high sensitivity toward oxygen and moisture render them difficult to use in many cases.<sup>15,16</sup> In addition to the necessity for careful handling, time-consuming protecting-group strategies have to be utilized when substrates bear alcohols or aldehydes.

Many of the functional group tolerance and oxophilicity problems in these early transition-metal systems were addressed by the development of well-defined ruthenium-based metathesis catalysts.<sup>6c,16,17</sup> Although the first reports regarding



**Figure 1.** First well-defined metathesis-active ruthenium alkylidene complex.



**Figure 2.** First- and second-generation ruthenium-based metathesis catalysts.

ill-defined ruthenium-catalyzed ROMP were published as early as the 1960s, using  $\text{RuCl}_3(\text{H}_2\text{O})_n$ ,<sup>18</sup> this late transition metal had to wait 20 more years until it came back into the metathesis game in the late 1980s.<sup>19</sup> Unlike its early transition-metal counterparts, ruthenium was remarkably tolerant toward oxygen, water, and functional groups, at least in these early ill-defined systems. Furthermore, one of the most important findings in these studies was the suggestion that the active species was a ruthenium alkylidene.<sup>20</sup> On this basis, the synthesis of the first metathesis-active ruthenium alkylidene complex (**1**, Figure 1) was accomplished in 1992;<sup>21</sup> nevertheless, catalyst **1** showed relatively low reactivity and was only effective in the ROMP of highly strained olefins.

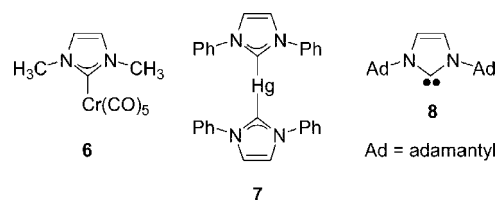
Although the basic structure of the currently used ruthenium-based catalysts still resembles that of the original complex, composed of a ruthenium alkylidene along with two anionic and two neutral ligands, contemporary catalysts (**2–5**, Figure 2) are much more robust and functional group tolerant. For example, first-generation catalyst **2** has much better functional group compatibility than all of the early transition-metal olefin metathesis initiators.<sup>22</sup> Substitution of one of the tricyclohexylphosphine ligands with the bulky *N*-heterocyclic carbene (NHC) ligand H<sub>2</sub>IMes produced ruthenium complex **3**, which displays improved catalytic activity, maintaining the high functional group tolerance and thermal stability of **2**.<sup>23</sup> This improvement has been attributed to the increased affinity of the NHC-substituted ruthenium center for  $\pi$ -acidic olefins relative to  $\sigma$ -donating phosphines (vide infra).<sup>24</sup> Furthermore, substitution of the second phosphine ligand for a bidentate alkylidene (complexes **4** and **5**) led to ruthenium-based catalysts with even higher thermal stability.<sup>25–27</sup> More recent studies have led to the development of ruthenium catalysts that, among others,<sup>28</sup> initiate asymmetric olefin metathesis reactions,<sup>29–36</sup> with applications in aqueous and protic solvent systems,<sup>37–43</sup> or even carry out the challenging formation of tetrasubstituted carbon–carbon double bonds.<sup>44,45</sup> All the above-mentioned developments in the field of heterocyclic carbene-coordinated ruthenium-based metathesis catalysts will be extensively discussed in the following sections of this article.

## 2. Introduction to the Use of Heterocyclic Carbenes as Ancillary Ligands in Ruthenium-Based Metathesis Catalysts

The earliest reports on the synthesis of carbene-coordinated organometallic complexes by Öfele and Wanzlick (complexes **6** and **7**, Figure 3) date back to the late 1960s.<sup>46</sup> Lappert and co-workers followed this work with a series of studies on the chemistry of late transition-metal carbene complexes in the early 1970s.<sup>47</sup> However, carbenes did not draw much of the chemical community's attention until 1991, when Arduengo reported the isolation of the first stable NHC (**8**, Figure 3).<sup>48</sup> Ever since, the use of heterocyclic carbenes has had a great impact both on organometallic chemistry,<sup>49</sup> where they are extensively utilized as ligands, and on organocatalysis.<sup>50</sup> Carbenes are strong Lewis bases, acting as excellent  $\sigma$ -donors and poor  $\pi$ -acceptors, and afford metal–carbon bonds that are usually less labile than the related metal–phosphine bonds.<sup>49a,51</sup> This decreased lability of carbenes, compared to the phosphine ligands, is believed to be one of the reasons for the improved thermal and oxidative stability of the corresponding organometallic complexes. Moreover, the electronic properties and the steric environment of heterocyclic carbenes can be easily and, in some cases, rationally modified, by changing the substituents on the carbene framework, thereby fine-tuning the catalytic properties of the resulting organometallic complexes.

Typically, heterocyclic carbene precursors are easily accessible through well-established synthetic routes starting from commercially available reagents.<sup>52</sup> Many of the existing carbenes are stable enough to be isolated; however, their in situ generation and subsequent reaction with the desired metal source is more straightforward and, consequently, more popular. The most common methods for the generation of free heterocyclic carbene ligands are illustrated in Scheme 3. Thus, deprotonation of imidazolium or imidazolium salts with a strong base, such as potassium hexamethyldisilazane (KHMDs) or potassium *tert*-butoxide (KO*t*-Bu), afford the corresponding free NHCs (eq 5).<sup>23,26,52–54</sup> Alternatively, the desired carbene species can be thermolytically generated from the related 2-trichloromethyl, 2-pentafluorophenyl, 2-carboxylated, or 2-dithiocarboxylated “protected” NHC adducts (eq 6).<sup>53,55</sup> The as-generated carbene can be then either isolated or in situ reacted with the appropriate ruthenium precursor, to afford the targeted organometallic complex. This is usually achieved by displacing one (or more) phosphine or pyridine ligand(s). In another approach, especially useful when the in situ generated carbenes tend to dimerize, Ag<sub>2</sub>O can be used to initially form the corresponding heterocyclic carbene–Ag complexes (eq 7);<sup>56</sup> these silver salts, which usually are very efficient carbene-transfer agents, subsequently afford the desired heterocyclic carbene-coordinated ruthenium species by transmetalation.

The heterocyclic carbenic frameworks used thus far in ruthenium-based metathesis catalysts are illustrated in



**Figure 3.** First reported NHC-coordinated organometallic complexes and isolable carbene.

### Scheme 3. Most Common Methods for the Generation of Free Heterocyclic Carbene Ligands

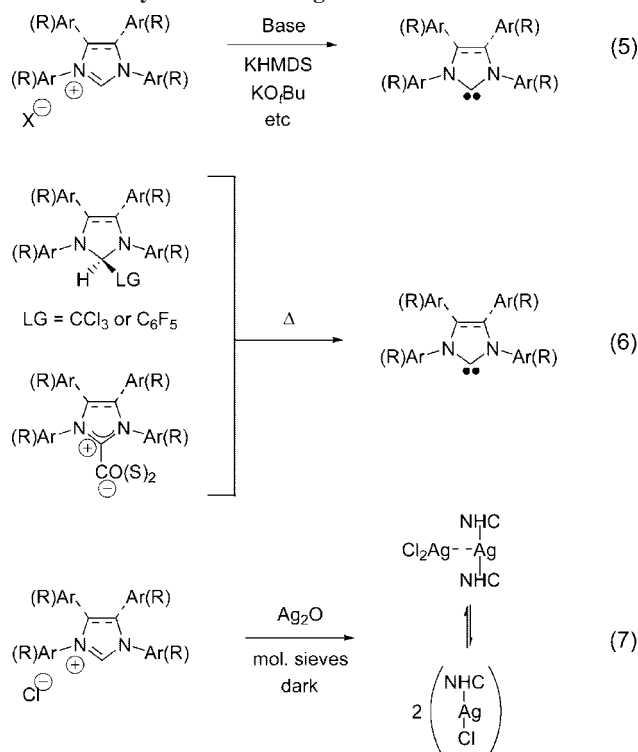


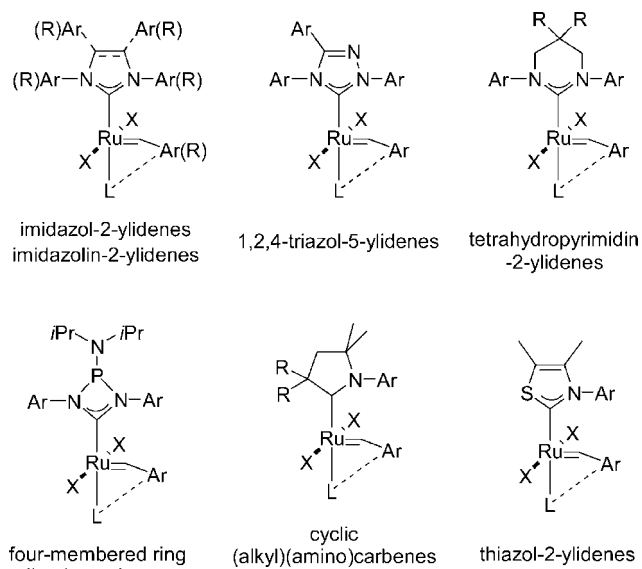
Figure 4.<sup>57</sup> The most successful and well-studied ruthenium catalysts bear either symmetrical or unsymmetrical imidazol- or imidazolin-2-ylidenes. Triazol-5-ylidenes, tetrahydropyrimidin-2-ylidenes, and a four-membered ring diaminocarbene have also been utilized, to afford the corresponding complexes. More recently, a series of ruthenium complexes coordinated with cyclic (alkyl)(amino)carbenes and thiazol-2-ylidenes have been synthesized. The synthesis, structure, and the catalytic activity of all (pre)catalysts families in Figure 4 will be thoroughly discussed in the following sections.

## 3. Heterocyclic Carbene Frameworks Used in Ruthenium-Based Metathesis Catalysts

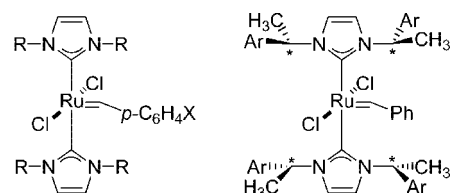
### 3.1. Symmetrical Imidazol- and Imidazolin-2-ylidenes

In 1998, Herrmann and co-workers reported the synthesis of the first heterocyclic carbene-containing ruthenium-based metathesis catalysts (**9**–**13**, Figure 5) in which both phosphine ligands were replaced by NHCs.<sup>58</sup> Despite their high stability, these complexes did not show a significant improvement in metathesis activity, mostly due to their slow initiation rates, attributed, in these carbene biscoordinated complexes, to one of the NHCs (less labile than phosphines),<sup>53,59</sup> which has to dissociate from the metal center for the catalyst to be initiated (*vide infra*).

Soon thereafter, the synthesis of heteroleptic ruthenium complexes **14a** and **14b** (Figure 6), by combining a nonlabile (1,3-dimesityl-imidazol-2-ylidene) with a labile (tricyclohexylphosphine or triphenylphosphine) ligand, was published.<sup>60–62</sup> Species **14a** and **14b** exhibited not only higher RCM activity affording even tetrasubstituted cycloolefins, at that time out of reach of ruthenium catalysts,<sup>60</sup> but also improved thermal stability compared to the parent bis(tri-



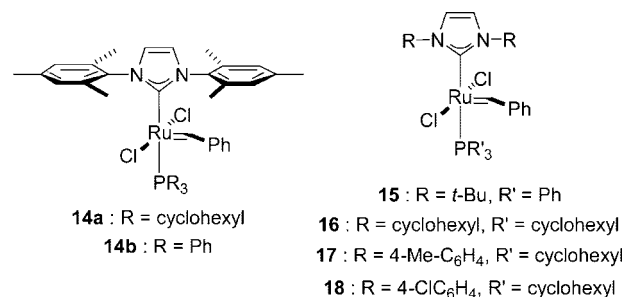
**Figure 4.** Ruthenium-based heterocyclic carbene-coordinated metathesis catalysts reported to date.



- 9:** R = *i*-Pr, X = H  
**10:** R = cyclohexyl, X = H  
**11:** R = *i*-Pr, X = Cl

- 12:** Ar = Ph  
**13:** Ar = naphthyl

**Figure 5.** First reported ruthenium-based carbene-coordinated metathesis catalysts.

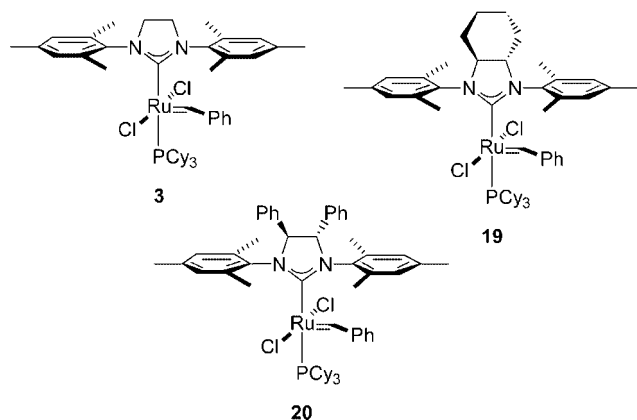


**Figure 6.** Ruthenium-based metathesis catalysts **14**–**18**.

cyclohexylphosphine) complex. Almost simultaneously, heteroleptic ruthenium-based metathesis catalysts **15**–**18** (Figure 6) were also reported.<sup>59,63,64</sup>

These first reports on heterocyclic carbene-coordinated ruthenium catalysts paved the way for one of the major breakthroughs in the field of olefin metathesis, which occurred with the synthesis of second-generation complex **3** (Figure 7).<sup>23</sup> The synthesis of carbene-coordinated ruthenium-based complexes **19** and **20** (Figure 7) was also published in that same work. The motivation for the preparation of complexes **3**, **19**, and **20** originated from the expected increased basicity of the corresponding saturated NHCs,<sup>65</sup> when compared to their unsaturated counterparts in Figure 6.<sup>23</sup> The increased basicity of these saturated NHCs was, in turn, anticipated to translate into an increased activity of the resulting ruthenium complexes. Complexes **3**, **19**, and **20** were synthesized in high yields, starting from the first-



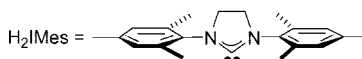
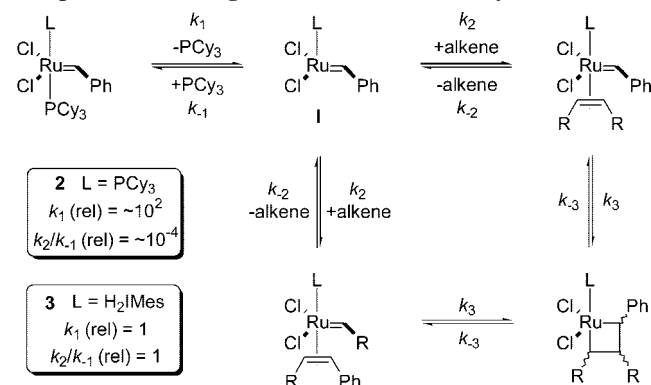


**Figure 7.** Ruthenium-based metathesis catalysts **3**, **19**, and **20**.

generation catalyst (**2**), by substituting one of the phosphine ligands with the in situ generated free carbenes.<sup>23</sup> Complex **3** expanded the scope of ruthenium metathesis catalysts significantly, as it was proved to be not only air-, water-, and functional group-tolerant<sup>66,67</sup> but also highly efficient in the RCM of sterically demanding dienes,<sup>23</sup> in the ROMP of low-strain substrates,<sup>68</sup> and in the realization of challenging CM reactions.<sup>66,69</sup> This kind of reactivity was previously possible only with the more active, though highly air- and water-sensitive, early transition-metal catalysts. What is more, **3** remains efficient at catalyst loadings as low as 0.05 mol % for RCM and 0.0001 mol % for ROMP reactions. An alternative, one-pot synthesis for complex **3** was published a couple of years later.<sup>70</sup> According to this report, potassium *t*-amylate can be used for the deprotonation of the carbene precursor, an imidazolium salt, whereas isolation of **3** can be achieved by simple filtration. Another route toward the preparation of **3** was reported in 2003.<sup>53</sup> In this work, the NHC–alcohol or –chloroform adducts were used as carbene precursors. These easy-to-synthesize and easy-to-use “protected” forms of NHCs are air-stable and easier to handle than their free carbene analogues, while the desired carbenes can be readily released in solution, providing direct access to the metal–NHC complexes.

The reasons for the increased activity of the second-generation phosphine-containing catalysts, compared to their first-generation analogues, have been investigated both experimentally and theoretically. Initially, it was assumed that the higher activity of the second-generation catalysts originates from the higher electronic *trans*-influence of the NHCs, compared to the phosphine ligands, that was in turn expected to lead to a lower barrier to phosphine dissociation (faster initiation). However, a series of mechanistic studies,<sup>24,71</sup> later on confirmed by gas-phase experiments,<sup>72</sup> showed that this is not the case. Thus, whereas both the first- (**2**) and second-generation (**3**) tricyclohexylphosphine-containing catalysts were found to initiate via a dissociative mechanism (Scheme 4), the initiation rate ( $k_1$ ) of **2** was measured to be 2 orders of magnitude higher than that of **3**.<sup>73</sup> Nevertheless, the overall catalytic activity of **3** was found to be about 2 orders of magnitude higher than that of **2**. To account for these contradictory observations, it was proposed that the partitioning ( $k_2/k_{-1}$ ) between the coordination of the alkene substrate ( $k_2$ ) and the phosphine ligand ( $k_{-1}$ , return to the resting state of the catalyst), by the corresponding 14-electron ruthenium intermediates (**I**, Scheme 4), is about 4 orders of magnitude greater for **3** relative to **2**.<sup>24,71</sup> Therefore, the increased activity of the second-generation catalyst(s) was rationalized on the basis of an increased affinity of the NHC-

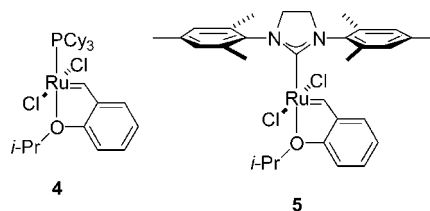
#### Scheme 4. Proposed Catalytic Mechanism of Phosphine-Containing Ruthenium-Based Catalysts



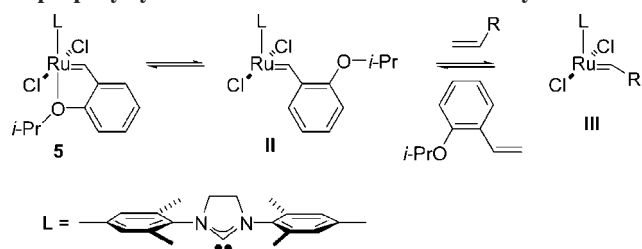
substituted ruthenium center for  $\pi$ -acidic olefins relative to  $\sigma$ -donating phosphines. It should be noted that improvement of initiation alone does not necessarily lead to a better catalyst, since catalyst efficiency depends on initiation, phosphine rebinding, reaction of the 14-electron ruthenium intermediate with olefin, and rate of catalyst decomposition.

As mentioned above, there are also a number of theoretical studies, sometimes contradictory to each other, dealing with the increased activity of the second-generation catalysts. For instance, differences in the barriers to the rotation of the ancillary neutral ligands (phosphine or NHC), in the 14-electron ruthenacyclobutane intermediates, were initially proposed as the source of the observed differences in activity between the first- and second-generation catalysts.<sup>74</sup> Later on, it was suggested that these differences in reactivity originate from the difference in the energy of the 14-electron benzylidenes and the corresponding 14-electron ruthenacyclobutane intermediates.<sup>75</sup> Other studies showed that both steric and electronic effects dictate the differences in reactivity.<sup>76,77</sup> Finally, in a more recent work, it was proposed that the difference in the initiation rates for phosphine- and NHC-coordinated catalysts is determined by attractive non-covalent interactions.<sup>78</sup>

In another significant contribution to the field of ruthenium-based metathesis, the Hoveyda group reported the synthesis of isopropoxystyrene-coordinated catalyst **5** in 2000,<sup>26</sup> one year after the report of its first-generation analogue **4** (Figure 8).<sup>25</sup> The Blechert group published the synthesis of the same phosphine-free catalyst almost simultaneously.<sup>27</sup> Compared to its phosphine-containing analogue **3**, catalyst **5** shows improved thermal stability, oxygen- and moisture-tolerance. On the other hand, the decreased initiation rate of **5** quite often comprises a major disadvantage. A variety of steric and electronic modifications of the chelating benzylidene



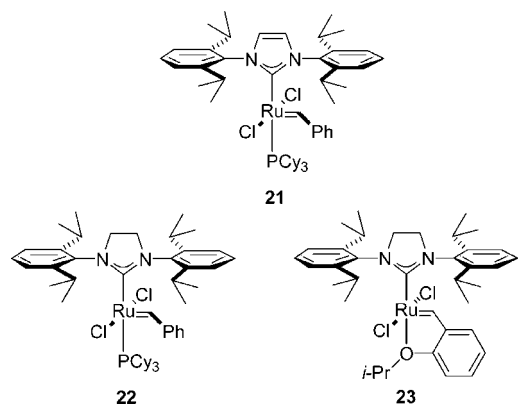
**Figure 8.** Isopropoxystyrene-coordinated ruthenium catalysts **4** and **5**.

**Scheme 5. Proposed Catalytic Mechanism of Isopropoxystyrene-Coordinated Ruthenium Catalysts**


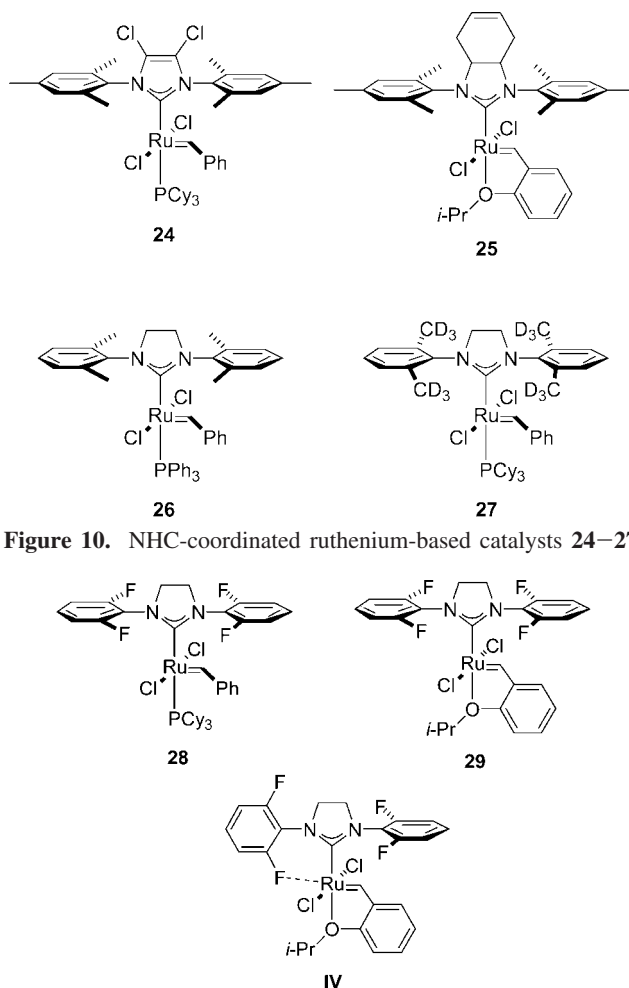
ether ligand were aimed at resolving this problem. These efforts will be discussed in section 4.1, which is exclusively dedicated to the chelating benzylidene ether ligands.

The proposed catalytic mechanism of the chelating benzylidene ether ruthenium complexes is slightly different from that discussed above for the phosphine-containing complexes. Initially, 14-electron intermediate **II** is formed through the dissociation of the benzylidene ether chelating group (Scheme 5). Coordination of the alkene substrate, followed by metathesis, leads to the formation of the catalytically active species **III** and a molecule of isopropoxystyrene (or a related derivative).<sup>25,26,79</sup> Therefore, the initial catalyst, or precatalyst, exists in equilibrium with the catalytically active species, and when the olefin is completely consumed, the catalyst may return to its resting state by rebinding the isopropoxystyrene that was eliminated at the first step (release/return mechanism).<sup>25,26</sup> Also note that both phosphine-containing (Scheme 4) and phosphine-free catalysts (Scheme 5) provide the same propagating species (**III**, Scheme 5) after a single turnover.

In 2000, Nolan and co-workers reported the synthesis of complex **21** (Figure 9), bearing two bulky aryl groups (2,6-diisopropylphenyl), in an effort to study the influence of the bulkiness of the NHCs on the catalytic activity of the corresponding complexes.<sup>80</sup> Likewise, the groups of Fürstner,<sup>81</sup> Mol,<sup>82</sup> and Wagener<sup>83</sup> reported the synthesis and the catalytic activity evaluation of complexes **22** and **23** (Figure 9), the saturated phosphine-containing and phosphine-free analogues of **21**. At ambient temperature, catalyst **22** shows effective turnover numbers 6 times higher than those of **3**,<sup>82</sup> along with very high initiation rates (turnover number is defined as the number of substrate molecules that are converted into product per catalyst molecule); nevertheless, its decomposition rate is also increased,<sup>83</sup> especially when utilized in challenging transformations.<sup>84</sup> In sharp contrast, phosphine-free catalyst **23** displays increased thermal stability



**Figure 9.** Ruthenium catalysts **21**–**23** bearing sterically demanding NHCs.



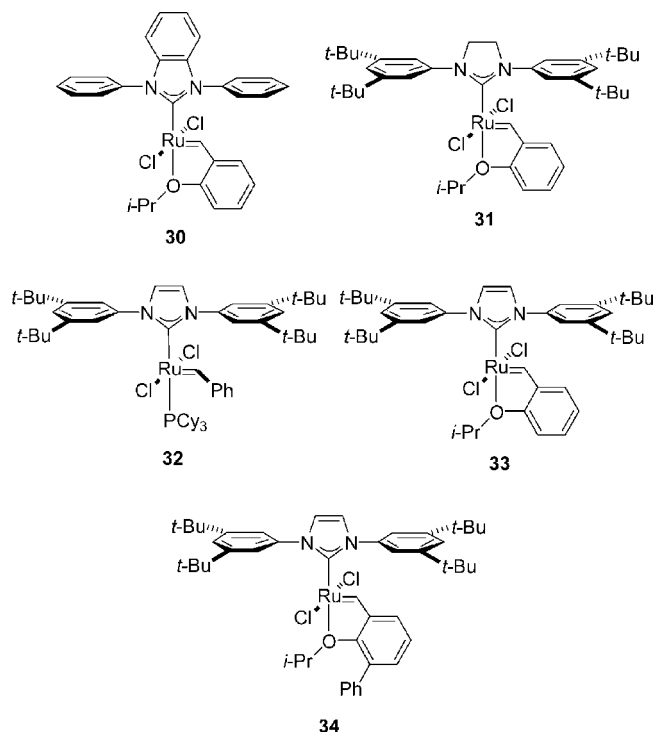
**Figure 10.** NHC-coordinated ruthenium-based catalysts **24**–**27**.

**Figure 11.** Fluorinated ruthenium-based catalysts **28** and **29**.

and improved ADMET polymerization efficiency compared to complex **22**.<sup>83</sup>

The Fürstner group has also published the preparation of complex **24** (Figure 10).<sup>81</sup> Remarkably, substitution of the backbone of this unsaturated NHC with two chlorine atoms has little effect on the reactivity of the resulting complex, despite the obviously altered electronics of the ligand. The synthesis of complexes **25**<sup>85</sup> and **26**,<sup>86</sup> presented in Figure 10, was published in 2005; **25**, bearing an internal double bond, was prepared in order to be used as a starting point for the preparation of further functionalized NHC-coordinated catalysts.<sup>85</sup> The unsaturated backbone in **25** remains intact even at elevated temperatures, most probably due to the low metathesis reactivity of unstrained cycloolefins such as cyclohexenes. The reactivity of **25** in the RCM of *N,N*-diallyl tosylamine was found to be slightly lower than that of the second-generation isopropoxystyrene-coordinated ruthenium catalyst **5** (Figure 8). Triphenylphosphine-containing complex **26** was reportedly purified by simple hexane washings (i.e., there was no need for column chromatography).<sup>86</sup> Its catalytic efficiency was evaluated in the self-CM of acrylonitrile, where it showed activity similar to the second-generation catalyst **3** (Figure 7). Complex **27** (Figure 10), bearing the deuterated analogue of the NHC in **26**, was prepared to investigate the mechanism of olefin isomerization in metathesis reactions carried out by H<sub>2</sub>IMes-containing ruthenium catalysts.<sup>87</sup>

Complexes **28** and **29** (Figure 11), bearing *o*-fluorinated aryl groups on the NHC ligand, were reported in 2006.<sup>88</sup>

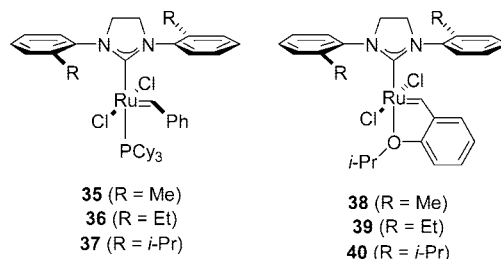


**Figure 12.** Ruthenium-based catalysts **30–34** without *o*-substituents on the *N*-bound aryl rings.

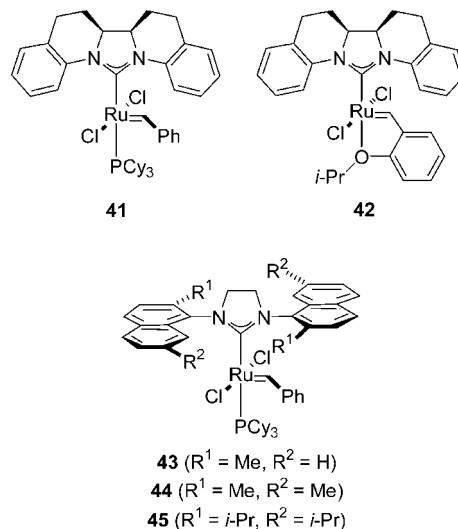
Phosphine-containing **28** catalyzes the RCM of diethyl diallylmalonate with a significantly increased reaction rate compared to both parent complexes **3** (Figure 7) and **5** (Figure 8), whereas, in the same benchmark reaction, phosphine-free **29** shows a slower rate than both **3** and **5**. This contradictory behavior of **28** and **29** was ascribed to an unprecedented fluorine–ruthenium interaction (Ru–F distance = 3.2 Å) observed in the solid-state structure of **29** (**IV**, Figure 11) via X-ray diffraction.

Despite the development of the highly active and functional group-tolerant catalysts described above, RCM to form tetrasubstituted olefins remained one of the weaknesses of ruthenium-catalyzed metathesis until 2007, when a series of new catalysts with increased activity for this transformation was published.<sup>44,45</sup> On the basis of an earlier observation, according to which catalysts with reduced bulk at the *ortho* position of the two *N*-bound aryl groups of the NHCs exert increased efficiency in the formation of sterically demanding substrates,<sup>34,35</sup> catalysts **30** and **31** (Figure 12) were designed and synthesized.<sup>44</sup> Indeed, these two catalysts, along with complex **29** in Figure 11, performed significantly better than all the ruthenium catalysts available at the time in the RCM formation of many tetrasubstituted olefins. Further improvements led to the syntheses of complexes **32–34** (Figure 12), bearing the unsaturated analogue of the NHC in **31**.<sup>44</sup> Overall, **34** was the most efficient catalyst in that work regarding RCM to afford tetrasubstituted olefins. It is also worth mentioning that the biphenyl group on the isopropoxybenzylidene moiety of complex **34** is known to afford rapidly initiating phosphine-free catalysts (refer to section 4.1).<sup>89</sup>

Unfortunately, however, the difficult preparation of catalyst **34** rendered its large-scale production uneconomical and imposed significant drawbacks regarding its commercialization. Research in the direction of more easily prepared catalysts eventually led to the evolution of **35–40** (Figure 13), the syntheses of which can be easily performed on a large scale.<sup>45</sup> Catalysts **35–40** proved to be very efficient in



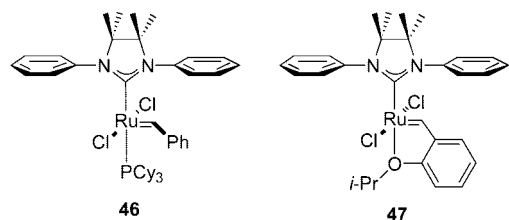
**Figure 13.** Ruthenium catalysts **35–40** with increased efficiency in the formation of tetrasubstituted olefins via RCM.



**Figure 14.** Ruthenium-based catalysts **41–45** bearing bulky NHC ligands.

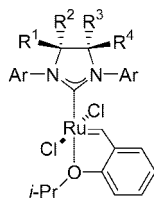
the RCM of dimethylallylmalonates, a family of sterically demanding benchmark substrates, while *N*-tolyl complexes **35** and **38** were the most successful catalysts in that work. Later on, **38** was also found to exert increased efficiency for the formation of sterically challenging disubstituted olefins by CM.<sup>90</sup> On the basis of solution- and solid-state structural data, and in conjunction with a series of theoretical calculations, the outstanding catalytic activity of **35** and **38** toward sterically demanding substrates was proposed to result from a significantly more open steric environment around the ruthenium center.<sup>91</sup> This was suggested to originate from the accessibility of conformations in which the *N*-tolyl rings are rotated away from approaching and coordinating olefins.

In two other recent reports, the syntheses of ruthenium-based catalysts **41**,<sup>92</sup> **42**,<sup>92</sup> and **43–45**<sup>93</sup> were described (Figure 14). Complexes **41** and **42** were initially targeted with the aim of increasing the diastereoselectivity of ring-rearrangement metathesis reactions. Although both **41** and **42** were found to be of limited stability in solution, even in the absence of olefin substrates, **41** indeed showed some promising results in diastereoselective ring-rearrangement metathesis reactions, affording improved *E/Z* selectivities.<sup>92</sup> In addition, **42** led to the isolation of a ruthenium complex relevant to the deactivation of NHC-coordinated ruthenium-based metathesis catalysts (refer to section 11). On the other hand, **43–45** were proven to be efficient RCM catalysts in benchmark reactions: **43** and **44** showed reactivity similar to that of the existing second-generation phosphine-coordinated catalyst (**3**), whereas **45** outperformed **3** by about an order of magnitude, in terms of turnover frequencies for complete conversion.



46

47

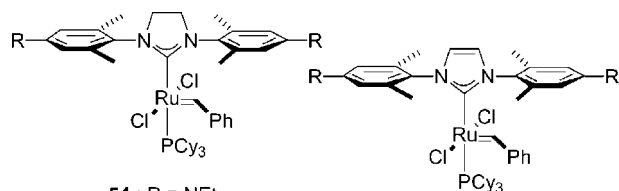


	Ar	R <sup>1</sup>	R <sup>2</sup>	R <sup>3</sup>	R <sup>4</sup>
48	mesityl	H	H	Me	Me
49	mesityl	Me	H	H	Me
50	mesityl	H	Me	Me	Me
51	<i>o</i> -tolyl	H	H	Me	Me
52	<i>o</i> -tolyl	H(Me)	Me(H)	H	Me
53	<i>o</i> -tolyl	Me	Me	Me	Me

Figure 15. NHC-backbone-substituted ruthenium catalysts 46–53.

A series of decomposition studies concerning NHC-substituted ruthenium complexes, extensively discussed in section 11 of the present article, has shown that *N*-aryl-substituted NHC complexes without *ortho*-substituents on the *N*-aryl groups are more prone to degradation compared to complexes bearing *ortho*-substituted *N*-aryl NHCs.<sup>92,94,95</sup> This lack of stability has been attributed to an easier rotation of the *N*-aryl groups in the former, which brings the *ortho*-aryl C–H bonds closer to the ruthenium center, thereby facilitating degradation through C–H bond activation. For this reason, it was anticipated that, by placing bulky substituents on the backbone of the NHC, the rotation of the *N*-aryl groups (about the N–C bond) should be restricted, thereby rendering this decomposition pathway unfavorable. In this context, complexes **46** and **47** (Figure 15), bearing a tetramethyl-substituted NHC ligand, were synthesized, and **47** was the first stable ruthenium metathesis catalyst coordinated with an *N,N*-diphenyl-substituted NHC with a saturated backbone.<sup>96</sup> Species **47** was proven to be an efficient olefin metathesis catalyst, carrying out a series of model RCM, CM, and ROMP reactions. **47** is also one of the most efficient catalysts in the RCM of the sterically demanding diethyl dimethylmalonate.

A subsequent more-detailed study, concerning the effects of NHC-backbone substitution on the efficiency of ruthenium metathesis catalysts, led to the synthesis of complexes **48–53** (Figure 15).<sup>97</sup> In that work, the catalytic activities of **48–53** were evaluated by the use of a highly sensitive Symyx robotic system. Both backbone and aryl substitution were found to significantly impact catalyst stability and activity. Thus, low *N*-aryl bulk on the NHC ligand led to increased activity and decreased stability, while increased backbone substitution increased catalyst lifetimes and decreased reaction rates. Furthermore, the relative importance of catalyst stability and activity on efficiency was found to depend on the steric encumbrance of the specific RCM reaction. Whereas for substrates with low steric demands catalyst stability is important for success at low catalyst loadings, for sterically hindered substrates catalyst activity becomes more important than catalyst stability.

54 : R = NEt<sub>2</sub>

56 : R = OMe

58 : R = Me

60 : R = H

62 : R = SMe

64 : R = F

66 : R = Cl

68 : R = Br

70 : R = I

72 : R = NMe<sub>2</sub>55 : R = NEt<sub>2</sub>

57 : R = OMe

59 : R = Me

61 : R = H

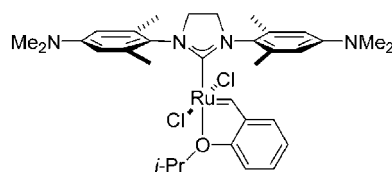
63 : R = SMe

65 : R = F

67 : R = Cl

69 : R = Br

71 : R = I



73

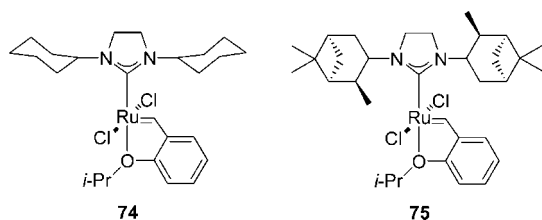
Figure 16. Catalysts 54–73 bearing saturated and unsaturated symmetrical NHC ligands.

In other work, based mostly on electrochemical and NMR studies, imidazolylidene- and imidazolynylidene-coordinated complexes **54–71** (Figure 16) were synthesized.<sup>98</sup> The major goal of this study was to investigate the existence of intramolecular  $\pi$ – $\pi$  interactions and whether such interactions influence the electronic density at the ruthenium center as well as the catalytic ability of the corresponding complexes. The reactivity of some representative complexes in selected RCM and CM reactions was found to systematically depend on the electronic properties of substituents R (Figure 16). Complex **54**, bearing the electron-donating NEt<sub>2</sub> group, was the most catalytically active complex. It was furthermore suggested by the authors that the differences in reactivity between saturated and unsaturated NHCs do not originate from different electron densities at the ruthenium center, and that the electron-donating abilities of the saturated and the unsaturated NHCs (bearing the same substituents R) are similar.

Complexes **72** and **73** (Figure 16), bearing a pH-responsive NHC ligand, have also been prepared by Schanz and co-workers.<sup>99</sup> In organic solvents, and in the absence of acid, **72** and **73** show reactivity similar to that of the parent H<sub>2</sub>IMes complexes **3** and **5** (Figures 7 and 8, respectively) in representative RCM and ROMP transformations. Upon addition of HCl, the NMe<sub>2</sub> groups in **72** and **73** get protonated, affording the corresponding dicationic complexes, which show increased decomposition rates. A protocol was developed to remove the residual ruthenium from RCM reaction mixtures by acidification and subsequent filtration of protonated **73** (refer also to section 10 dedicated to this issue).

Phosphine-free complexes **74** and **75** (Figure 17) were the first reported isolable ruthenium-based catalysts bearing aliphatic side groups on both nitrogen atoms of their saturated NHC ring.<sup>100</sup> Despite their higher catalytic activity in the ROMP of 1,5-cyclooctadiene, compared to the parent bis(mesityl)-substituted catalyst **5** in Figure 8, both **74** and **75** show decreased activity in model RCM and CM reactions. The authors suggested that this low efficiency originated from





**Figure 17.** Catalysts **74** and **75** bearing saturated NHC ligands with two aliphatic side groups.

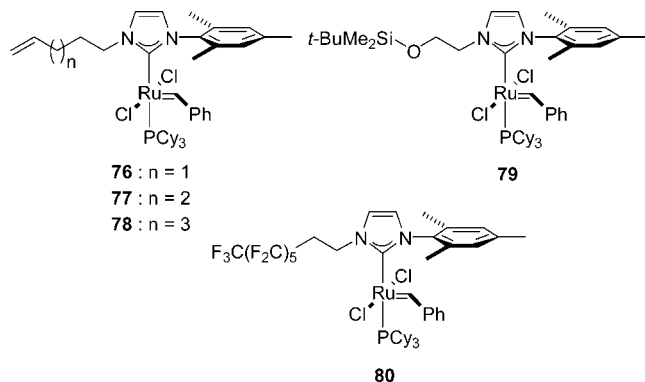
the increased steric bulk of the alkyls relative to the usual aromatic groups.

### 3.2. Unsymmetrical Imidazol- and Imidazolin-2-ylidenes

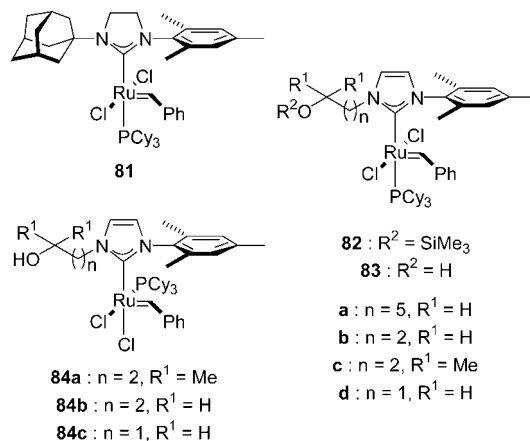
The first report on ruthenium complexes coordinated with unsymmetrical NHCs came from the Fürstner group in 2001.<sup>81</sup> Specifically, **76–78** (Figure 18) were targeted as complexes able to metathesize their own heterocyclic carbene ligands, affording the corresponding chelates, with the goal of regenerating themselves after the quantitative consumption of the substrate. In that same work, complexes **79** and **80** (Figure 18), incorporating a silylether and a perfluoroalkyl chain, respectively, were also reported. Complexes **76–80** are efficient in the RCM of *N,N*-dimethyl-*N*-tosylamide to form the corresponding tetrasubstituted carbon–carbon double bond. The catalytic activity of **76–78** also showed a systematic dependence on the tether length between the alkene group and the ruthenium center. This effect was postulated to depend on the different capacities of **76–78** to form chelate complexes in situ.

To further enhance the steric bulk and the electron-donating ability of the NHC *N*-substituents in the second-generation ruthenium catalysts, Mol and co-workers attempted the synthesis of  $[\text{RuCl}_2(=\text{CHPh})(\text{H}_2\text{IAd})(\text{PCy}_3)]$  ( $\text{H}_2\text{IAd}$  = 1,3-di(1-adamantyl)-4,5-dihydroimidazol-2-ylidene).<sup>101</sup> Although the synthesis of this symmetrical NHC complex was proven impossible, supposedly due to the increased three-dimensional bulkiness of the  $\text{H}_2\text{IAd}$  ligand, its unsymmetrical counterpart **81** (Figure 19), bearing the mixed 1-adamantyl/mesityl ligand, was isolated as a green solid in good yield. However, **81** was proved to be a very poor olefin metathesis catalyst and only catalyzed the ROMP of norbornene, one of the least challenging cyclic olefins to polymerize. The explanation offered for the exceptionally low reactivity of **81** was based on the extreme steric hindrance imposed by its NHC ligand.

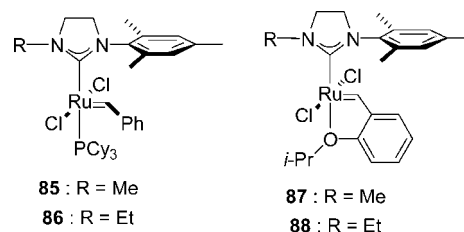
Unsymmetrical complexes **82a–82d** and **83a–83c** (Figure 19), bearing protected or unprotected hydroxyl groups on



**Figure 18.** Complexes **76–80** coordinated with unsymmetrical NHC ligands.



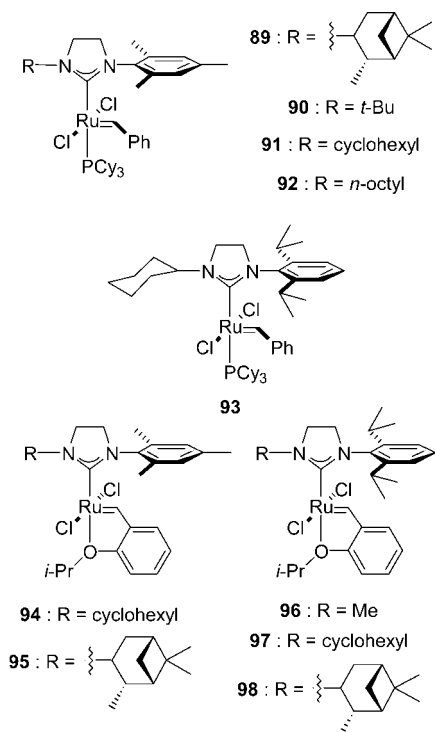
**Figure 19.** Ruthenium-based complexes **81–84** bearing unsymmetrical NHC ligands.



**Figure 20.** Complexes **85–88** coordinated with unsymmetrical NHCs.

the side-chains of their NHC ligands, were synthesized in an attempt to prepare catalysts capable of undergoing immobilization on various supports (for a discussion on ruthenium metathesis catalysts tagged with insoluble materials or soluble functionalities, refer to section 10).<sup>102</sup> An unanticipated molecular rearrangement was observed during the deprotection of **82d** under acidic or mildly basic conditions. Thus, instead of the expected **83d**, rearranged **84c** with its neutral ligands in a *cis*-configuration was isolated in high yield (Figure 19). The same phenomenon was observed during immobilization attempts of **83b** and **83c** on silica gel, when rearranged complexes **84b** and **84a** were respectively isolated. It was speculated that this reorganization process is promoted by the terminal hydroxyl groups. The ability of the hydroxyl function to effect this transformation becomes increasingly facile as this group is brought closer to the ruthenium center. *cis*-Configured **84a–84c** are active metathesis catalysts at elevated temperatures, where, as suggested by <sup>31</sup>P NMR data, they revert into their *trans*-isomers **83b–83d**.

The design of complexes **85–88** (Figure 20) was based on the anticipation that the unsymmetrical nature of their NHC ligands might alter the environment of key intermediates in the metathesis pathway, leading to improved *E/Z* selectivity in CM reactions and diastereoselectivity in RCM reactions.<sup>103</sup> Moreover, the enhanced electron-donating ability of alkyl substituents was anticipated to lead to increased catalyst activity. Complexes **85–88** were synthesized from commercially available reagents in good to high yields. NOE-difference NMR experiments (NOE = nuclear overhauser effect) suggest that only one rotational isomer exists for both **85** and **86** in solution, with the benzylidene moiety located directly under the mesityl ring of the NHC. Similarly, in the solid state, a single isomer was isolated for **87** and **88**, with the mesityl group situated directly above the benzylidene proton. In a model RCM reaction, complexes **85–88** showed

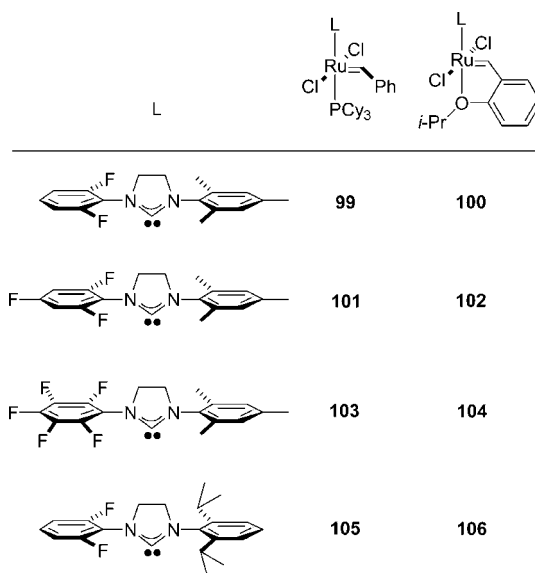


**Figure 21.** Unsymmetrical NHC-coordinated complexes **89**–**98**.

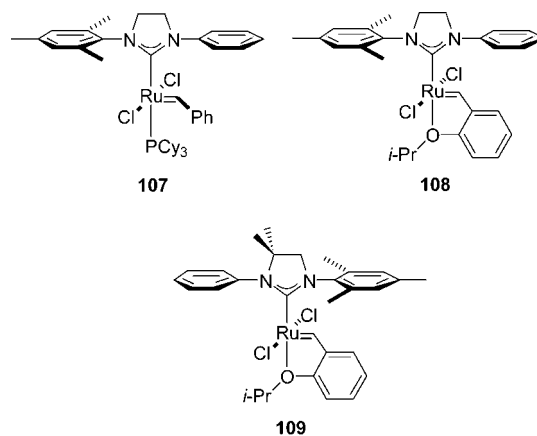
activities similar to those of their parent bis(mesityl)-substituted complexes **3** and **5** (Figures 7 and 8, respectively). Moreover, **85** and **87** showed significantly different *E/Z* ratios in selected CM transformations and improved selectivities in a diastereoselective RCM reaction compared to the parent complexes **3** and **5**.

Ledoux, Verpoort, and co-workers synthesized and evaluated another series of ruthenium catalysts coordinated with *N*-alkyl-*N*-aryl-substituted NHCs (**89**–**98**, Figure 21).<sup>100,104,105</sup> Phosphine-containing **89**, **91**, and **92** were demonstrated to surpass the parent second-generation catalyst (**3**) in the ROMP of 1,5-cyclooctadiene,<sup>104</sup> whereas **93** showed only fair metathesis activity.<sup>105</sup> The decreased catalytic activity of **90** was attributed to its increased steric bulk in close proximity to the metal center.<sup>104</sup> Phosphine-free complexes **94**, **96**, and **97** display reduced catalytic activity compared to the parent bis(aryl) *N*-substituted symmetrical catalysts (**5** and **23**, Figures 8 and 9, respectively).<sup>100</sup>

A family of ruthenium-based complexes bearing unsymmetrical NHCs with fluorinated *N*-aryl groups (**99**–**106**, Figure 22) has been also synthesized.<sup>106,107</sup> These complexes are readily accessible in one or two steps from commercially available first-generation catalyst **2**. Among others, **99**–**106** promote the RCM of diethyl diallylmalonate and diethyl allylmethylmalonate, the ROMP of 1,5-cyclooctadiene, and the CM of allyl benzene with *cis*-1,4-diacetoxy-2-butene, in some cases surpassing the existing second-generation catalysts **3** and **5** in efficiency. Especially in the CM of allyl benzene with *cis*-1,4-diacetoxy-2-butene, complexes **99**–**106** demonstrate similar or higher activity than the second-generation ruthenium catalysts and, more importantly, afford improved *E/Z* ratios of the desired cross-product at conversion above 60%. This was quite an important finding, since, as mentioned in the Introduction, compared to RCM and ROMP, CM is an underutilized olefin metathesis transformation, not only because it lacks the entropic driving force of RCM and the ring-strain release of ROMP, but also because



**Figure 22.** Fluorinated unsymmetrical NHC-coordinated complexes **99**–**106**.

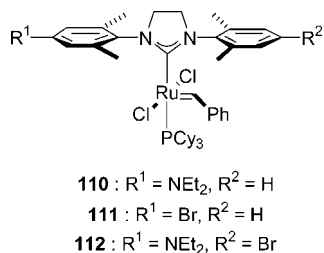


**Figure 23.** Complexes **107**–**109** coordinated with 1-mesityl-3-phenyl-substituted unsymmetrical NHC ligands.

it often leads to relatively low statistical yields of the desired cross-product, as well as poor *E/Z* cross-product selectivity.<sup>108</sup> The *E/Z* selectivity in CM reactions at high conversion is usually governed by thermodynamic factors; that is, secondary metathesis promotes isomerization of the product to the favored *E* isomer, with the *E/Z* selectivity being controlled by the stability of the olefin isomers rather than the selectivity of the catalyst.

The influence of the unsymmetrical NHC ligands in **99**–**106** on the initiation rate of the irreversible reaction of these ruthenium complexes with butyl vinyl ether was also studied.<sup>106,107</sup> The measured rate constants and activation parameters for all phosphine-containing catalysts in Figure 22 suggest rate-determining phosphine dissociation. On the contrary, rate constants and activation parameters for the phosphine-free catalysts **5**, **100**, **102**, **104**, and **106** are indicative of an associative mechanism.<sup>106,107,109</sup> Finally, the synthesis of the related Rh(CO)<sub>2</sub>Cl(NHC) complexes allowed for the study of the electronic properties of all unsymmetrical NHC ligands in **99**–**106**, by measuring the corresponding carbonyl stretching frequencies.<sup>107</sup>

Complexes **107**–**109**, coordinated with the 1-mesityl-3-phenyl-substituted NHC ligands presented in Figure 23, have been also synthesized. **107** and **108** were prepared as model complexes during a series of catalyst decomposition studies



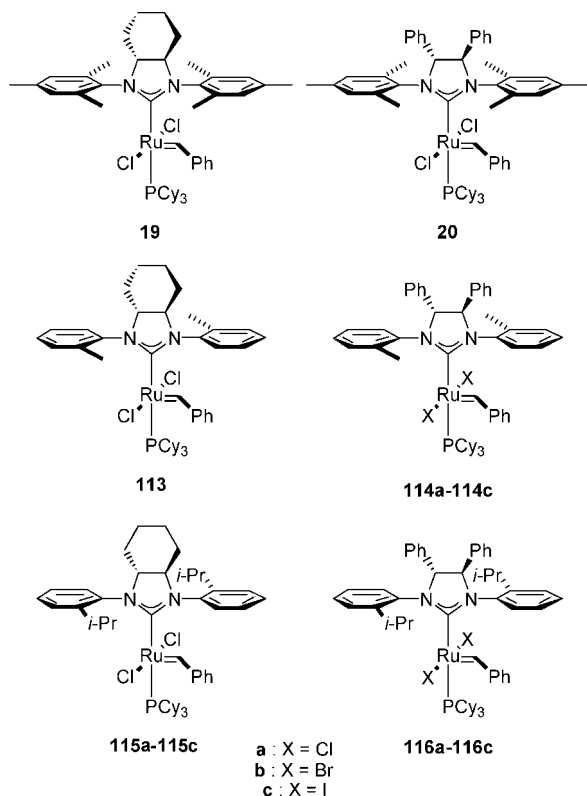
**Figure 24.** Unsymmetrical NHC-coordinated complexes **110**–**112**.

(see section 11) and, being highly unstable, their metathesis catalytic activity has not been evaluated.<sup>92</sup> On the other hand, **109** was targeted as a stabilized analogue of **108** and efficiently catalyzes the RCM of diethyl diallyl, diethyl allylmethyl, and diethyl dimethylmalonate, as well as the CM of allyl benzene with *cis*-1,4-diacetoxy-2-butene.<sup>96</sup>

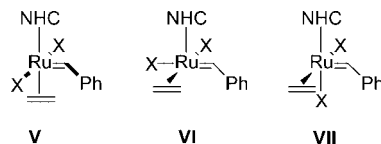
In 2008, phosphine-containing complexes **110**–**112** (Figure 24), coordinated with unsymmetrical bis(*N*-aryl)-substituted NHCs, were reported.<sup>98</sup> As had been found earlier for other similar unsymmetrical systems,<sup>106,107</sup> complexes **110**–**112** exist as pairs of atropisomers.<sup>98</sup> During a series of electrochemical studies, it was also observed that the orientation of the aryl rings relative to the benzylidene moiety dictates the ruthenium redox potential. The metathetic catalytic activity of **110**–**112** has not been evaluated.

### 3.3. Chiral Monodentate *N*-Heterocyclic Carbenes

Although the first ruthenium-based catalysts bearing chiral monodentate NHCs<sup>110</sup> (**19** and **20**, Figure 25) were reported in 1999,<sup>23</sup> the first asymmetric metathesis reaction catalyzed by these kinds of complexes was published two years later.<sup>29</sup> Besides **19** and **20**, chiral complexes **113**–**116** (Figure 25)



**Figure 25.** Ruthenium complexes **19**, **20**, and **113**–**116** coordinated with chiral monodentate NHCs.



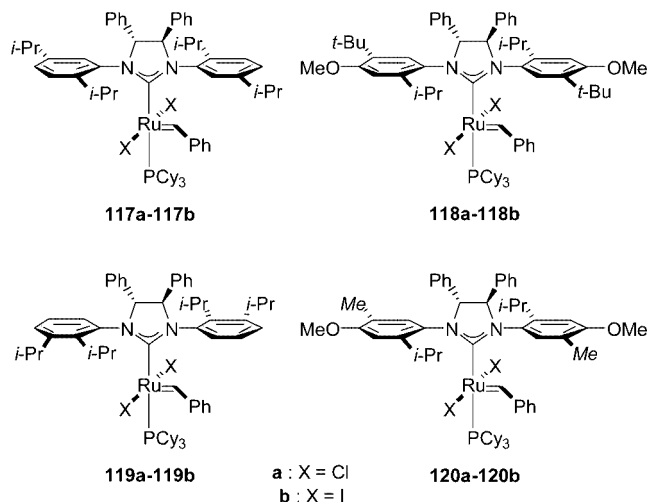
**Figure 26.** Possible geometries of the intermediate olefin complex.

were synthesized and evaluated. In these asymmetric complexes, the chirality is transferred from the 4- and 5-positions of the NHC imidazolyl ring to the *N*-bonded aromatic groups, forcing the *ortho*-substituents of the *N*-aryl rings to reside on the NHC-face opposite to the bulky groups on the backbone (a so-called “gearing” effect). Complexes **113**, **114a**, **115a**, and **116a** are air-stable solids easily purified on the bench by column chromatography, whereas **114b**–**116b** and **114c**–**116c** can be generated in situ by the addition of excess LiBr or NaI (vide infra). Crystallographic evidence of the conformation of these chiral NHCs was obtained by conversion of **114a** to the corresponding bis(pyridine) complex (see section 4.3).

Complexes **19**, **20**, and **113**–**116** were evaluated in the enantioselective desymmetrization of achiral trienes (3-allyloxy-2,4-dimethylpenta-1,4-dienes), also known as asymmetric ring-closing metathesis (ARCM).<sup>29</sup> It was found that catalysts encompassing the (1*R*,2*R*)-1,2-diaminocyclohexane group (**19**, **113**, and **115**) exhibit lower enantioselectivities than those having the (1*R*,2*R*)-1,2-diphenylethylenediamine moiety (**20**, **114**, and **116**). Replacement of the mesityl substituents (in **19** and **20**) with *o*-methylaryl (in **113** and **114**) or *o*-isopropylaryl groups (in **115** and **116**) also increases the enantioselectivity. Finally, changing the halide ligands from chlorides to iodides improves the enantioselectivity; however, the conversion to the metathesized products is simultaneously reduced, supposedly due to the lower stability of the diiodide ruthenium intermediates. None of these catalysts showed a significant temperature- or solvent-dependent change in its enantioselectivity. Catalyst **116c** afforded the highest enantiomeric excess measured in that study.

On the basis of the ligand effects described above and the stereochemical outcome of the studied reactions, a bottom-face (*trans* to the NHC) olefin binding pathway (intermediate **V** in Figure 26) was excluded. Among the two side-on (*cis* to the NHC) olefin binding pathways in Figure 26, intermediate **VII** was favored, although **VI** was not excluded.<sup>29</sup> On the contrary, theoretical work published in 2004 suggested bottom-face olefin binding (**V**, Figure 26), given that the other two intermediates (**VI** and **VII**) were calculated to be of remarkably higher energy.<sup>111</sup> For a more detailed discussion on olefin coordination and the geometry of ruthenacyclobutane intermediates, the reader may refer to section 4.6.

Subsequent studies, aimed at the enhancement of the enantioselectivity displayed by **116**, together with the goal of expanding the substrate scope of ARCM, led to the synthesis of chiral complexes **117**–**120** (Figure 27).<sup>34,35</sup> While **117** and **118** showed enantioselectivities similar to those of catalyst **116**, **119** displayed increased enantioselectivity to the extent that, in a number of substrates, even its dichloride version (**119a**) could be used at very low catalyst loadings (<1 mol %) to afford high enantiomeric excesses and conversions.<sup>34</sup> Thus, **116c** and **119a** were utilized to ring-close alkenyl ether- and silyl ether-prochiral trienes, affording five- to seven-membered rings; conversions up to >98% and enantiomeric excesses up to 92% were obtained. The

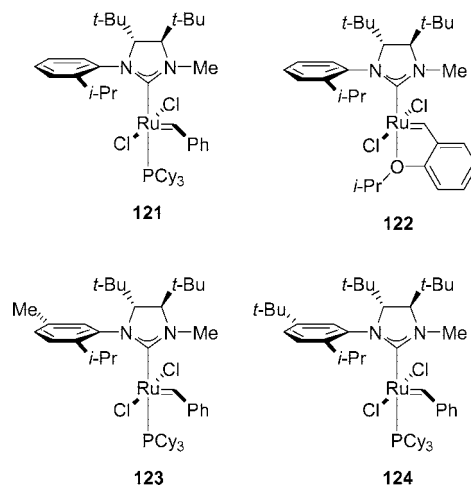


**Figure 27.** Ruthenium complexes **117–120** bearing chiral mono-dentate NHC ligands.

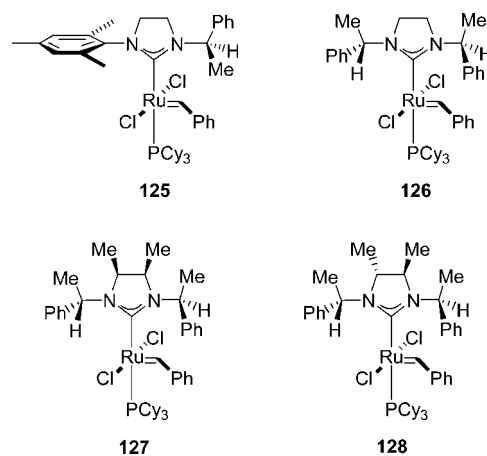
influence of solvent and temperature on conversion and enantiomeric excess was also studied. Finally, according to the olefin-binding pathways proposed, if the incoming olefin binds *cis* to the NHC, the stereodefining interaction is the face of the ruthenium to which the olefin binds. If, on the other hand, the incoming olefin binds *trans* to the NHC, the stereodefining interaction is the position of the alkylidene under the *N*-bound aryl ring. Either way, the position of the pendent olefin in the forming ring also plays an important role in the transition state.

**116–120** (Figures 25 and 27) were later proven to also be highly active in asymmetric ring-opening cross-metathesis (AROCM) reactions.<sup>35</sup> **118a** was found to be the most selective of dichloride catalysts **116–120**, whereas the use of diiodide catalyst **118b** slightly improved the enantiomeric excess values (up to 82% in the AROCM of norbornene derivatives with styrene). Nevertheless, since diiodide catalysts are generally less reactive than their dichloride counterparts, the loading of **118b** had to be increased to 3 mol % to achieve activity similar to that observed with 1 mol % loading of **118a**. A ruthenium benzylidene, rather than a ruthenium methylidene as the propagating species, along with a *trans* coordination pathway were proposed to be operative in these AROCM reactions. Moreover, in the same work, the first examples of asymmetric cross-metathesis (ACM) reactions, the most challenging of the asymmetric metathesis transformations, were reported.<sup>35</sup> The enantiomeric excess values obtained in the ACM reactions of protected 1,4-pentadien-3-ols, hexa-1,5-diene-3,4-diol, or hepta-1,6-diene-3,5-diol with *cis*-1,4-diacetoxy-2-butene ranged from 37% to 52%.

Collins and co-workers prepared another family of ruthenium catalysts coordinated with chiral mono-dentate NHC ligands (**121–124**, Figure 28).<sup>112,113</sup> Instead of the 1,2-diphenyl enantioinducing backbone of the NHCs in **20**, **114**, and **116–120** (Figures 25 and 27), complexes **121–124** encompass a bulky 1,2-di-*tert*-butyl unit. Furthermore, the NHCs in **121–124** are unsymmetrical, having one *N*-aryl and one *N*-methyl substituent adjacent to the carbenic center. **121–124** showed high reactivities and high enantiomeric excess values in representative AROCM reactions, without the use of halide additives. It was also proposed that the barriers to the rotation of the NHC ligands in **121–124** play a significant role in determining the reactivity of the corresponding catalysts.



**Figure 28.** Ruthenium complexes **121–124** bearing chiral mono-dentate NHC ligands.



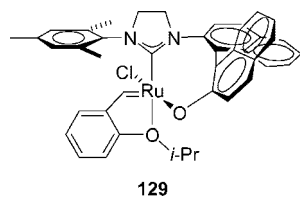
**Figure 29.** Ruthenium complexes **125–128** coordinated with chiral mono-dentate NHCs.

In 2008, the synthesis of complexes **125–128** (Figure 29) was reported by the groups of Buchmeiser, Blechert, and Grisi.<sup>114,115</sup> The catalytic activity of **125** was not investigated extensively, since it was essentially prepared as the precursor of the corresponding phosphine-free, pyridine-coordinated complex, utilized in alternating copolymerizations (refer to section 4.3).<sup>114</sup> **126–128**, bearing saturated NHCs with two nonaromatic *N*-substituents, were found to promote RCM, AROCM, CM, and ROMP reactions.<sup>115</sup> In these benchmark ROMP and CM reactions, **126–128** showed activities between that of the first- and second-generation phosphine-containing catalysts (Figure 2, catalysts **2** and **3**, respectively), with **127** being the most catalytically active complex in the series. In the CM of allyl benzene with *cis*-1,4-diacetoxy-2-butene, **126–128** afforded improved *E/Z* ratios toward *Z* double bond formation. It should be noted that **126**, which does not have chirality in the backbone of the NHC, was completely unable to give enantioinduction in AROCM, whereas, in the same transformation, **128** afforded modest enantioselectivities (33%). This difference in reactivity was a key observation and highlights the significance of chiral substitution on the backbone and the minor role of the chiral *N*-substituents in chirality induction with this catalyst type.

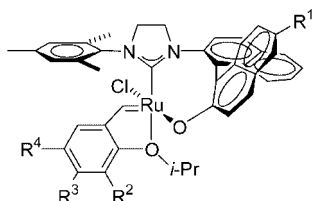
### 3.4. Chiral Bidentate *N*-Heterocyclic Carbenes

Hoveyda and co-workers have developed a series of ruthenium complexes coordinated with bidentate NHC





**Figure 30.** Ruthenium complex **129** bearing a chiral bidentate NHC.



**130** :  $R^1 = \text{H}$ ,  $R^2 = \text{H}$ ,  $R^3 = \text{H}$ ,  $R^4 = \text{NO}_2$

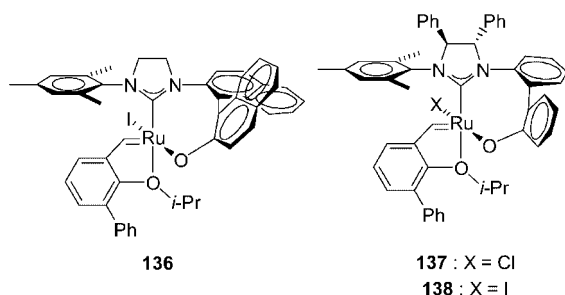
**131** :  $R^1 = \text{H}$ ,  $R^2 = \text{H}$ ,  $R^3 = \text{H}$ ,  $R^4 = \text{OMe}$

**132** :  $R^1 = \text{H}$ ,  $R^2 = \text{H}$ ,  $R^3 = \text{OMe}$ ,  $R^4 = \text{H}$

**133** :  $R^1 = \text{H}$ ,  $R^2 = \text{Ph}$ ,  $R^3 = \text{H}$ ,  $R^4 = \text{H}$

**134** :  $R^1 = \text{CF}_3$ ,  $R^2 = \text{H}$ ,  $R^3 = \text{H}$ ,  $R^4 = \text{H}$

**135** :  $R^1 = \text{CF}_3$ ,  $R^2 = \text{Ph}$ ,  $R^3 = \text{H}$ ,  $R^4 = \text{H}$



**Figure 31.** Ruthenium complexes **130–138** coordinated with chiral bidentate NHCs.

ligands, bearing biphenolate or binaphtholate moieties that displace one of the chlorides in the coordination sphere of ruthenium. More specifically, in 2002 they reported the synthesis of chiral complex **129** (Figure 30), bearing a bidentate binaphthol NHC moiety.<sup>30</sup> This was the first report regarding a ruthenium-based metathesis catalyst in which the chiral information of the NHC ligand is transferred directly to the ruthenium center. Complex **129**, isolated in >98% diastereo- and enantiomeric purity without resolution, is air- and moisture-stable and can be recycled at the end of the reaction, by column chromatography, with up to 96% catalyst recovery. Because of the less electronegative nature and the increased steric bulk of the naphthoxide ligand in **129**, compared to the corresponding chloride ligand in parent complex **5**, **129** is less active, requiring longer reaction times and elevated temperatures for the same transformations. Nevertheless, **129** was proven to efficiently catalyze a series of AROCM reactions to afford high enantioselectivities.<sup>30</sup>

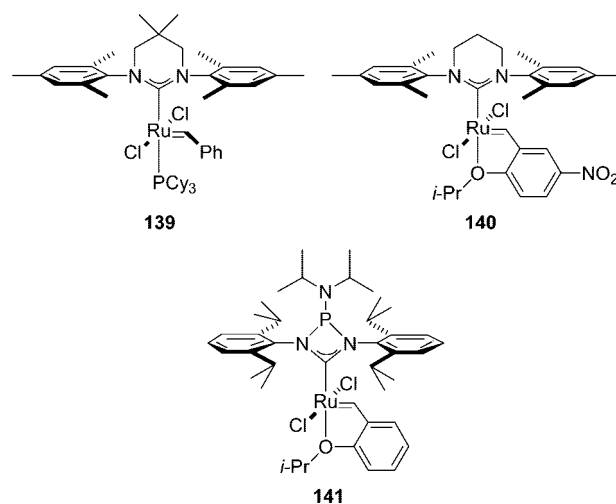
Aiming at the enhancement of the activity of **129**, by increasing the electronegativity of the naphtholate moiety, the Hoveyda group developed the trifluoromethyl-substituted chiral NHC ligand incorporated in complexes **134** and **135** (Figure 31).<sup>31</sup> Indeed, **134** and **135** showed reactivities more than 2 orders of magnitude higher than parent complex **129**. A number of modifications of the chelating isopropoxybenzylidene ligand (in complexes **130–133** and **135**), addressing

the low initiation rate of **129**, were also reported in that same work (for a detailed discussion on this issue, see section 4.1). Complexes **130–135** showed enhanced catalytic activity, in general requiring lower catalyst loadings than **129**, and in some cases promoting asymmetric reactions that cannot be effected by **129**.<sup>31,116</sup> More recently, complex **136** (Figure 31), the iodide-containing analogue of complex **133**, was also reported.<sup>32</sup> Both **133** and **136** were found to be efficient and highly enantioselective, affording up to 98% enantiomeric excesses in the AROCM of low-strain oxabicyclic olefins, allowing access to a variety of 2,6-disubstituted pyrans.<sup>32</sup> **136** was shown to catalyze these AROCM reactions with significantly higher asymmetric induction than **133**.

The most significant drawback to the synthesis and, therefore, the extensive use of the above binaphthyl-based catalysts is their lengthy, chiral auxiliary directed synthesis. To overcome these difficulties, Hoveyda and co-workers synthesized biphenolate, NHC-coordinated complexes **137** and **138** (Figure 31).<sup>33</sup> The synthetic route to the precursor of the asymmetric carbene contained in **137** and **138** is considerably shorter and, more significantly, does not require the use of optically pure, axially chiral amino alcohols. Although **137** is not stable to chromatography, it can be prepared and in situ catalyze a series of AROCM reactions.<sup>33</sup> On the contrary, iodide-containing **138**, while less active than **137**, can be chromatographically purified and promotes a variety of AROCM reactions, in many cases affording higher enantioselectivities than its binaphthyl-based analogues, **133** and **136**.<sup>33,36,117</sup>

### 3.5. Four- and Six-Membered Ring *N*-Heterocyclic Carbenes

With the purpose of investigating the role of the NHC ring size on the activity of ruthenium-based catalysts, additional structural modifications of the diaminocarbene family led to the synthesis of complexes **139–141** (Figure 32). **139**, coordinated with a six-membered NHC, was synthesized in moderate yield via a four-step synthetic route.<sup>118</sup> Unfortunately, however, **139** displayed lower catalytic activity than its counterparts with five-membered NHCs, most probably due to the increased steric bulk of its six-membered NHC in close proximity to the ruthenium center. This pronounced steric influence, clearly observed in the X-ray structure of **139**, was proposed to disfavor olefin



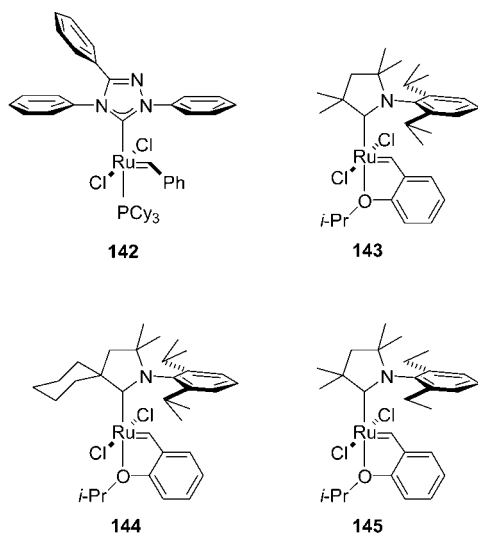
**Figure 32.** Complexes **139–141** bearing four- and six-membered NHC ligands.

binding and/or ruthenacyclobutane formation, resulting in reduced activity. Soon thereafter, complex **140**, featuring a six-membered NHC similar to that in **139** along with a chelating benzylidene ether ligand, was also reported.<sup>119</sup> **140** is highly active in benchmark RCM and ROCM reactions and moderately active in enyne metathesis. The significantly different activity of **139** and **140** is most probably related to the existence of the chelating benzylidene ether ligand in **140**, versus the tricyclohexylphosphine in **139**, rather than to the difference in the backbone structure of the corresponding NHCs.

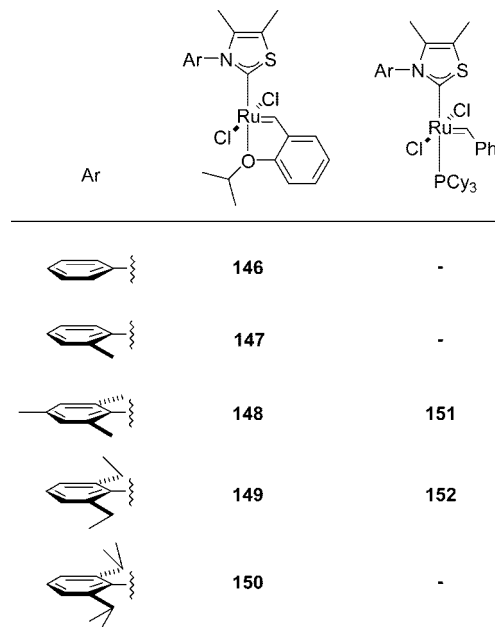
In order to study the impact of employing more strained diaminocarbene frameworks than in the ordinary five-membered NHCs, complex **141** was synthesized.<sup>120</sup> X-ray crystallographic analysis of **141** showed that the geometry around the nitrogen atoms is not strictly planar, indicating a reduced  $p_\pi$  overlap between the carbenic carbon atom and the adjacent nitrogen atoms. Moreover, by measuring the carbonyl stretching frequencies in the corresponding  $\text{Rh}(\text{CO})_2\text{Cl}(\text{NHC})$  complex, it was found that the four-membered NHC ligand in **141** is a slightly less effective  $\sigma$ -donor than its dihydroimidazol-2-ylidene analogue. This difference was attributed to the more bent carbene angle in the former. Complex **141** was shown to catalyze selected RCM, CM, and ROMP transformations, albeit in a slower rate than the parent, phosphine-free second-generation catalyst (**5**).

### 3.6. 1,2,4-Triazol-5-ylidenes, Cyclic (Alkyl)(amino) Carbenes, Thiazol-2-ylidenes, and Other Heterocyclic Carbene Ligands

The first report of the employment of a carbene structure, other than the typical diaminocarbene framework in a ruthenium-based metathesis catalyst, was published in 2001 by Fürstner et al. (complex **142**, Figure 33).<sup>81</sup> Despite the straightforward synthesis of **142**, given that the 1,2,4-triazol-5-ylidene is commercially available, this complex is not an efficient metathesis catalyst, due to its high instability in solution.<sup>53,81</sup> The rapid decomposition of **142** was proposed to originate from the facile dissociation of the triazolylidene from the metal center.<sup>53</sup> Nevertheless, **142** was shown to exert a high initial activity in the formation of tetrasubstituted cycloalkenes,<sup>81</sup> providing one of the first hints regarding the



**Figure 33.** 1,2,4-Triazol-5-ylidene-coordinated complex **142** and cyclic (alkyl)(amino) carbene-coordinated complexes **143–145**.

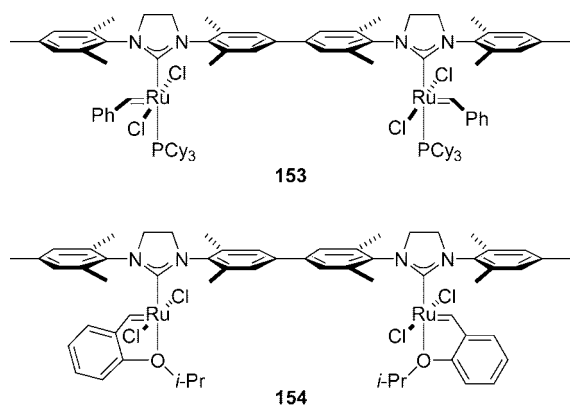


**Figure 34.** Ruthenium-based complexes **146–152** bearing thiazol-2-ylidene ligands.

creation of a “more open” steric environment around the ruthenium center in order to accommodate more sterically demanding substrates; this effect is discussed above for complexes **30–40** (Figures 12 and 13) and complexes **46**, **47**, and **51–53** (Figure 15).

In a more recent work, a series of ruthenium catalysts bearing cyclic (alkyl)(amino) carbenes was synthesized and characterized (**143–145**, Figure 33).<sup>121</sup> Cyclic (alkyl)(amino) carbenes are more  $\sigma$ -electron-donating than their conventional NHC counterparts and, at the same time, introduce a unique  $C_s$ - or  $C_1$ -symmetric steric environment. These unusual steric properties of cyclic (alkyl)(amino) carbenes may have implications for the microscopic reversibility of the olefin binding and cycloreversion steps along the metathesis catalytic cycle. Complexes **143–145** are air- and moisture-stable compounds that can be isolated and purified by column chromatography in low (**145**) to high (**144**) yields. In the solid state, **143–145** position the *N*-aryl rings of their cyclic (alkyl)(amino) carbenes above the benzylidene moiety and the quaternary carbon adjacent to the carbenic center over the empty coordination site. <sup>1</sup>H NMR spectroscopy data suggest that the solid-state conformation of **143–145** is maintained in solution. The catalytic activity of **143–145** was evaluated in RCM,<sup>121</sup> CM, and ethenolysis reactions.<sup>122</sup> The RCM efficiency of **143–145**, in the formation of representative di- and trisubstituted cycloalkenes, was found to be comparable to that of the second-generation complexes **3** and **5** (Figures 7 and 8, respectively).<sup>121</sup> In the CM of allyl benzene with *cis*-1,4-diacetoxy-2-butene, **143–145** exhibit lower *E/Z* ratios relative to most NHC-substituted complexes.<sup>122</sup> Furthermore, in the ethenolysis of methyl oleate, **143–145** afford good selectivity for the formation of terminal olefins versus internal olefins (originating from undesired self-metathesis and secondary metathesis), with complex **145** being the most efficient ethenolysis catalyst examined to date, achieving 35 000 turnover numbers.

Another family of ruthenium-based metathesis catalysts, coordinated with a series of thiazol-2-ylidene ligands (**146–152**, Figure 34), was reported in 2008.<sup>123</sup> The steric



**Figure 35.** Homodinuclear ruthenium catalysts **153** and **154**.

environment of the thiazol-2-ylidenes encompassed in **146–152** is unique, in the sense that they bear only one exocyclic substituent adjacent to the carbenic center. The synthesis of the thiazol-2-ylidene precursors, namely, the corresponding 3-aryl-4,5-dimethylthiazolium chlorides, is a two-step, straightforward procedure, while **146–152**, which are stable to chromatography, can be prepared in one step from commercially available **2** or **4** (Figure 2). In the solid state, the *N*-aryl substituents of the thiazol-2-ylidene ligands are located above the empty coordination site of the ruthenium center. This is a rather interesting find, since all phosphine-free ruthenium complexes bearing unsymmetrical carbenes with only one exocyclic aryl substituent adjacent to the carbenic center, reported thus far, are isolated with this aryl group located directly above the benzylidene proton.

Despite the decreased steric protection of their ligands, complexes **146–152** were demonstrated to efficiently promote a series of benchmark RCM, macrocyclic RCM, ROMP, and CM reactions, showing stability and activity comparable to the conventional NHC-containing ruthenium catalysts.<sup>123</sup> The phosphine-free catalysts of this family were found to be more stable than their phosphine-containing counterparts. Upon removing the steric bulk from the *ortho*-positions of the *N*-aryl group of the thiazol-2-ylidenes, the phosphine-free catalysts lose stability, but when the substituents become too bulky, the resulting catalysts show prolonged induction periods. Among the five thiazol-2-ylidene ligands examined, 3-(2,4,6-trimethylphenyl)- and 3-(2,6-diethylphenyl)-4,5-dimethylthiazol-2-ylidene afforded the most efficient and stable catalysts (**148** and **149**). Unlike all previously evaluated catalysts, the steric bulk of these thiazol-2-ylidene-containing complexes is correlated to the observed *E/Z* ratio of the cross-product in the cross-metathesis reaction of allyl benzene with *cis*-1,4-diacetoxy-2-butene. Thus, decreasing the steric demand of the *ortho* substituents on the *N*-aryl groups from *i*-Pr to H results in an increased kinetic *E*-selectivity from  $\sim 4$  to  $\sim 6.5$ . In addition, in the macrocyclic ring-closing of a 14-membered lactone, the *E/Z* profile of catalysts **146–152** is completely different than that of H<sub>2</sub>IMes catalysts **3** and **5** (Figures 7 and 8, respectively) and more similar to the stereoselectivity displayed by the first-generation catalyst **2** (Figure 2).

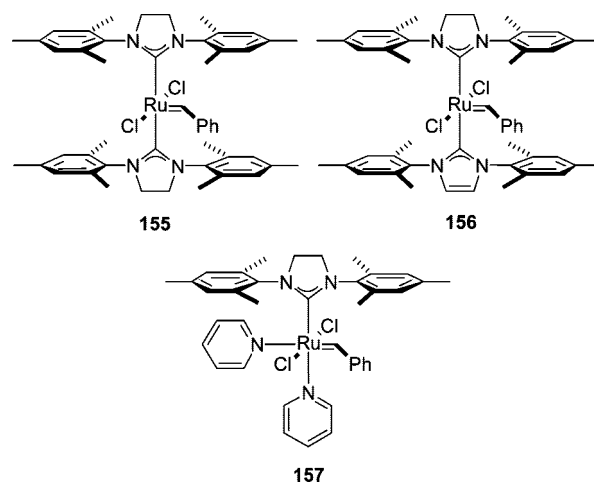
Homodinuclear ruthenium complexes **153** and **154** (Figure 35) were designed as “double-centered” metathesis catalysts that should, upon reaction with the appropriate  $\alpha,\omega$ -dienes, promote cyclodimerization rather than cyclization or oligomerization.<sup>124</sup> Indeed, although **153** is unstable and decomposes after some hours in solution, phosphine-free **154** was shown to competently promote dimer ring-closing metathesis

of dienes with the appropriate length, at the suitable effective molarity. A trapping experiment suggested that both ruthenium centers in homobimetallic **154** are simultaneously metathetically active.

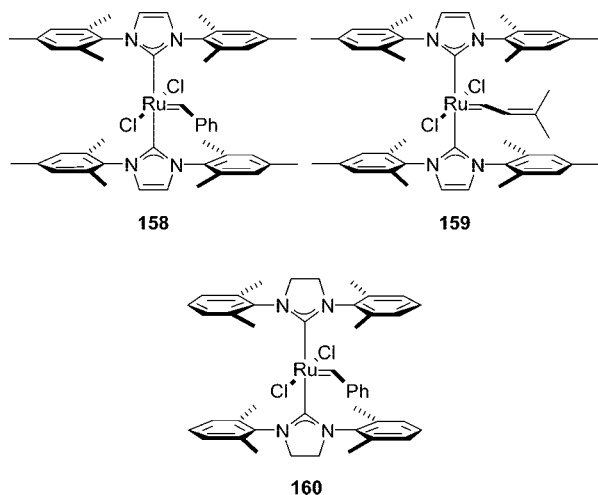
### 3.7. Carbene Biscoordination

Ruthenium-based complexes bearing two heterocyclic carbene ligands are prepared in one or two steps via the substitution of two or more labile ligands by the corresponding carbenes. The ease of this carbene biscoordination has been suggested to depend both on the steric and the electronic properties of the utilized carbene(s).<sup>53,123</sup> Moreover, according to the established mechanistic model, one of the carbenes has to dissociate from the metal center for a biscarbene ruthenium complex to initiate.<sup>24–26,71,79</sup> In this regard, although it is generally accepted that carbene ligands bind strongly to the metal centers,<sup>49,51</sup> carbene dissociation/transfer have been repeatedly proven feasible.<sup>53,100,105,125,126</sup>

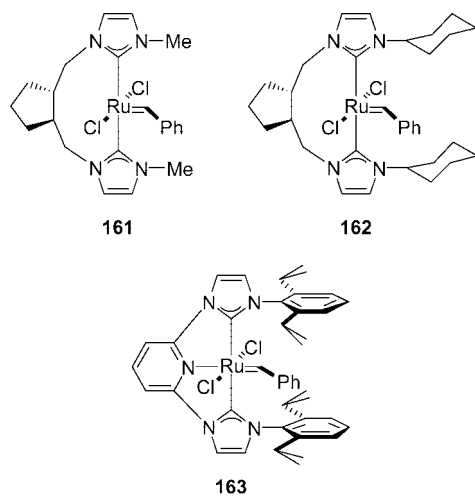
As mentioned earlier, the first heterocyclic carbene biscoordinated ruthenium complexes were reported in 1998 (**9–13**, Figure 5).<sup>58</sup> These complexes were applied in the ROMP of functionalized norbornenes,<sup>127</sup> as well as in benchmark RCM reactions,<sup>128</sup> albeit displaying slow initiation rates due to the relatively low lability of the corresponding NHCs. Later on, carbene biscoordinated ruthenium complexes **155** and **156** (Figure 36) were also prepared.<sup>53</sup> The complexes **155** and **156** could not be obtained directly from first-generation catalyst **2** (Figure 2), even when a large excess of the NHC was used. This was attributed to the significant decrease of the phosphine exchange rate when one of the tricyclohexylphosphine ligands was replaced by a NHC.<sup>53</sup> Nevertheless, bis-substitution was achieved using complex **157** (Figure 36) bearing two labile pyridine ligands (see section 4.3).<sup>129</sup> Both **155** and **156** are highly stable and can be purified by column chromatography on silica gel.<sup>53</sup> In the solid state, both of the Ru–NHC distances in **156** are longer than those in either of the corresponding monocarbene complexes (complexes **14** and **3** in Figures 6 and 7, respectively), which was suggested to originate from the greater steric congestion in **156** and possibly also from a more electron-rich ruthenium center. **155** shows low RCM and ROMP activities below 40 °C, but this picture significantly improves at 80 °C. Therefore, elevated temperatures are required for an efficient initiation of **155** to occur. When **155** is heated in the presence of PCy<sub>3</sub> or the first-generation



**Figure 36.** Carbene biscoordinated ruthenium complexes **155** and **156** and bis(pyridine) complex **157**.



**Figure 37.** Heterocyclic carbene biscoordinated complexes **158–160**.

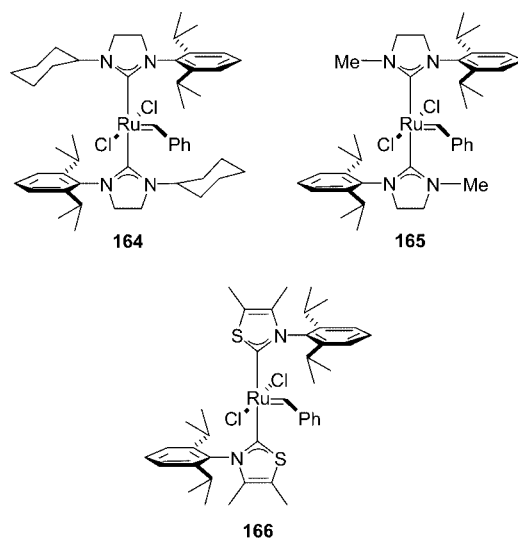


**Figure 38.** Complexes **161–163** coordinated with chelating NHC ligands.

catalyst **2** (Figure 2), the heteroleptic, second-generation catalyst **3** (Figure 7) is formed, confirming NHC dissociation. It should also be noted that a bimolecular NHC transfer mechanism has been similarly proposed by Herrmann and co-workers for the formation of complex **16** (Figure 6).<sup>63</sup>

Arylphosphines are generally weaker donor ligands and bind more weakly to the metal centers than their alkylphosphine analogues (for a related discussion, refer to section 6). On this basis, complexes **158–160** (Figure 37) were prepared in one step by simply reacting their corresponding bis(triphenylphosphine) precursors with the appropriate NHC ligand.<sup>126,130</sup> **158** was isolated as a crystalline, air-stable solid and was fully characterized, whereas the isolation of **159** was proven impossible and was only observed in situ, because of its high solubility.<sup>130</sup> The metathetical catalytic activities of **158** and **159** have not been evaluated. Moreover, **160** shows a rather low RCM activity at 40 °C, ascribed to its slow initiation, but at 80 °C it efficiently ring-closes diethyl diallylmalonate and diallyl malononitrile.

Carbene biscoordinated complexes **161–163** (Figure 38) have been also prepared.<sup>131,132</sup> **161** and **162**, bearing two 9-membered chiral bidentate NHCs, were isolated as air-stable solids, but their metathesis activity has not yet been evaluated.<sup>131</sup> On the other hand, the catalytic activity of “pincer” pyridine–dicarbene complex **163** was examined in benchmark RCM and ROMP reactions.<sup>132</sup> Both the first- and



**Figure 39.** Heterocyclic carbene biscoordinated complexes **164–166**.

the second-generation phosphine-containing catalysts (complexes **2** and **3**, respectively, Figure 2) outperformed **163**, as the same metathesis transformations required higher catalyst loadings and longer reaction time with **163**.

More recently, the synthesis of complexes **164** and **165** (Figure 39) was accomplished by substituting both tricyclohexylphosphine ligands in the first-generation catalyst **2** (Figure 2) in one step.<sup>105</sup> The exclusive formation of the NHC biscoordinated complexes **164** and **165**, when even an equimolar amount of the corresponding heterocyclic carbene was utilized, was assigned to a higher phosphine exchange rate in the heteroleptic (phosphine–NHC) intermediate complex compared to its precursor **2**. Interestingly, it was also found that both NHCs on biscoordinated complexes **164** and **165** can be exchanged with an excess of tricyclohexylphosphine, affording the initial bis(phosphine) complex (**2**). **164** and **165** were found to be catalytically active in the ROMP of 1,5-cyclooctadiene at elevated temperatures, and initiation was proposed to occur via NHC dissociation.

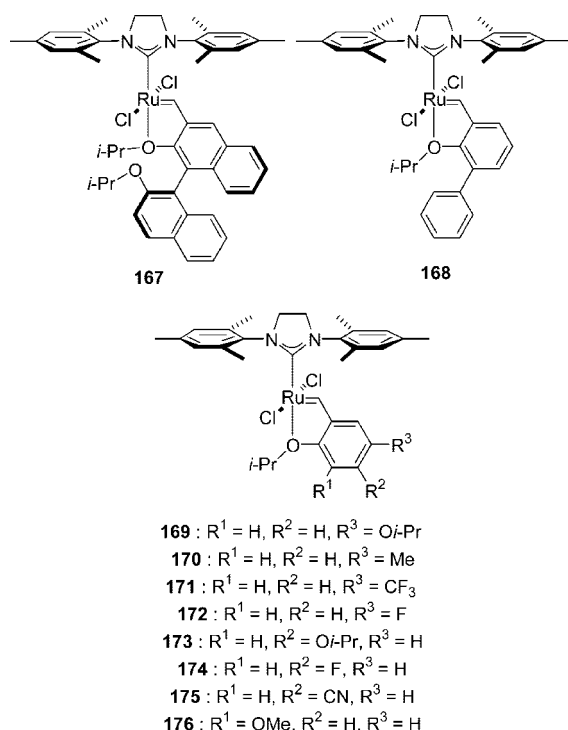
An analogous situation was observed during a series of attempts to isolate the tricyclohexylphosphine-containing ruthenium complex bearing a 3-(2,6-diisopropylphenyl)-4,5-dimethylthiazol-2-ylidene, when only the formation of the carbene biscoordinated complex **166** (Figure 39) was observed by <sup>1</sup>H NMR and high-resolution mass spectroscopy.<sup>123</sup> In that case, it was proposed that the coordination of the first bulky thiazol-2-ylidene ligand at the ruthenium center, followed by the dissociation of the remaining tricyclohexylphosphine and coordination of a second thiazol-2-ylidene, is highly energetically favorable due to the formation of an “empty pocket” in the coordination sphere of the intermediate complex. This empty pocket was suggested to better accommodate the second unsymmetrical carbene ligand compared to the C<sub>3</sub>-symmetric tricyclohexylphosphine. Complex **166** is not stable enough to be purified by column chromatography.

## 4. Phosphine-free Heterocyclic Carbene-Coordinated Ruthenium Catalysts

### 4.1. Chelating Alkoxybenzylidene Ligands

As mentioned in section 3.1, the synthesis of the first isopropoxystyrene-containing heterocyclic carbene-coordinated catalyst (**5**, Figure 8) was independently and almost



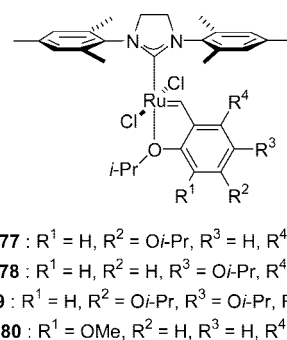


**Figure 40.** Ruthenium-based complexes **167**–**176** bearing chelating isopropoxybenzylidene ligands.

simultaneously published by the Hoveyda and the Blechert groups in 2000.<sup>26,27</sup> Compared to its phosphine-containing counterpart (**3**, Figure 7), catalyst **5** displays enhanced oxygen- and moisture-tolerance; however, its decreased initiation rate presents a major disadvantage. To increase initiation rate, either the bulk around the ether moiety is increased or a *para*-electron-withdrawing substituent that decreases the basicity of the ether group is introduced. In all these cases, the catalyst activity is controlled by initiation. After the first turnover, the properties of the catalytically active species are the same for all. The modifications of the chelating benzylidene ether moiety's sterics and electronics that have been attempted thus far are comprehensively discussed below.

The first and rather adventitious advancement in this direction came from the group of Blechert in 2002.<sup>133</sup> Highly active and air-stable **167** (Figure 40), bearing a binol-based ruthenium alkylidene, was prepared as a potent ARCM catalyst. Despite the absence of asymmetric induction in ARCM, **167** showed a large improvement in catalytic activity. This high reactivity was suggested to originate from an improved leaving group ability of the binol-substituted isopropoxystyrene, because of its increased steric bulk in comparison with the isopropoxystyrene in the parent complex (**5**, Figure 8). Soon thereafter, the synthesis of catalyst **168**, showing a markedly greater catalytic efficiency than either **5** or **167**, and without any loss of stability in air, was published.<sup>89</sup> Again, the enhanced reactivity of **168** was attributed to the faster dissociation of the phenyl-substituted isopropoxystyrene ligand, owing to a weakening of the chelation bond as a result of steric crowding. This assumption was later confirmed via a series of ligand-exchange experiments.<sup>134</sup> A more efficient and practical synthetic route to **168** was also reported in the same work.

In order to obtain more detailed information regarding the effect of the steric and the electronic environment of the chelating isopropoxybenzylidene ligands on the rate of

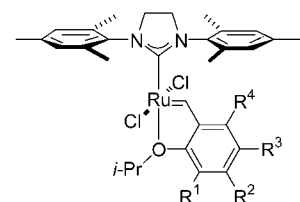
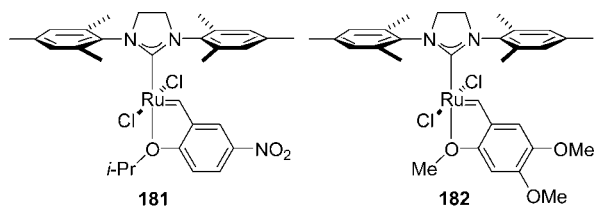


**Figure 41.** Ruthenium complexes **177**–**180** coordinated with chelating isopropoxybenzylidene ligands.

metathesis, Blechert and co-workers prepared complexes **169**–**176** (Figure 40).<sup>135</sup> By comparing the RCM activity of **5** and **168**–**176**, and by taking into account the  $\sigma_m^+$  and  $\sigma_p^+$  values of the corresponding substituents, they concluded that an increase in the electrophilicity of either substituent (R<sup>1</sup> through R<sup>3</sup>), namely, decreasing the electron density at both the Ru=C and the Ru–O bonds, leads to a faster initiation rate, with the electronic character of the Ru=C bond being the dominant factor. As expected, increased steric hindrance *ortho* to the isopropoxy group was also found to enhance initiation rates. In another publication, addressing the lower catalyst loading limit that can effect a RCM transformation, complexes **177**–**180** (Figure 41) were reported.<sup>136</sup> **177**–**179** were found to deliver similar turnover numbers to each other, whereas the sterically modified **180** delivered lower turnover numbers, perhaps due to its faster initiation rate, which was proposed to result in faster decomposition.

A variety of electronically and sterically modified catalysts, bearing chelating alkoxybenzylidene ligands, have been also synthesized by Grela and co-workers. Thus, **181** (Figure 42) was found to be significantly more reactive than its parent complex (**5**, Figure 8), without being less air- or moisture-stable.<sup>137</sup> The drastically increased reactivity of **181** was rationalized in terms of a reduced chelating ability of the isopropoxy fragment, due to a decrease in the electron density of the corresponding oxygen atom. Moreover, complex **182** (Figure 42), encompassing an inexpensive and easily accessible chelating methoxystyrene fragment, was synthesized as a cheap alternative of the parent catalyst (**5**, Figure 8).<sup>138</sup> **182** was successfully tested in RCM, CM, and enyne metathesis reactions, showing slightly improved reactivities in comparison with **5**. A more detailed study regarding the activity of catalysts bearing nitro-substituted chelating alkoxybenzylidenes (**181** and **183**–**187**, Figure 42) in RCM, CM, and enyne metathesis reactions was subsequently published.<sup>139</sup> It was found that catalysts coordinated with *meta*- and *para*-nitro-substituted isopropoxybenzylidenes (**181** and **183**) are significantly more active than the parent catalyst **5**, although not as reactive as **168** (Figure 40). On the other hand, attempts to combine electronic and steric activation in the same isopropoxybenzylidene induced a drastic decrease in the stability of the resulting complexes (**184**–**186**); furthermore, **187** proved to be a less efficient catalyst than its isopropyl counterpart (**181**). Subsequently, an improved synthetic route to various 3- and 5-substituted alkoxybenzylidenes, and a practical, large-scale preparation of the corresponding NHC-coordinated alkoxybenzylidene complexes, was also published.<sup>140,141</sup>

Further research led to the synthesis of phosphine-free complexes **188** and **189** (Figure 43), the initiation efficiency

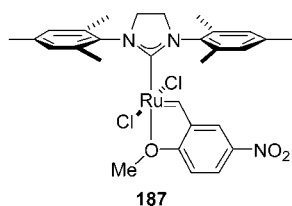


183 : R<sup>1</sup> = H, R<sup>2</sup> = NO<sub>2</sub>, R<sup>3</sup> = H, R<sup>4</sup> = H

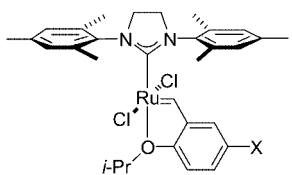
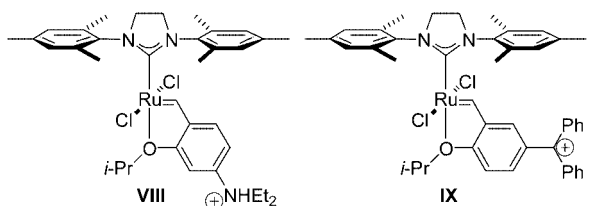
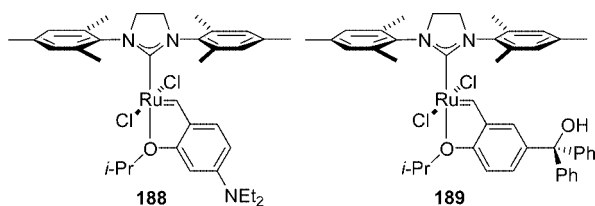
184 : R<sup>1</sup> = NO<sub>2</sub>, R<sup>2</sup> = H, R<sup>3</sup> = H, R<sup>4</sup> = H

185 : R<sup>1</sup> = Ph, R<sup>2</sup> = H, R<sup>3</sup> = NO<sub>2</sub>, R<sup>4</sup> = H

186 : R<sup>1</sup> = OMe, R<sup>2</sup> = H, R<sup>3</sup> = NO<sub>2</sub>, R<sup>4</sup> = H



**Figure 42.** Ruthenium-based complexes **181–187** bearing chelating alkoxybenzylidene ligands.



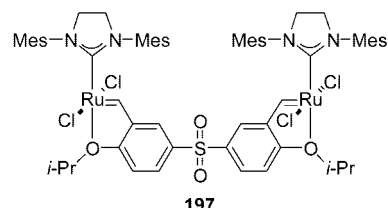
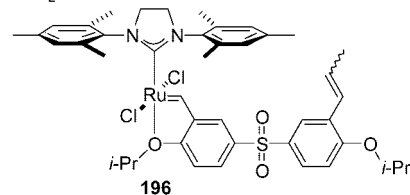
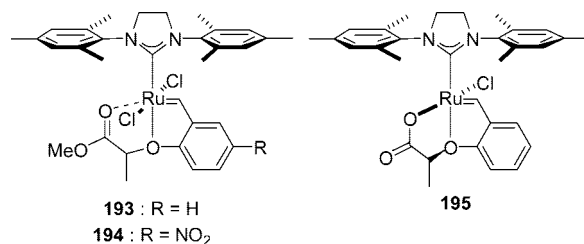
190 : X = Cl

191 : X = Br

192 : X = SO<sub>2</sub>C<sub>4</sub>F<sub>9</sub>

**Figure 43.** Ruthenium complexes **188–192** coordinated with chelating isopropoxybenzylidene ligands.

of which can be controlled on demand.<sup>142</sup> Thus, in the absence of acid, **188** shows no activity in the RCM of diethyl allylmethylmalonate, whereas its in situ formed salts (**VIII**) via the addition of 1 equiv of organic acids are highly active, in one case outperforming even the parent complex **5** (Figure

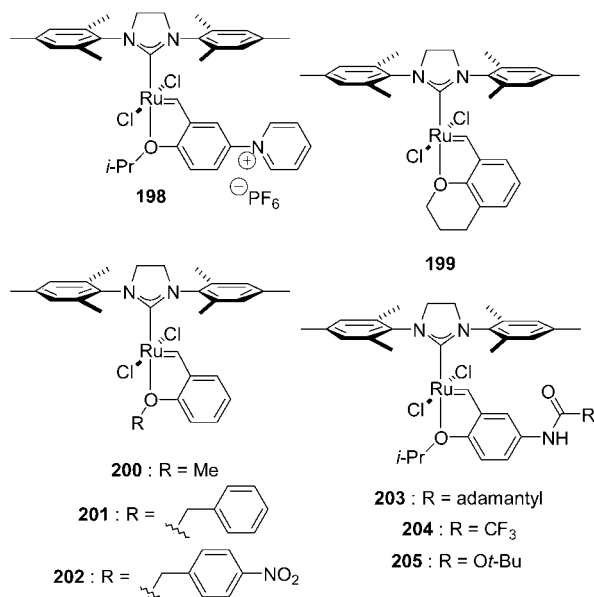


**Figure 44.** Complexes **193–197** bearing chelating alkoxybenzylidene ligands.

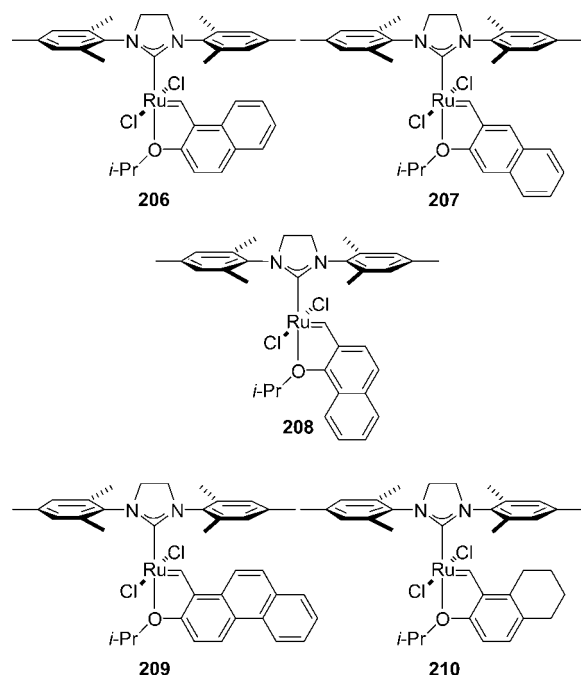
8). Similarly, the reactivity of **189** can be dramatically enhanced using Ph<sub>2</sub>SnCl<sub>2</sub>, due to the formation of carbocation **IX** (Figure 43). Complexes **190–192** have been also prepared.<sup>139,143</sup> **190** and **191** are slightly less efficient than the parent catalyst **5**, while the metathetical catalytic behavior of **192** has not been reported.

In complexes **193–195** (Figure 44), the aliphatic end group of the styrenyl ether has been functionalized by the attachment of an ester or an acid moiety.<sup>144,145</sup> “Scorpio catalysts” **193** and **194** were shown to be highly efficient in model RCM and CM reactions, sometimes outperforming even the very active **168** (Figure 40).<sup>144</sup> Interestingly, **194**, which combines a coordinating ester function with an electron-withdrawing NO<sub>2</sub> group, requires 10 times lower catalyst loadings than the parent NO<sub>2</sub>-bearing complex **181** (Figure 42) in order to afford the same result under identical conditions in a model CM reaction. Moreover, during an attempt to prepare the free carboxylic acid analogue of **193**, ruthenium carboxylate **195** was isolated in 84% yield.<sup>145</sup> Although catalytically dormant, **195** can be chemically (via the addition of 1 equiv of acid) and thermally activated in situ, promoting a series of RCM and CM reactions. **196** and **197** (Figure 44) were also synthesized and evaluated in benchmark RCM reactions, mainly because their isopropoxybenzylidene moiety can be simply prepared in three steps from inexpensive starting materials.<sup>146</sup> Both **196** and its dimeric analogue **197** show catalytic activity higher than that of the parent complex **5**.

Additional studies led to the synthesis of complexes **198–205** (Figure 45). **198** was prepared with the purpose of carrying out metathesis reactions both in organic and aqueous solvents, as well as in ionic media (for a survey on water-soluble and ionic liquid tagged catalysts, see sections 9 and 10, respectively).<sup>147</sup> However, although highly active in model RCM reactions, the recyclability levels of **198** in ionic solvents were very low. Complexes **199**, **201**, and **202** were also shown to be significantly more active than the



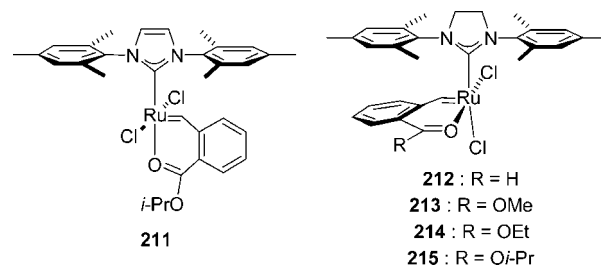
**Figure 45.** Ruthenium-based complexes **198–205** coordinated with chelating alkoxybenzylidene ligands.



**Figure 46.** Ruthenium complexes **206–210** coordinated with chelating isopropoxyarylidene ligands.

parent complex **5** (Figure 8);<sup>148</sup> nevertheless, **201** and **202** are also less thermally- and air-stable and, therefore, less efficient than both **199** and **5**. Finally, phosphine-free catalysts **203–205** were targeted in view of the tunable steric and electronic properties of their aminocarbonyl group (amide or carbamate).<sup>149</sup> **203–205** initiate faster than **5**, while **204** is the best-performing and **203** is the worst-performing catalyst in the series. These differences in the initiation rates were rationalized on the basis of the switchable electronic properties of the aminocarbonyl function.

In 2008, Barbasiewicz et al. reported the preparation of complexes **206–210** (Figure 46), bearing five different isopropoxyarylidene chelates.<sup>150</sup> **207**, which was found to be the most efficient RCM catalyst in the series, showed metathesis activity similar to **5** (Figure 8). On the contrary, systems **206** and **208** were found to be latent, initiating only



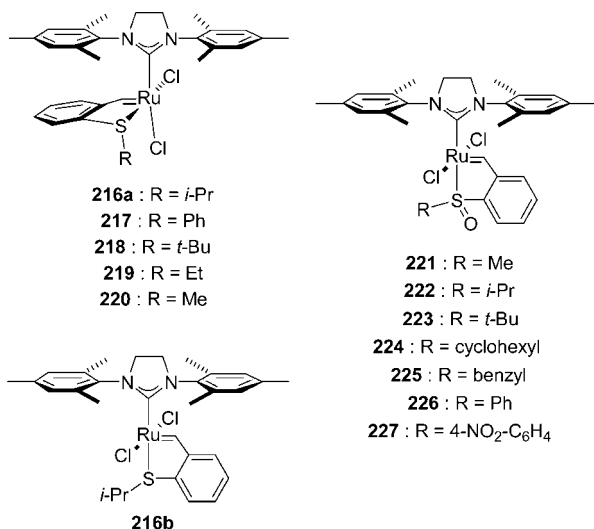
**Figure 47.** Complexes **211–215** coordinated with chelating benzylidene ligands.

at temperatures above 110 °C. These pronounced differences in the catalytic activity of **206–210**, also taking into consideration a series of structural and spectroscopic studies, were attributed to the partially aromatic character of the ruthenafurane ring, present in all ruthenium alkoxybenzylidenes, which inhibits initiation and thereby decreases the catalytic activity of the complexes.

An analogous class of NHC-coordinated complexes bearing carbonyl- or carboxyl-substituted chelating benzylidene ligands (**211–215**) is presented in Figure 47. **211** is significantly less metathesis active than both first-generation catalyst **2** (Figure 2) and its heteroleptic (phosphine-NHC) analogues **14a** and **14b** (Figure 6).<sup>151</sup> On the contrary, complexes **212–215**, which have an unusual *cis*-dichloro arrangement, most commonly observed in complexes bearing strong chelating ligands such as pyridyl or quinoline (vide infra), were found to be thermally switchable in the ROMP of functionalized norbornenes.<sup>152</sup> For example, aldehyde derivative **212**, which showed the lowest initiation efficiency in this study, is barely active at room temperature but is an efficient polymerization catalyst at temperatures higher than 45 °C. In the ester series (**213–215**), initiation efficiencies were found to increase with the decreasing steric bulk of the alkoxy substituent (R). It should be noted that the development of thermally switchable, chemically switchable, or photoswitchable catalysts is highly important in polymer chemistry, as quite often the mixing of the monomer with the catalyst and the polymerization reaction have to be carried out at different times (and/or reactors) and, therefore, accurately controlled. This is vital in processes such as spraying or inkjet printing, where a constant and low viscosity is required, or when the monomer/catalyst mixture has to be shaped and profiled prior to polymerization (“curing”).

## 4.2. Chelating Thioether and Chelating Sulfoxide Benzylidene Ligands

In 2008, Lemcoff and co-workers published the synthesis of ruthenium-based complexes **216a** and **217–220** (Figure 48) bearing a series of chelating thioether benzylidene ligands.<sup>153,154</sup> As demonstrated by NMR experiments and single-crystal X-ray analysis data, these complexes display a *cis*-dichloro arrangement similar to that of **212–215** (Figure 47). **216a** and **217–220** are highly stable toward oxygen and moisture and, equally importantly, thermally switchable. For example, catalyst **216a** could be repeatedly switched on and off in the RCM of diethyl diallylmalonate by heating to 80 °C and cooling to 25 °C, respectively.<sup>153</sup> It was also found that the initiation efficiency of **216a** and **217–220** systematically depends on the steric bulk of substituent R, with **218** being the most reactive catalyst in the series.

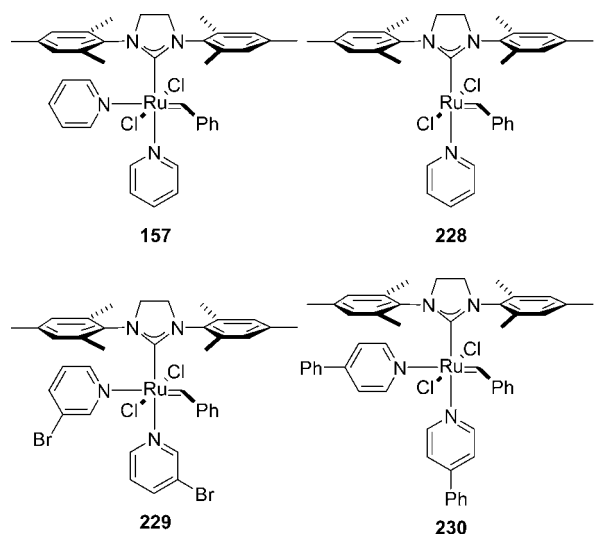


**Figure 48.** Complexes **216**–**227** coordinated with chelating thioether and chelating sulfoxide benzylidene ligands.

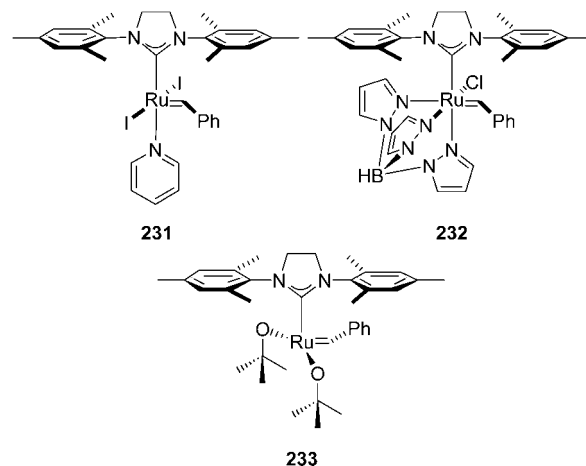
More recently, Grela and co-workers reported the synthesis and catalytic activity evaluation of complexes **221**–**227** and **216b**, an isomer of **216a** having the usual *trans*-dichloro arrangement (Figure 48).<sup>155</sup> **221**–**227**, which are coordinated with chelating sulfoxide benzylidene ligands, were proven to be metathetically inactive at room temperature but showed good diene and enyne RCM catalytic activity at elevated temperatures. **227** was found to be the most efficient metathesis catalyst in this study, combining thermal and air stability with good catalytic activity.

### 4.3. Mono- and Bis(pyridine)-Coordinated Catalysts

Further modifications of the ligand environment in heterocyclic carbene-coordinated ruthenium complexes led to the synthesis of catalysts **157** and **228**–**230** (Figure 49), bearing one or two pyridine ligands. As mentioned earlier, because of the lability of these pyridine ligands, mono- and bis(pyridine)-coordinated complexes can be used as versatile starting materials for the synthesis of other NHC-coordinated ruthenium complexes.<sup>53,129,156</sup> Complexes **157**, **229**, and **230** can be easily prepared and purified on a multigram scale,



**Figure 49.** Bis(pyridine)-coordinated H<sub>2</sub>IMes complexes **157** and **228**–**230**.



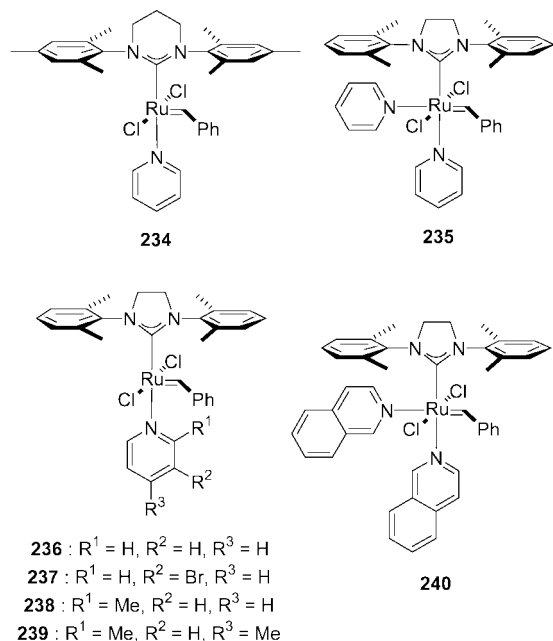
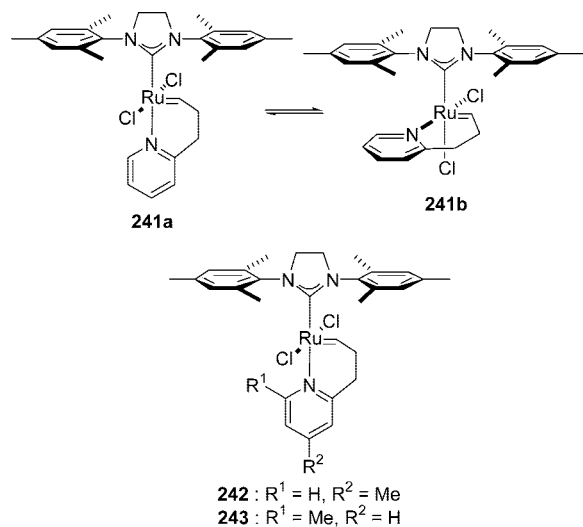
**Figure 50.** Ruthenium-based NHC-coordinated complexes **231**–**233**.

requiring little or no solvent, by simply adding an excess of the appropriate pyridine to **3** (Figure 7).<sup>129,157</sup> As shown in Figure 49, pyridine ligands bind in a *cis* geometry, occupying the coordination sites *trans* to the benzylidene and the NHC ligands. In the solid-state structure of **157**, the Ru–N bond of the pyridine located *trans* to the benzylidene is more than 0.15 Å longer than the Ru–N bond of the pyridine positioned *trans* to the NHC, indicating that the benzylidene exerts a significantly larger *trans* influence than the NHC.<sup>129</sup> Besides being the precursor of bis(NHC)-coordinated complexes **155** and **156** (Figure 36),<sup>53</sup> **157** reacts instantaneously with PCy<sub>3</sub> to regenerate the parent complex **3**, with NaI to afford mono(pyridine) complex **231**, with potassium tris(pyrazolyl)borate to give **232**, or with potassium *t*-butoxide to afford complex **233** (Figure 50).<sup>129</sup> Mono(pyridine) complex **228** can be prepared from **157** upon loss of one pyridine ligand under vacuum.

Probably even more importantly, bis(pyridine) ruthenium benzylidenes were proven to be efficient in the challenging CM of acrylonitrile, and they are among the fastest-initiating ruthenium systems studied thus far.<sup>157</sup> Specifically, the initiation rate in the irreversible reaction of complex **229** with ethyl vinyl ether is at least 6 orders of magnitude higher than the corresponding initiation rate of second-generation catalyst **3**. This very fast initiation of catalyst **229** has proven to be extremely useful in the production of polymers with very narrow polydispersity and for the synthesis of block copolymers.<sup>158</sup>

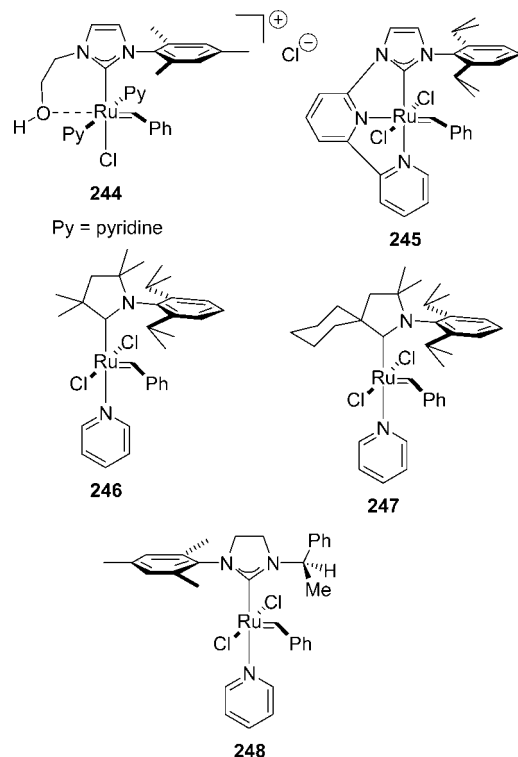
The procedure for the preparation of complexes **234**–**240** (Figure 51) is analogous to that of **157** and **229**.<sup>86,159</sup> The isolation of mono(pyridine)-coordinated **234**, instead of the expected bis(pyridine) complex, was rationalized on the basis of the increased steric bulk and donor ability of the ancillary six-membered NHC ligand, compared to the five-membered NHC in **157** (Figure 49).<sup>159</sup> **234** was used in the ROMP of two enantiomerically pure norbornene derivatives. Bis(pyridine)-coordinated **235** was shown to be highly efficient in the CM of acrylonitrile with various functionalized alkenes.<sup>86a,b</sup> The activity of **235** decreases in coordinating solvents, whereas utilization of Lewis acids, which prevent the coordination of the cyano functionality with the ruthenium center, improves both the reaction rate and the yield of the CM reactions. In another more detailed study, mono(pyridine) complexes **236**–**239** were prepared from the corresponding triphenylphosphine-containing NHC-coordinated **26** (Figure 10).<sup>86c</sup> Complex **236** can also be prepared from



Figure 51. NHC-coordinated ruthenium complexes **234**–**240**.Scheme 6. Latent Ruthenium-Based Metathesis Catalysts **241**–**243**

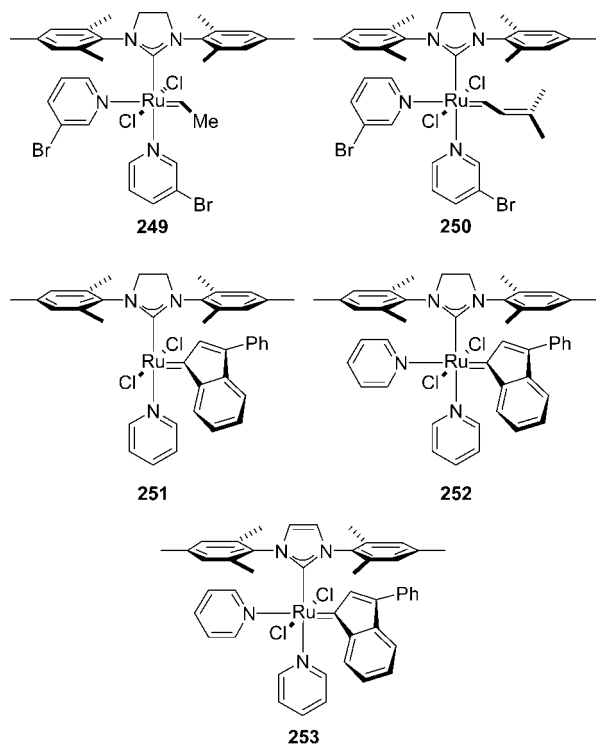
bis(pyridine)-coordinated **235** under vacuum, and conversely, **236** can be transformed into **235** in the presence of an excess of pyridine. The metathetic catalytic activity of complexes **235** and **236** was shown to be quite similar, while **238** was the most catalytically active complex studied, namely, among complexes **235**–**240**, in the RCM of diallyl malononitrile and the CM of acrylonitrile with terminal olefins.

On a different note, pyridine-containing tethered catalysts **241**–**243** (Scheme 6) initiate slowly, but since the same propagating species is provided after one turnover, they maintain the high activity of parent catalyst **3** (Figure 7).<sup>160</sup> As mentioned earlier, metathesis catalysts exerting attenuated initiation rates are very important in a number of ROMP applications, because they allow for longer fabrication times of the monomer/catalyst mixture and, therefore, for a more uniform polymeric material to be synthesized.<sup>161</sup> Complexes **241a** and **241b**, of  $C_s$  and  $C_1$  symmetry, respectively, are isomers in equilibrium, with **241b** being the thermodynamically favored species. Also, **241a** and **241b** are both latent initiators relative to complexes **3**, **5** (Figures 7 and 8,

Figure 52. Pyridine-containing ruthenium-based complexes **244**–**248**.

respectively), and **157** (Figure 49), with **241b** initiating much slower than **241a** in RCM and ROMP transformations. The difference in initiation rate between **241a** and **241b** was attributed to the fact that the tethered pyridine ligand in **241a** is *trans* to the strongly  $\sigma$ -donating NHC ligand and, as a result, dissociates to give the active 14-electron species much more quickly than that in **241b**. Substitution on the pyridine ring was found to have a much less significant effect on catalytic activity, and **243** was found to be a faster initiator than **241** and **242**, presumably due to the steric crowding of the *o*-methyl group on the tethered pyridine.

A series of other heterocyclic carbene-coordinated ruthenium complexes bearing pyridine or pyridine-based ligands are presented in Figure 52. Cationic complex **244** was isolated in an attempt to enforce intramolecular displacement of one of the chloride atoms, by the hydroxyl group in the side chain, to form a chelate structure.<sup>102</sup> **244** is metathesis inactive in standard RCM reactions, supposedly due to the pyridine ligands that are tightly bound to the cationic metal center and cannot be released even upon addition of *p*-toluenesulfonic acid. On the other hand, the tridentate carbene in **245** was designed as a more labile and less rigid alternative of the pincer NHC ligand in **163** (Figure 38) and was anticipated to lead to an improved metathesis catalyst compared to **163**.<sup>132</sup> Nevertheless, **245** was isolated in a very low yield, preventing evaluation of its catalytic activity. Pyridine adducts **246** and **247** (Figure 52) were also isolated, during attempts to prepare the corresponding (not observed) tricyclohexylphosphine complexes.<sup>121</sup> Complexes **246** and **247**, coordinated with cyclic (alkyl)(amino)carbenes, showed relatively low RCM efficiency, which was suggested to result from increased catalyst decomposition. Finally, **248** was targeted as a catalyst with improved initiation efficiency compared to its tricyclohexylphosphine-containing counterpart **125** (Figure 29).<sup>114</sup> Indeed, **248** was shown to be an efficient ROMP initiator in sequence-selective copolymeriza-

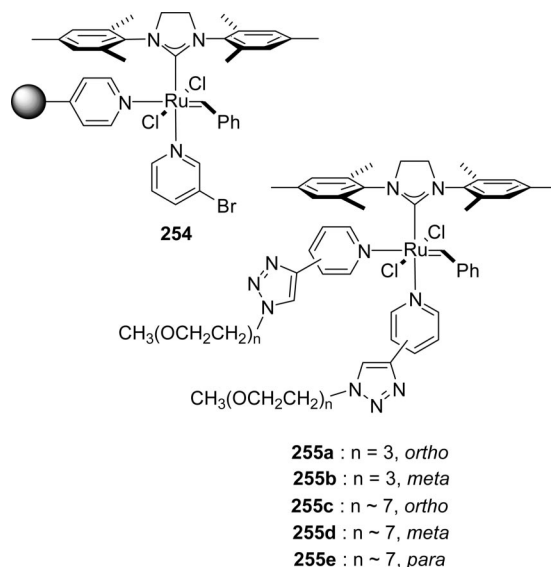


**Figure 53.** Pyridine-containing ruthenium complexes **249**–**253**.

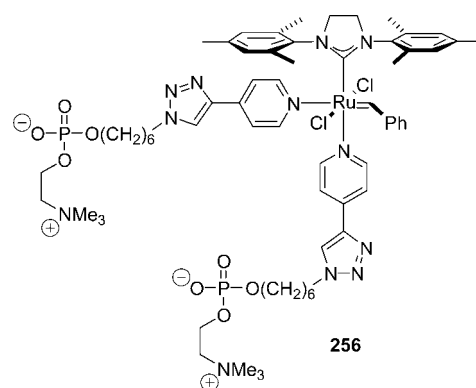
tions. This alternating ROMP selectivity by **248** was attributed to the steric interaction of the 2-phenethyl substituent of the NHC with the growing polymer chain.

The concept of using labile pyridine ligands to prepare faster-initiating and highly active ruthenium metathesis catalysts that do not suffer from incomplete initiation has been also employed in complexes **249**–**253** (Figure 53), which bear alkylidene ligands other than benzylidene (note that section 5 is dedicated to the systematic variation of the alkylidene ligand in heterocyclic carbene-coordinated catalysts). Thus, Wagener and co-workers developed catalysts **249** and **250**, bearing a ruthenium ethylidene and a ruthenium dimethylvinylidene, respectively, and successfully used them in ADMET and ROMP transformations.<sup>162,163</sup> In other work, **251** was prepared by treatment of the corresponding tricyclohexylphosphine-coordinated indenylidene complex with an excess of pyridine.<sup>164</sup> Displacing the phosphine ligand by pyridine in the indenylidene precursor of **251** is significantly slower than the same substitution reaction in benzylidene-bearing complex **3** (Figure 7). This was attributed to the stronger electron-donating ability and, therefore, *trans* influence, as well as to the increased steric bulk of the indenylidene, as compared to the benzylidene ligand. Nevertheless, **251** is also more thermally stable and, furthermore, more active in both RCM and ROMP compared to its benzylidene counterpart **228** (Figure 49).<sup>164,165</sup> Quite similarly, both pyridine-coordinated ruthenium indenylidenes **252** and **253** were shown to be highly active in the ROMP of 1,5-cyclooctadiene.<sup>166</sup>

Finally, polyvinyl-, poly(ethylene glycol)-, and phosphocholine-substituted pyridine ligands, in complexes **254**, **255**, and **256**, respectively (Figures 54 and 55), have been successfully utilized to prepare immobilized (**254**)<sup>167</sup> (see section 10) or water-soluble metathesis catalysts (**255** and **256**)<sup>168</sup> (see section 9).



**Figure 54.** Pyridine-coordinated  $H_2IMes$  ruthenium complexes **254** and **255**.

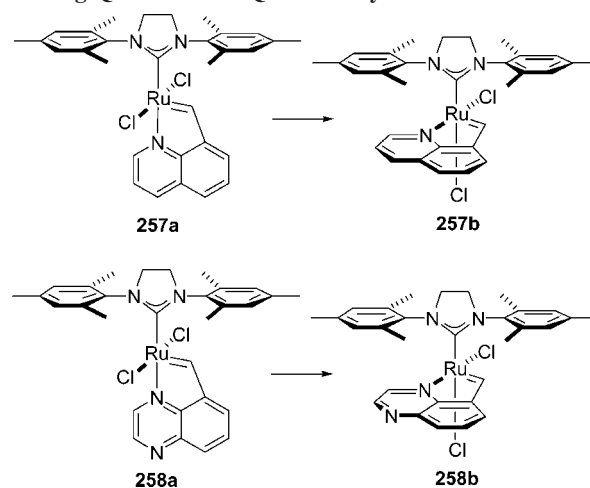


**Figure 55.** Water-soluble, pyridine-coordinated complex **256**.

#### 4.4. Chelating Quinolin- and Quinoxalin-ylidenes

Quinoline- and quinoxaline-containing tethered complexes **257** and **258** (Scheme 7), bearing five-membered chelate rings, have also been prepared.<sup>169</sup> Similarly to their pyridine-containing counterparts **241**–**243** (Scheme 6),<sup>160</sup> these complexes are initially isolated in the *trans*-dichloro geometry (**257a** and **258a**); nevertheless, upon prolonged storage in solution they isomerize to the thermodynamically favored

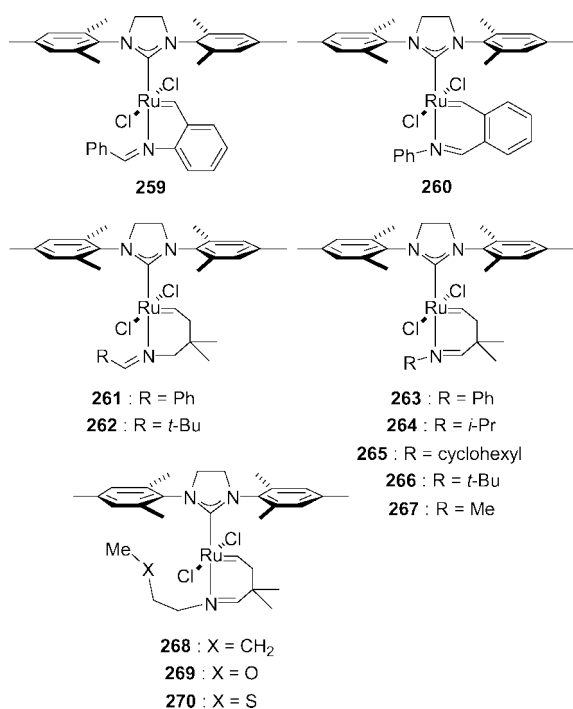
#### Scheme 7. Ruthenium-Based Catalysts **257** and **258** Bearing Chelating Quinolin- and Quinoxalin-ylidenes



*cis*-dichloro isomers (**257b** and **258b**, respectively). Both **257** and **258** are air-stable in solution, showing RCM, enyne metathesis, and thermally triggered ROMP activity.<sup>169,170</sup> Moreover, *trans*-dichloro complexes **257a** and **258a** initiate faster than their *cis*-dichloro isomers **257b** and **258b**, while the quinoxaline-containing **258a** is faster than its quinoline analogue (**257a**) in model RCM and enyne metathesis reactions.<sup>169</sup>

#### 4.5. Bidentate Alkylidenes Chelated through Imine Donors

The first NHC-coordinated ruthenium alkylidenes containing an imine donor tethered to the alkylidene (**259** and **260**, Figure 56) were reported in 2005 by Slugovc et al.<sup>171</sup> These air- and moisture-stable complexes exert thermally switchable ROMP behavior, showing high efficiency at temperatures around 110 °C and very low initiation rates at room temperature. **260** has a higher switching temperature and a lower polymerization rate than **259**. This difference in the initiation rates of **259** and **260** was ascribed to the varying chelate ring sizes (five- versus six-membered, respectively).<sup>171</sup> However, this hypothesis was challenged one year later, by the suggestion that the placement of the imine bond (exocyclic in **259** versus endocyclic in **260**) is the factor that primarily determines the initiation behavior.<sup>172</sup> In that study, complexes **261–270** (Figure 56) were prepared and evaluated in RCM and ROMP transformations. Exocyclic imine catalysts **261** and **262** were found to be highly active, and certainly not latent, in the RCM of diethyl diallylmalonate, and **261** initiated somewhat faster than **262**. On the contrary, endocyclic imine complexes **263–267** are thermally triggered latent catalysts that show an almost on/off polymerization behavior in the ROMP of dicyclopentadiene. This different initiation behavior among the exocyclic and the endocyclic imine frameworks was attributed to unfavorable steric interactions in the exocyclic case with the rest of the catalyst framework. Thus, a weaker Ru–N bond results in a more



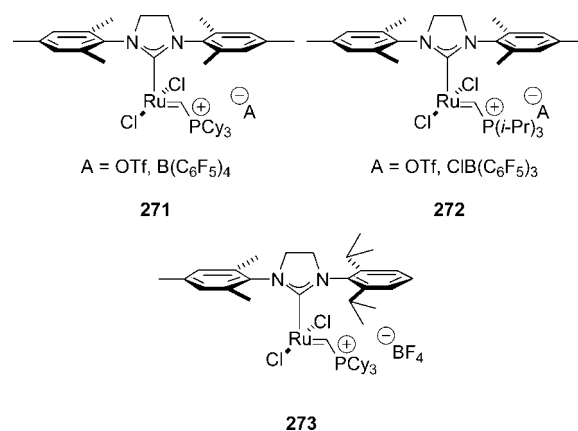
**Figure 56.** Ruthenium-based metathesis catalysts **259–270** bearing chelating carbenes with imine functionalities.

efficient initiator and, ultimately, leads to a higher activity. Moreover, endocyclic imine complexes **263–267** efficiently ring-close diethyl diallylmalonate at elevated temperatures, with an order of activity **263** > **264** > **265** > **266** > **267**. This result was rationalized on the basis of the relative donating ability and steric demand of the imine substituents. Namely, the electron-poor phenyl substituent affords the fastest-initiating catalyst and the small methyl group affords the slowest-initiating catalyst. The three-point chelating alkylidenes in **269** and **270** were designed as potentially even slower metathesis initiators since two successive ligand dissociation events must take place before a catalytically active fragment is generated. However, **268** and **269** show essentially identical RCM activities, indicating that the oxygen atom does not bind tightly enough to measurably impact the catalysis. Complex **270**, on the other hand, shows a lower initiation rate than both **268** and **269**, which suggests that incorporating an appropriate third point of attachment may indeed have a major impact on catalysis.

#### 4.6. 14-Electron Phosphonium Alkylidenes

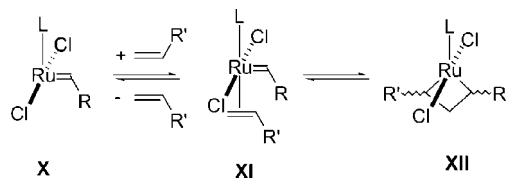
In 2004, Piers and co-workers published the synthesis of NHC-coordinated ruthenium complex **271** (Figure 57) bearing a 14-electron phosphonium alkylidene.<sup>173</sup> Surprisingly, the four-coordinate complex **271**, which models the presumed active species formed upon dissociation of the labile ligand in NHC-coordinated catalysts, is air- and moisture-stable and, furthermore, highly active in model RCM reactions. More importantly, this system provides rapid metathesis initiation, outperforming even bis(3-bromopyridine) complex **229** (Figure 49). Initiation in these 14-electron phosphonium alkylidenes is more energetically favorable than in the classic five- or six-coordinated systems, as it consists of a low-barrier olefin-binding event without the need for a ligand to dissociate. Soon after the synthesis of **271**, the analogous 14-electron complexes **272** and **273** (Figure 57) were also prepared.<sup>174,175</sup>

The ability of these phosphonium alkylidenes to initiate at very low temperatures has additionally proven useful in a series of low-temperature mechanistic studies that resulted in the direct observation of ruthenacyclobutane intermediates relevant to olefin metathesis.<sup>174–177</sup> Given that ruthenacyclobutanes are known to play a key role in the determination of the regio- and stereochemical outcome of metathesis, a better understanding of their geometry is essential to the rational design of diastereo- and enantioselective catalysts. These studies are suggestive of bottom-face olefin coordina-

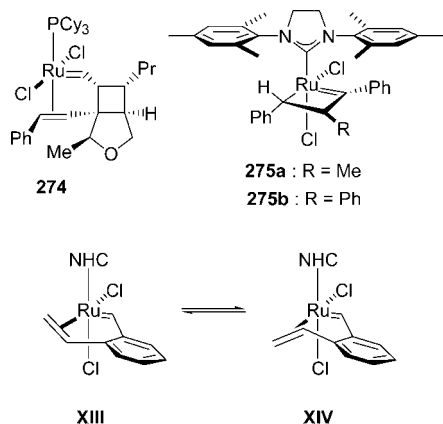


**Figure 57.** 14-electron NHC-coordinated ruthenium catalysts **271–273** bearing phosphonium alkylidenes.

**Scheme 8. Initial Steps Proposed for the Bottom-Face Pathway in the Ruthenium-Catalyzed Olefin Metathesis Mechanism**



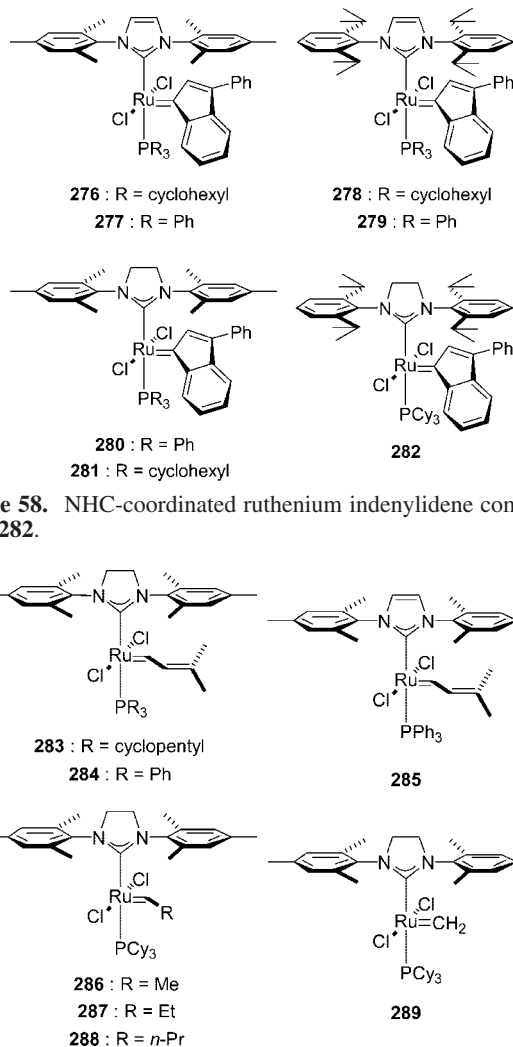
**Scheme 9. Side-on and Bottom-Face Bound Ruthenium Olefinic Complexes**



tion and metallacycle generation, that is, *trans* to the NHC ligand. Spectroscopic data for all reported ruthenacyclobutanes are consistent with a symmetric structure with a flat, kite-shaped four-membered ring (species **XII**, Scheme 8).<sup>174–178</sup> Ruthenacyclobutanes show dynamic structure, proceeding through a series of nonproductive metallacycle formations/cycloreversions prior to olefin exchange. However, most systems studied to date are relatively simple, and therefore, one should be very careful in generalizing these observations to more complicated ruthenacyclobutane species. Also note that there has been a long-standing debate regarding the site of olefin coordination to the ruthenium catalyst that leads to ruthenacyclobutane formation (side- or bottom-bound). Thus, in 1997 Snapper and co-workers reported the isolation of complex **274** (Scheme 9) in which a chelating olefin coordinates *trans* to the PCy<sub>3</sub> ligand (bottom face).<sup>179</sup> Complexes **275a** and **275b** (Scheme 9) were also subsequently isolated, suggesting a side-bound olefin intermediate.<sup>180</sup> In a similar vein, the reaction between 1,2-divinylbenzene and a series of NHC-coordinated ruthenium complexes led to the formation of two types of side-bound olefin adducts (**XIII** and **XIV**, Scheme 9) that undergo dynamic interconversion.<sup>181,91</sup>

**5. Ruthenium Alkylidene Variation: Fischer-Type Carbenes, Indenylidenes, Vinylidenes, Cyclic Ruthenium Alkylidenes, and Other Alkylidene Ligands**

The first NHC-coordinated ruthenium indenylidenes (**276–279**, Figure 58) were reported in 1999 by Nolan and co-workers.<sup>182,183</sup> These complexes were demonstrated to be highly thermally stable and efficient in the RCM of benchmark  $\alpha,\omega$ -dienes, forming five-, six-, and seven-membered di-, tri-, and tetrasubstituted cycloalkenes, in the ROMP of 1,5-cyclooctadiene, as well as in a series of CM transformations.<sup>166,182–186</sup> The preparation of indenylidene complexes **280**, **281**, and **282** (Figure 58), bearing NHC ligands with



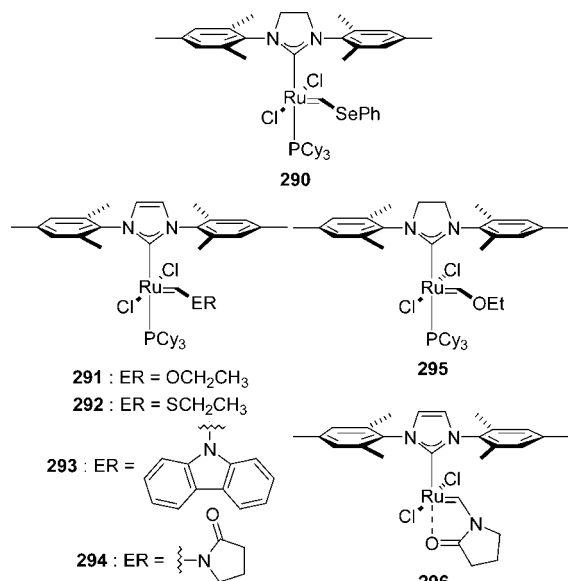
**Figure 58.** NHC-coordinated ruthenium indenylidene complexes **276–282**.

**Figure 59.** Ruthenium complexes **283–289** bearing dimethylvinylidene and alkylidene ligands.

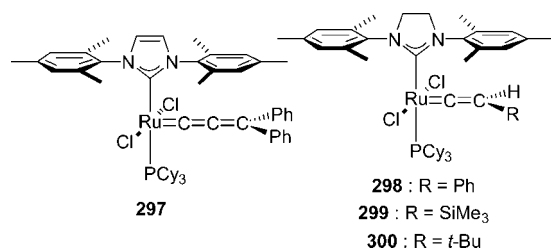
saturated backbones, was published in 2001, 2008, and 2009, respectively.<sup>164,187,188</sup> Complex **280** was found to initiate the ROMP of 1,5-cyclooctadiene faster than both **281** and **3** (Figure 7), due to the more labile nature of the PPh<sub>3</sub> ligand as compared to the PCy<sub>3</sub> (also refer to section 6). Moreover, **281** shows an increased induction period compared to its benzylidene analogue **3** (Figure 7) and, therefore, lower activity in both RCM and ROMP transformations. It should also be noted that (pre)catalysts **3**, **280**, and **281**, as well as all H<sub>2</sub>IMes-coordinated ruthenium complexes, provide the same propagating species (**X**, Scheme 8) after a single turnover. That is, as long as ligand “L” and the two anionic ligands in **X** are the same in two (pre)catalysts, the catalytic behavior of these species will only differ in the initiation step. Finally, complex **282** was found to be more competent than both **276** and **281** in the RCM of unhindered and moderately hindered dienes and enynes.

Ruthenium vinylalkylidene complexes **283–285** (Figure 59) have also been isolated.<sup>66a,130,162</sup> **283** was successfully utilized in the RCM and CM of a variety of electron-deficient olefins,<sup>66a</sup> whereas **285** and ruthenium ethylidene **286** were shown to be efficient ADMET and ROMP catalysts.<sup>162,163</sup> Ruthenium alkylidenes **286–288** (Figure 59) initiate faster than the parent benzylidene complex **3** (Figure 7),<sup>189</sup> while, in contrast, methylidene **289** is a very poor metathesis catalyst, in part as a result of its extremely low phosphine





**Figure 60.** Ruthenium complexes **290**–**296** bearing Fischer-type carbenes.

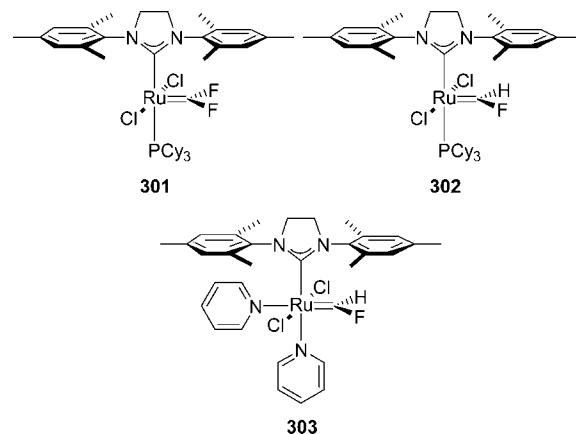


**Figure 61.** Ruthenium-based complexes **297**–**300**.

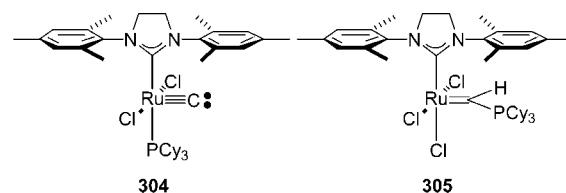
dissociation rate.<sup>24</sup> **289** represents an important intermediate of low stability in metathesis reactions of terminal olefins initiated by H<sub>2</sub>IMes catalyst **3**, but can be isolated and purified by column chromatography.<sup>24</sup> All related catalyst decomposition studies are discussed in section 11.

Ozawa and co-workers were the first to report the preparation of an NHC-coordinated ruthenium complex bearing a Fischer-type carbene (**290**, Figure 60),<sup>190</sup> shown to be efficient in the ROCM of *endo*-5,6-disubstituted norbornenes using phenyl vinyl selenide as an acyclic olefin. Soon thereafter, Fischer-type ruthenium complexes **291**–**295** (Figure 60) were also synthesized and were demonstrated to be structurally similar, but inherently more stable than their carbon analogues.<sup>191</sup> In solution, complex **294** exists in a temperature-dependent equilibrium with the chelate complex **296** and free PCy<sub>3</sub>. Complexes **291**–**295** efficiently catalyze a series of model RCM and ROMP reactions, although with significantly lower rates than their corresponding alkylidene counterparts. The rate of the RCM reaction of diethyl diallylmalonate was found to be highly dependent on the  $\alpha$ -heteroatom; complex **293** was proven to be the most active catalyst in the series with the relative activities following the trend E = C > N > S > O. Along these lines, care should be taken when ethyl vinyl ether is used as the quenching agent in ROMP reactions, since complex **295** is metathesis active, at least under some conditions.

Furthermore, ruthenium allenylidene **297** (Figure 61), reported in 1999, shows high thermal stability but very low RCM activity, supposedly due to the relatively high bonding energy of the allenylidene moiety.<sup>192</sup> However, vinylidenes **298**–**300** (Figure 61) are efficient RCM and ROMP catalysts,



**Figure 62.** Ruthenium fluoromethylidene complexes **301**–**303**.



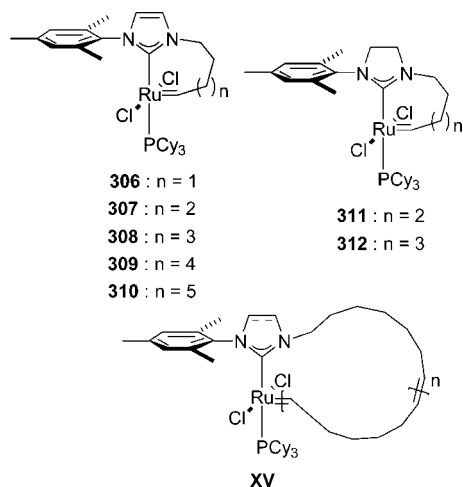
**Figure 63.** Terminal carbide **304** and phosphoniomethylidene **305**.

although not as reactive as the corresponding benzylidene complex **3** (Figure 7).<sup>193</sup>

Despite the great progress that has been made in the field of ruthenium-catalyzed metathesis, ruthenium catalysts do not efficiently carry out the metathesis of directly halogenated alkenes (i.e., vinyl halides and related substrates), because of the electron-withdrawing nature of the pendent halogens. This is especially true in CM, since there are some examples of RCM transformations involving  $\alpha$ -chloro- and  $\alpha$ -fluoro- $\alpha,\omega$ -dienes.<sup>194</sup> The first example of a successful metathesis reaction between an NHC-coordinated ruthenium complex and a vinyl halide was reported in 2001, where ruthenium difluoromethylidene **301** (Figure 62) was prepared by treating the parent benzylidene complex (**3**, Figure 7) with an atmosphere of 1,1-difluoroethylene.<sup>195</sup> Although the F<sub>2</sub>C=CH<sub>2</sub> double bond was cleaved metathetically, this reaction was proven not catalytic. Nevertheless, **301** effects the ROMP of 1,5-cyclooctadiene, albeit significantly less efficiently than **3**. The poor catalytic activity of **301** was attributed to its insufficient initiation and, therefore, could be slightly improved by additives that promote phosphine dissociation.

On the basis of another study, Johnson and co-workers published a procedure toward the synthesis of monofluoromethylidene complexes **302** and **303** (Figure 62).<sup>196</sup> **302** and **303** are significantly more reactive than **301**, but slow compared to **3**, in the RCM and CM of model alkenes. Bis(pyridine) complex **303** initiates more quickly than **302**, as anticipated; however, it also suffers from a higher decomposition rate. Isolation of the monochloromethylidene analogue of **302** was not possible, even though its transient formation could be observed at  $-70$  °C by NMR.<sup>197</sup> Instead, terminal carbide **304** and phosphoniomethylidene **305** (Figure 63) were formed upon reaction of ruthenium benzylidene **3** with vinyl chloride.

In 2001, Fürstner et al. reported the synthesis of complexes **306** and **307** (Figure 64), featuring a chelating N-to-Ru tether, as catalysts that could be regenerated upon consumption of monomer; nevertheless, the catalytic activities of **306** and



**Figure 64.** Cyclic ruthenium alkylidene complexes **306**–**312**.

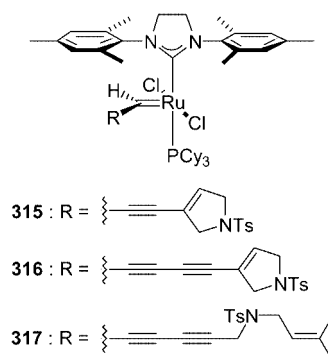
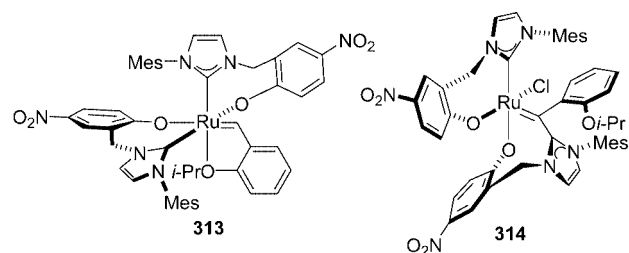
**307** were not evaluated in that early work.<sup>81</sup> Later on, however, catalyst **309** (Figure 64) was found to mediate the synthesis of cyclic polymers via ROMP of strained cyclic monomers such as *cis*-cyclooctene,<sup>198</sup> 1,5-cyclooctadiene, and 1,5,9-*trans-cis-trans*-cyclododecatriene.<sup>199</sup> In brief, this ring-expansion metathesis polymerization (REMP) was suggested to proceed via a ring-expansion initiation event, from a cyclic ruthenium alkylidene catalyst, and propagate as cyclic monomers are incorporated into the growing cyclic polymer (**XV**, Figure 64) that remains attached to the metal center throughout the entire polymerization process. This approach circumvents the problems involved in other more typical routes to cyclic polymers, which require the intramolecular macrocyclization of linear precursors at very low concentrations. Further investigations, with the aim of systematically studying the impact of the tether length and the electronic properties of the NHC, via backbone saturation, on different aspects of the polymerization mechanism, led to the synthesis of cyclic catalysts **307**–**312**, presented in Figure 64.<sup>200</sup> Whereas increasing the N-to-Ru tether length was found to result in enhanced rates of polymerization, shorter tethers were more efficient for catalyst release from the polymer. Utilizing a saturated NHC backbone (**311** and **312**) was shown to boost polymerization rates to a greater extent than increasing the length of the tether.

Attempts to prepare active chelated catalysts led to the preparation of an unusual imidazolium-substituted ruthenium alkylidene (**314**, Figure 65).<sup>201</sup> Complexes **313** and **314** were isolated during attempts to synthesize a ruthenium alkylidene complex monocoordinated with the corresponding bidentate aryloxy–NHC ligand. **313** and **314** were purified by column chromatography and fully characterized, although in very low isolated yields (6 and 12%, respectively). As expected, **314** proved to be a poor olefin metathesis catalyst.

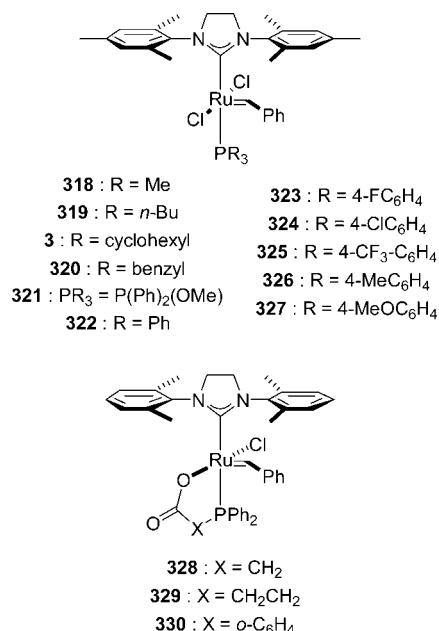
The isolation of alkynyl-substituted alkylidene ruthenium complexes **315**–**317** (Figure 65) was reported in 2009.<sup>202</sup> In that work, Lee and co-workers showed that substituents on alkynyl ruthenium alkylidenes can efficiently adjust their reactivity and metallotropic [1,3]-shift behavior. **315**, characterized via single-crystal X-ray analysis, was proved to be moderately active in the RCM of a model enyne substrate.

## 6. Variation of the Phosphine Ligand

With regard to phosphine-containing NHC ruthenium catalysts, it should be re-emphasized that complexes which



**Figure 65.** Ruthenium-based complexes **313**–**317**.



**Figure 66.** Phosphine-coordinated ruthenium catalysts **3** and **318**–**330**.

are different only in their phosphine ligand provide the same propagating species (**X**, Scheme 8) upon phosphine dissociation. Consequently, by varying the phosphine, one can manipulate initiation and phosphine rebinding without changing the metathesis ability of the catalyst. Accordingly, phosphine-containing complexes **318**–**327** (Figure 66) were prepared for a systematic study of the effect of different phosphine ligands.<sup>24,129,156,203</sup> The data obtained for complexes **322**–**327** (bearing phosphine ligands with the same cone angle)<sup>204</sup> by either magnetization transfer experiments or by the stoichiometric initiation with ethyl vinyl ether<sup>24,156</sup> revealed the existence of a linear free energy relationship between the phosphine dissociation rate constant and the Hammett constant  $\sigma_p$  (that is, phosphine  $\sigma$ -donor strength), with the more electron-rich phosphines dissociating at slower rates than electron-poor ones.<sup>156</sup> Moreover, arylphosphine

dissociation was generally found to be faster than alkylphosphine dissociation. Thus, initiation in  $\text{H}_2\text{IMes}$  phosphine-containing catalysts can be easily adjusted by tuning phosphine electronics. On the other hand, phosphine reassociation showed no direct correlation with phosphine electronics. In addition to electronics, the steric properties of phosphine ligands have a major impact on phosphine dissociation, and thus complex **318** was essentially metathesis inactive at room temperature.<sup>203</sup>

Recently, complexes **328**–**330** (Figure 66), coordinated with a series of chelating phosphine–carboxylate ligands, were prepared.<sup>205</sup> These chelated complexes exhibit slow initiation rates at temperatures up to 40 °C; nevertheless, at elevated temperatures, **328** and **330** efficiently ring-close diethyl diallylmalonate and diallyl malononitrile, outperforming **329**.

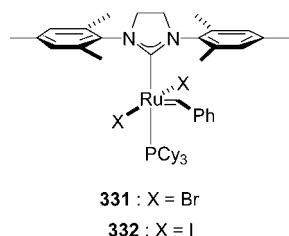
## 7. Anionic Ligand(s) Variation

### 7.1. Halides

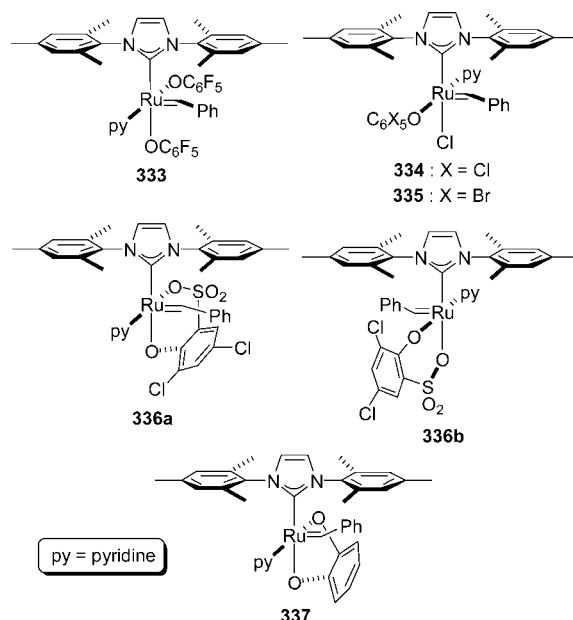
It has been already mentioned that, in some cases, changing the halide ligands from chlorides to iodides improves the enantioselectivity of chiral ruthenium metathesis catalysts (sections 3.3 and 3.4). In the case of chiral monodentate NHCs, the diiodide complexes are prepared in situ, by dissolving the dichloride catalyst in THF in the presence of  $\text{NaI}$ ,<sup>29,34,35</sup> whereas chiral bidentate iodide complexes are stable enough to be isolated and chromatographically purified.<sup>32,33</sup> Additionally, halide ligands have been shown to have a significant impact on the initiation rates of second-generation catalysts.<sup>24,206</sup> For example, dibromide **331** and diiodide **332** (Figure 67) initiate 3 and 250 times faster than the dichloride parent complex **3** (Figure 66), respectively.<sup>24</sup> This initiation rate enhancement was predominantly attributed to the increased steric bulk of bromide or iodide ligands, since *cis* electronic effects (i.e., between the halide(s) and the phosphine ligand) are generally relatively small in dissociative ligand-substitution reactions. However, despite the increased initiation efficiency of **332**, its olefin metathesis activity is comparable to, or even lower than, that of the parent dichloride complex **3** due to slower turnover rates.

### 7.2. Monodentate and Bidentate Aryloxides

Motivated by the easily tunable steric and electronic properties of aryloxides, and in order to inhibit the formation of chloride-bridged ruthenium species that lead to catalyst decomposition, Fogg and co-workers developed “pseudohalide” ruthenium catalysts **333**–**337** (Figure 68).<sup>207–210</sup> “Halide-free” **333**, the first NHC-coordinated complex of this type to be reported, proved to be a highly active metathesis catalyst, efficiently carrying out the ring-closing of model  $\alpha,\omega$ -dienes, even at very low catalyst loadings.<sup>207</sup> Equally



**Figure 67.** Dibromide and diiodide ruthenium catalysts **331** and **332**.



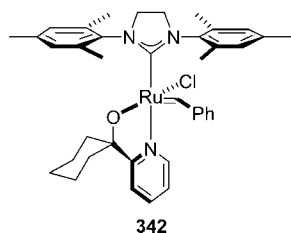
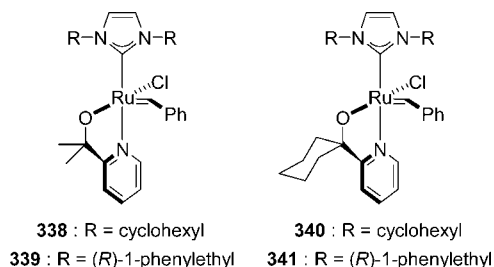
**Figure 68.** Ruthenium-based catalysts **333**–**337** bearing aryloxide ligands.

efficient metathesis catalysts **334** and **335** followed soon thereafter.<sup>208</sup> Remarkably, **333**–**335** also showed very high affinity for silica gel, facilitating their efficient removal from the metathesized compound(s). For example, in the RCM of diethyl diallylmalonate using 5 mol % catalyst loading of **333**–**335**, followed by flash chromatography, ruthenium levels lower than 100 ppm in the product were achieved. This is quite important since difficulties in removing residual ruthenium impose major drawbacks in multistep synthetic procedures that employ metathesis (for a more extended discussion on this issue, refer to section 10). Finally, *o*-sulfonato and catecholato aryloxide complexes **336** and **337** were also synthesized and evaluated.<sup>209</sup> As can be seen in Figure 68, *o*-sulfonato complex **336** is isolated in the form of two isomers (**336a** and **336b**); while catecholato derivative **337** was shown to be a highly active RCM catalyst, the pyridine ligand in **336** is nonlabile, and consequently, **336** shows modest RCM activity.

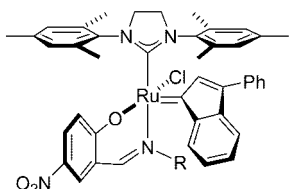
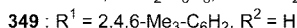
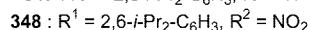
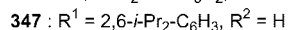
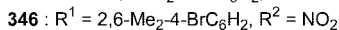
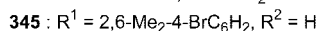
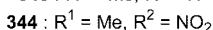
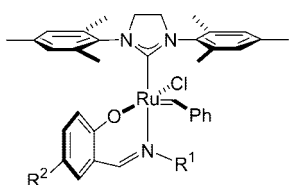
### 7.3. *N,O*-, *P,O*-, and *O,O*-Bidentate Ligands

The first ruthenium catalysts featuring this class of ligands to be reported are complexes **338**–**341** (Figure 69), prepared by exchanging tricyclohexylphosphine with the corresponding chelating pyridinyl alcoholate ligand, which display low metathesis activity at room temperature.<sup>211</sup> This effect was attributed to the chelate stabilization induced by the dangling pyridine ligand. Nevertheless, at 60 °C, **338**–**341** effect the ROMP of both norbornene and cyclooctene, showing reactivities similar to the tricyclohexylphosphine-containing parent complexes. In a more recent study, Jordaan and Vosloo prepared the structurally similar complex **342** (Figure 69) and evaluated its catalytic performance in the self-metathesis of 1-octene in the absence of a solvent.<sup>212</sup> Complex **342** displays a lower initiation rate than phosphine-containing **3** (Figure 66); however, at 60 °C, **342** has a higher activity and stability compared to **3**.

Schiff base *N,O*-bidentate ligands were introduced for the first time in NHC-coordinated ruthenium complexes by Verpoort and co-workers.<sup>213–215</sup> Utilizing this ligand framework is quite appealing, not only because of the fine-tuning

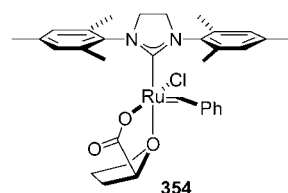
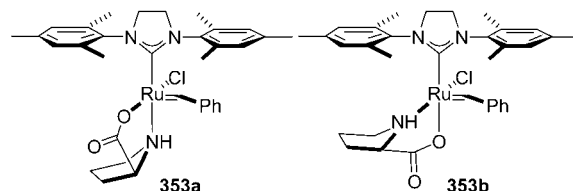
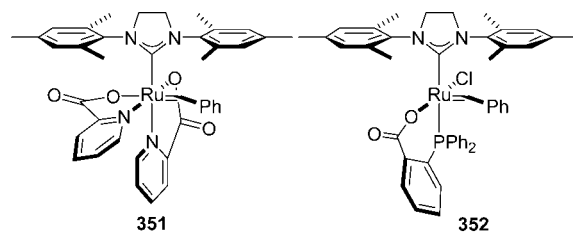


**Figure 69.** Ruthenium catalysts **338**–**342** coordinated with chelating pyridinyl–alcoholato ligands.



**Figure 70.** NHC-coordinated ruthenium catalysts **343**–**350** bearing bidentate Schiff base ligands.

possibility of both the sterics and electronics at the ruthenium center but also because of the high-yielding and usually single-step procedures by which they are accessible. Thus, complexes **343**–**349** (Figure 70) were synthesized and shown to efficiently catalyze the RCM and ROMP of a series of benchmark substrates.<sup>213,214,216</sup> The catalytic activity of **343**–**348** was proved to depend strongly and systematically on the steric and electronic environment of the Schiff base, with an order of activity **343** > **344** > **345** > **346** > **347** > **348**. In addition, complexes **346**–**349** initiate extremely slowly compared to their phosphine-containing analogue **3** (Figure 66), showing very low metathesis activity at room temperature. Nevertheless, at 90 °C, **346**–**349** are very efficient ROMP initiators, on account of their very high thermal stability.<sup>216</sup> It was also found that the initiation efficiency of latent **346** can be chemically controlled on demand.<sup>217</sup> Specifically, upon addition of Brønsted or Lewis acids, such as HSiCl<sub>3</sub>, HSiMeCl<sub>2</sub>, BF<sub>3</sub>, or AlCl<sub>3</sub>, at room temperature, **346** can be transformed into a very reactive catalyst, affording high turnover numbers in the ROMP of



**Figure 71.** Ruthenium catalysts **351**–**354** bearing chelating carboxylate ligands.

both 1,5-cyclooctadiene and dicyclopentadiene, as well as in the RCM of diethyl diallylmalonate. The triggering mechanism was proposed to involve the reversible formation of an adduct between the acid and the electron pair on the nitrogen of the Schiff base. Ruthenium indenylidene **350** (Figure 70), with both ROMP and controlled radical polymerization reactivity, has been also prepared.<sup>218</sup>

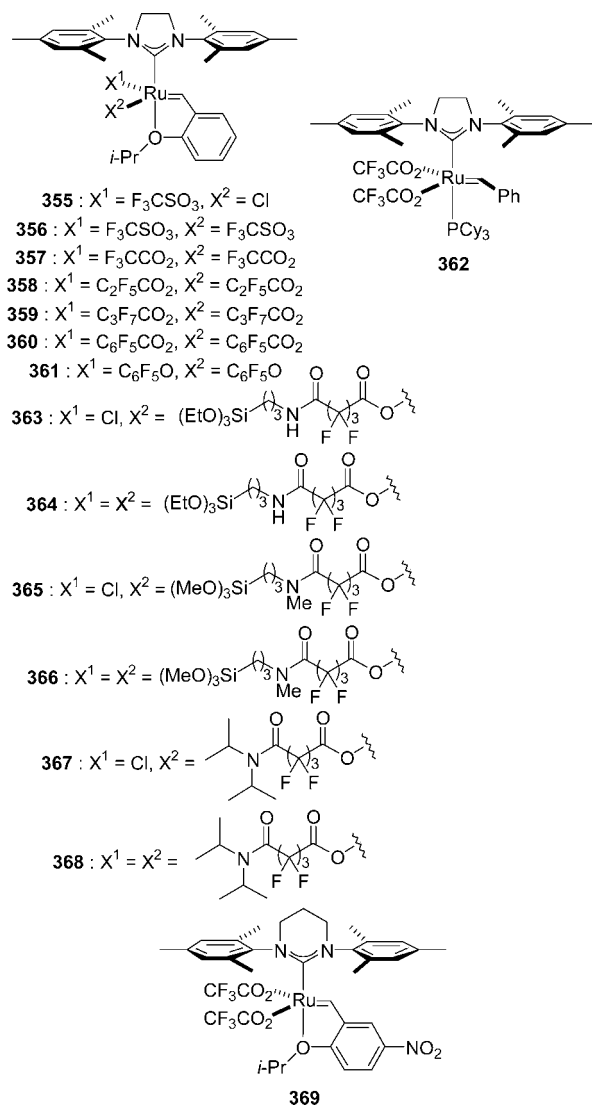
In 2005, Hahn et al. reported the synthesis of halide-free **351** (Figure 71), coordinated with two bidentate 2-pyridine–carboxylato ligands.<sup>219</sup> Although complex **351** is metathesis inactive, upon addition of 2 equiv of HCl it generates a catalytically active species by protonation of at least one of the 2-pyridine–carboxylato ligands. While less active than second-generation catalyst **3** (Figure 66), this in situ generated species effects the RCM of model  $\alpha,\omega$ -dienes in CH<sub>2</sub>Cl<sub>2</sub> and MeOH.

In another approach, *N,O*-, *P,O*-, and *O,O*-bidentate complexes **352**–**354** (Figure 71) were developed.<sup>220</sup> Quite similar to many of the above-reported chelated catalysts, **352**–**354** exert low metathesis activity at room temperature, while *O,O*-chelate **354** also suffers from a high decomposition rate. Interestingly, however, the initiation of both **352** and **353** is significantly enhanced upon addition of CuCl. Whereas CuCl-activated **352** shows reduced stability, CuCl-activated **353** is a quick-initiating and highly efficient catalytic system in the RCM of diethyl diallyl and diethyl allylmethylmalonate. Additionally, intermediate trapping experiments suggest that this CuCl-assisted initiation mechanism involves reversible coordination of the proline ligand to CuCl, thereby facilitating an open coordination site on ruthenium.

#### 7.4. Carboxylates and (Alkyl)sulfonates

Substitution of the anionic chloride ligand(s) by perfluorosulfonates and, more often, perfluorocarboxylates, in ruthenium metathesis catalysts is typically connected with the preparation of immobilized catalysts on solid supports (see section 10). However, homogeneous catalytic applica-





**Figure 72.** Ruthenium-based catalysts **355**–**369** coordinated with carboxylate and (alkyl)sulfonate ligands.

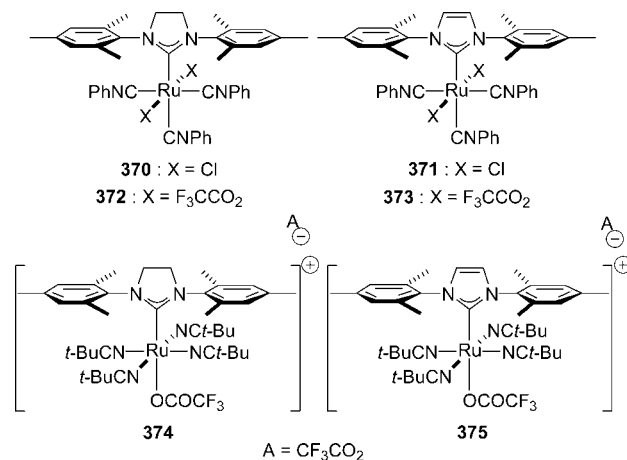
tions of this family of complexes turned out to be quite successful as well. Thus, catalysts **355**–**357** (Figure 72) were prepared and found to be efficient in the RCM of diethyl diallylmalonate, 1,7-octadiene, diallyldiphenylsilane, *N,N*-diallyltrifluoroacetamide, and other related substrates, as well as in enyne metathesis and ROCM reactions.<sup>221</sup> In other work, **357**–**362** were tested in a series of benchmark RCM transformations.<sup>222</sup> These complexes proved to exert similar or lower reactivity compared to the parent chlorine-containing systems (catalysts **3** and **5**, Figures 66 and 8, respectively). Quite similarly, **363**–**368** (Figure 72) were prepared by substituting one or two of the chloride ligands in complex **5** with 1 or 2 equiv of the corresponding silver carboxylates, respectively.<sup>223,224</sup> Note that this rather typical substitution reaction is usually complete within minutes, driven by the precipitation of silver(I) chloride. In terms of catalytic efficiency, monosubstituted catalysts (**363**, **365**, and **367**) outperform those in which both chloride ligands are exchanged (**364**, **366**, and **368**), with the most efficient, **363**, showing activity similar to the parent dichloride catalyst **5**. Complex **369** was shown to be a highly active metathesis catalyst in both RCM and ROCM transformations.<sup>119</sup>

In 2006, Braddock and co-workers published a related study on Cl-, Br-, CF<sub>3</sub>CO<sub>2</sub>-, and C<sub>2</sub>F<sub>5</sub>CO<sub>2</sub>-substituted ruthenium isopropoxybenzylidenes, the results of which reveal significant implications for all kinds of anionic substituents in these types of ruthenium complexes.<sup>225</sup> In solution, all examined complexes were shown to constantly undergo anionic ligand exchange, under mild conditions typical for olefin metathesis reactions. The mechanism that was proposed to account for this ligand exchange involves the intermediacy of halide-bridged dimers, which are more easily accessible in the case of carboxylate-containing complexes due to steric reasons. This effect should be taken into consideration in the design of both homogeneous and heterogeneous ruthenium catalysts in the case of immobilization through the anionic ligand(s). One year later, the same group reported the vacuum-driven anionic ligand exchange of free perfluorocarboxylic acids with ruthenate-bound perfluorocarboxylates.<sup>226</sup>

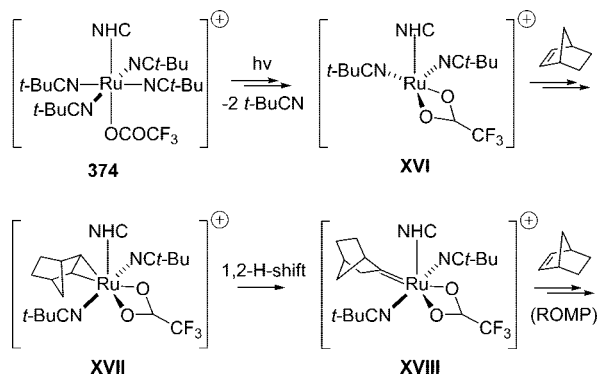
ium isopropoxybenzylidenes, the results of which reveal significant implications for all kinds of anionic substituents in these types of ruthenium complexes.<sup>225</sup> In solution, all examined complexes were shown to constantly undergo anionic ligand exchange, under mild conditions typical for olefin metathesis reactions. The mechanism that was proposed to account for this ligand exchange involves the intermediacy of halide-bridged dimers, which are more easily accessible in the case of carboxylate-containing complexes due to steric reasons. This effect should be taken into consideration in the design of both homogeneous and heterogeneous ruthenium catalysts in the case of immobilization through the anionic ligand(s). One year later, the same group reported the vacuum-driven anionic ligand exchange of free perfluorocarboxylic acids with ruthenate-bound perfluorocarboxylates.<sup>226</sup>

## 7.5. Nitrile- and Isonitrile-Coordinated Alkylidene-Free Ruthenium Catalysts

This class of compounds was targeted by Buchmeiser and co-workers with the aim of developing phototriggered ROMP catalysts. Whereas both **370** and **371** (Figure 73) were shown to initiate the ROMP of norbornene at room temperature in the absence of irradiation, therefore being unsuitable phototriggered initiators for this monomer, polymerization of norborn-5-ene-2-ylmethanol required UV irradiation (172 nm) and concurrent heating at 40 °C.<sup>227</sup> Thus, **370** and **371** are in principle suitable for the UV-initiated ROMP of this monomer. Initiation of **370** and **371** was postulated to involve the phototriggered dissociation of at least two of the three phenyl isonitrile groups. Although structurally similar to **370** and **371**, carboxylate-containing catalysts **372** and **373** (Figure 73) decompose upon heating in the presence of a series of functionalized norbornenes, supposedly due to an imine metathesis-type reaction of dissociated phenyl isonitrile with any in situ generated ruthenium alkylidene complex.<sup>228</sup> Nevertheless, the turning point in this family of catalysts occurred with the preparation of nitrile-coordinated cationic complexes **374** and **375** (Figure 73).<sup>229</sup> These two complexes proved to be the first thermally stable, UV-initiated ROMP catalysts. Both **374** and **375** can be handled in air and, in the absence of light, are completely unreactive toward cyclooctene, dicyclopentadiene, and a number of norbornene derivatives up to 45 °C. Exposing mixtures of either **374** or **375** with these same monomers to 308 or 254 nm irradiation, at room temperature, led to the formation of the correspond-



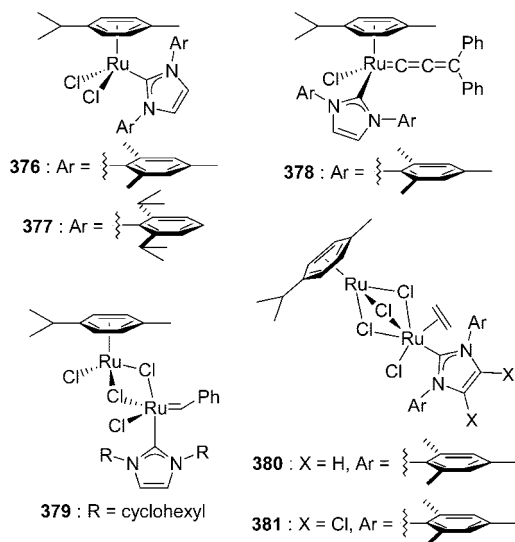
**Figure 73.** Nitrile- and isonitrile-coordinated ruthenium-based complexes **370**–**375**.

**Scheme 10. Proposed Mechanism for the Photoinitiated ROMP Activity of Complex 374**


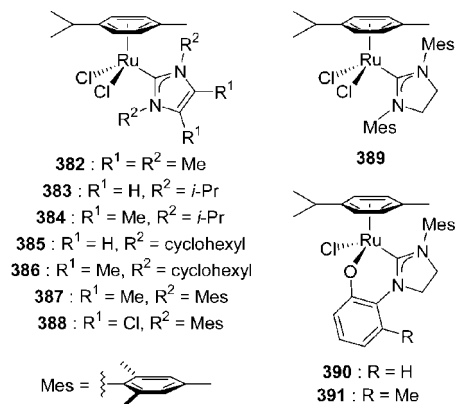
ing polymers, with 254 nm excitation being considerably more efficient. On the basis of NMR data, laser flash and steady-state photolysis experiments, and a series of theoretical calculations, the mechanism shown in Scheme 10 was proposed to account for the phototriggered ROMP activity of **374**. According to their proposal, photolysis of the precatalyst (**374**) initially leads to the formation of species **XVI**, which then binds one monomer molecule to form intermediate **XVII**. In the key step for the alkylidene formation, a 1,2-hydrogen atom shift on the carbon-carbon double bond of the alkene  $\pi$ -complex (**XVII**) affords the active ruthenium(IV) species (**XVIII**) that initiates the ROMP cascade.

**8. *N*-Heterocyclic Carbene-Coordinated ( $\eta^6$ -Arene)ruthenium Metathesis Catalysts**

Complexes **376–378** depicted in Figure 74 were the first ( $\eta^6$ -arene)ruthenium species<sup>230</sup> bearing NHC ancillary ligands to be reported.<sup>231</sup> These half-sandwich complexes, which are isolated in high yields and display high thermal stability, outperform their phosphine-containing counterparts in the RCM of diethyl diallylmalonate. It should be noted that the typical alkylidene moiety that serves as the precursor for the generation of the well-established ruthenacyclobutane intermediates (via a [2 + 2]-cycloaddition step) is not preinstalled in **376** and **377** and, therefore, an in situ generated alkylidene species is likely operating in this case.



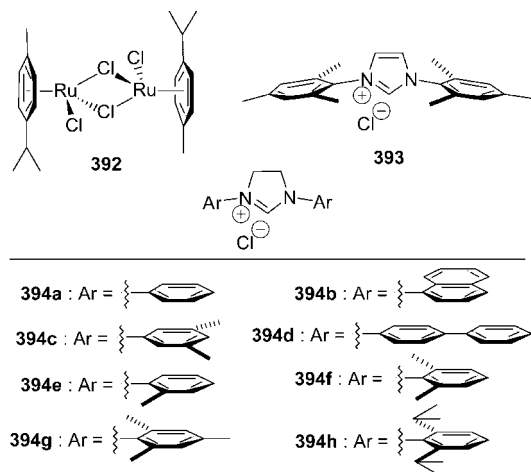
**Figure 74.** Half-sandwich NHC-coordinated ruthenium metathesis catalysts **376–381**.



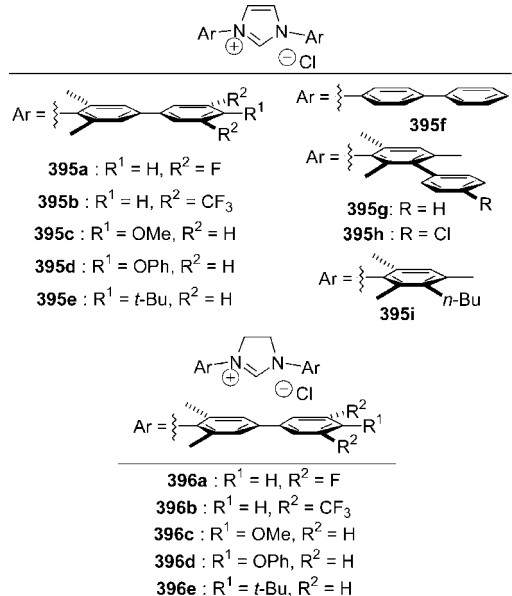
**Figure 75.** NHC-coordinated half-sandwich ruthenium complexes **382–391**.

The metathetic activity of **376–378** in the RCM of diethyl diallylmalonate was proven not to be photoinduced, since exposure to UV or neon light, known to accelerate or in some cases to be necessary for the initiation of the phosphine-containing analogues, had no effect on these systems.<sup>231</sup> More recently, **376** was shown to efficiently promote the CM of functionalized styrenes to afford the corresponding symmetrical and unsymmetrical stilbenes, as well as the ring-closing of dimethylallyl tosylamide.<sup>232</sup> Homobimetallic complex **379** (Figure 74), which bears structural resemblance to **376–378**, was also isolated and shown to be efficient in RCM and ROMP transformations.<sup>127,128</sup> In a more recent study, the isolation of homobimetallic ruthenium species **380** and **381** (Figure 74) was reported as well.<sup>233</sup> Upon reacting with  $\alpha,\omega$ -dienes, **380** and **381** were found to unselectively catalyze both ring-closing and cycloisomerization transformations simultaneously.

Noels and co-workers conducted a series of more detailed investigations on this kind of NHC-coordinated ( $\eta^6$ -arene)ruthenium metathesis catalysts. Specifically, they initially synthesized complexes **382–389** (Figure 75) and tested their metathesis activity in the ROMP of cyclooctene, including complexes **376** and **377** (Figure 74) for comparison.<sup>234</sup> While all alkyl-substituted imidazol-2-ylidene-containing complexes (**382–386**) showed extremely low catalytic activity, their aryl-substituted imidazol- and imidazolin-2-ylidene-coordinated counterparts (**376** and **377**, as well as **387–389**) efficiently polymerize cyclooctene, either by visible light activation or by trimethylsilyldiazomethane initiation. Trimethylsilyldiazomethane was proposed to act through the formation of an  $[\text{Ru}]=\text{CHSiMe}_3$  intermediate species, as had been previously observed with other analogous systems. Alternatively, visible light irradiation was observed to lead to *p*-cymene decoordination, generating highly reactive, coordinatively unsaturated ruthenium species that were suggested to trigger metathesis. In the absence of trimethylsilyldiazomethane, the ROMP of cyclooctene by **376** and **377** was found to depend on the presence of light, in contrast to the RCM of diethyl diallylmalonate discussed above. Photoinitiation only required an ordinary 40 W “cold white” fluorescent tube or a 250 W incandescent light bulb fixed at 10 cm from the Pyrex reaction flasks. The most efficient ROMP catalyst in this study proved to be **376**, slightly outperforming the second most efficient, **377**. In related more recent work, Ledoux et al. reported that preparation of **389** is extremely problematic due to its high decomposition rate.<sup>235</sup> Instead, they prepared chelated complexes **390** and **391** (Figure 75), the phenolate ligand of which dissociates



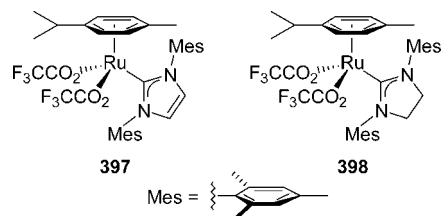
**Figure 76.** Ruthenium complex **392**, imidazolium chloride **393**, and imidazolium chlorides **394a–394h**.



**Figure 77.** Imidazolium chlorides **395a–395i** and imidazolium chlorides **396a–396e**.

upon treatment with HCl to afford the corresponding monodentate analogues of **389**. These species were highly unstable as well.

Interestingly, it was also found that preformed **376** is almost as catalytically efficient as when generated in situ from the homobimetallic complex **392** (Figure 76) and the corresponding NHC, which is also obtained in situ from imidazolium chloride **393** (Figure 76) by deprotonation with KO<sup>*t*</sup>-Bu.<sup>234,236</sup> This three-component catalytic system (i.e., [RuCl<sub>2</sub>(*p*-cymene)]<sub>2</sub>/NHC-precursor salt/base) is simpler and more straightforward to utilize, as it requires only stable and commercially available reagents to generate the active species. Subsequently, the same approach was utilized with imidazolium and imidazolium chlorides **394–396** (Figures 76 and 77) as NHC ligand precursors.<sup>237–239</sup> It was found that the presence of a C4–C5 double bond in the imidazole ring of the NHC ligand is not a prerequisite for high catalytic activities in the photoinduced ROMP of cyclooctene and norbornene.<sup>237,238</sup> However, blocking all the *ortho* positions on the *N*-aryl substituents of the NHCs is necessary to afford efficient photoinitiating ROMP polymerization catalysts. This effect was proposed to originate from the tendency of ruthenium complexes lacking *ortho* substituents to undergo

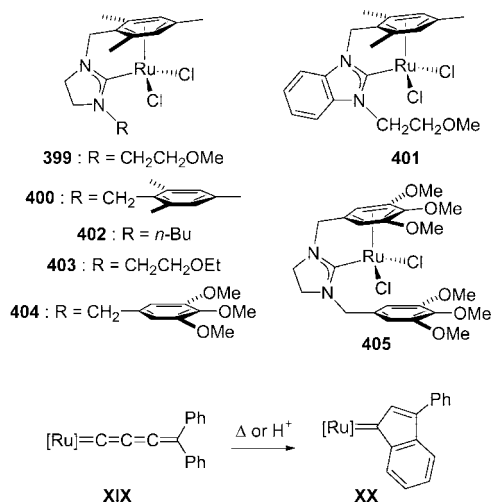


**Figure 78.** NHC-coordinated half-sandwich ruthenium complexes **397** and **398**.

*ortho*-metalation<sup>240</sup> of the *N*-aryl moiety (also refer to section 11). Moreover, changing the sterics and the electronics of the remote aryl groups of the biphenyl units in imidazolium chlorides **395a–395h** and imidazolium chlorides **396a–396e** (Figure 77) had only limited influence on the polymerization activity.<sup>239</sup> Mesityl-based in situ generated **376** and **389** were the most efficient catalysts in these studies. Finally, Buchmeiser and co-workers prepared complexes **397** and **398** (Figure 78), which are the trifluoroacetate-coordinated analogues of **376** and **389**, and examined their thermally initiated and photoinitiated ROMP activity.<sup>227,228</sup> While **397** and **398** were indeed shown to be suitable for the UV-triggered polymerization of norborn-5-ene-2-yl-methanol, norbornene was uncontrollably polymerized by both **397** and **398** in the absence of irradiation at room temperature.

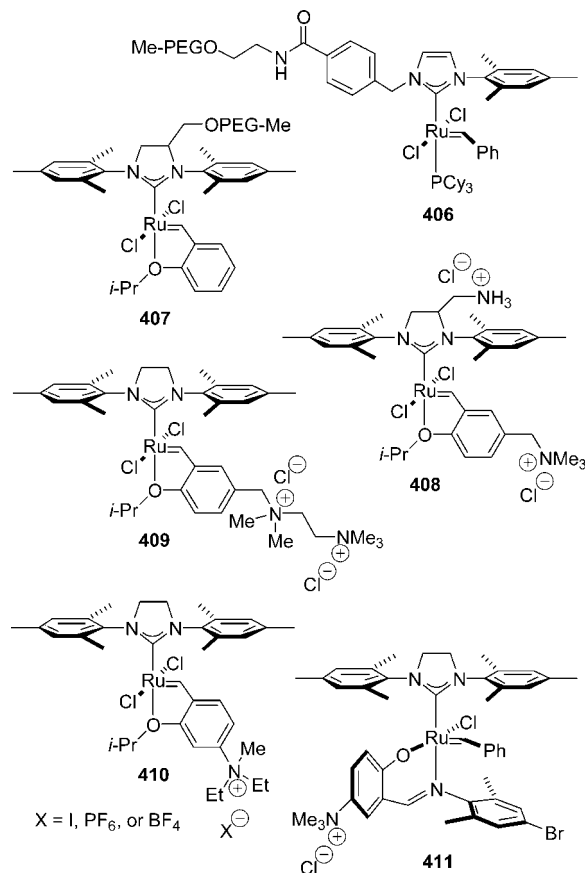
Dixneuf and co-workers utilized a quite similar, though thermally initiated rather than photoinitiated, three-component catalytic system (i.e., [RuCl<sub>2</sub>(*p*-cymene)]<sub>2</sub>/NHC-precursor salt/Cs<sub>2</sub>CO<sub>3</sub>) to carry out enyne metathesis and RCM reactions.<sup>241–244</sup> The presence of a terminal alkyne as an activator was necessary in the latter set of transformations. Furthermore, the same in situ prepared three-component system was found to promote the ROMP of cyclooctene.<sup>245</sup> Thus, heating of [RuCl<sub>2</sub>(*p*-cymene)]<sub>2</sub> (**392**), NHC-precursors **394g** or **394h**, and Cs<sub>2</sub>CO<sub>3</sub> at 80 °C in chlorobenzene led to high- and moderate-yielding cyclooctene polymerization with **394g** and **394h**, respectively. Two different experimental procedures were used, with addition of cyclooctene to the catalytic system either before or after its activation process. Cs<sub>2</sub>CO<sub>3</sub> was proposed not only to deprotonate the NHC precursor but also to modify the catalyst, possibly by substituting the chloride ligand(s) and/or favoring the dissociation of *p*-cymene.

Electron-rich bis(imidazolinyldiene) olefins, containing at least one pendant *N*-arylmethyl group on each imidazolinyldiene moiety, have also been used as carbene precursors to afford chelated NHC-coordinated ( $\eta^6$ -arene)ruthenium complexes **399–405** (Scheme 11).<sup>246–248</sup> Complexes **399–405** are not metathesis-active; however, chloride abstraction with AgOTf and reaction with 1,1-diphenyl propargyl alcohol (HC≡CCPh<sub>2</sub>OH) afford the corresponding unstable ruthenium allenylidene intermediates **XIX** (Scheme 11) that, depending on the nature of the substrate, catalyze the RCM and/or the cycloisomerization of  $\alpha,\omega$ -dienes.<sup>246,247</sup> Furthermore, following the same activation procedure, **399**, **400**, and **402–405** effect the ROMP of norbornene, with **402** and **403** being the most efficient catalysts in this work.<sup>248</sup> The metathetically active ruthenium species in these studies were proposed to be indenylidene intermediates **XX** (Scheme 11), in situ generated by rearrangement of the initially formed allenylidenes **XIX**.<sup>249</sup>

**Scheme 11. NHC-Coordinated ( $\eta^6$ -Arene)ruthenium Complexes 399–405**

**9. N-Heterocyclic Carbene-Coordinated Ruthenium Catalysts Designed for Homogeneous Metathesis in Water and Protic Solvents**

In addition to the potential environmental and economic benefits of aqueous olefin metathesis, successful materialization of such a process would also be important for numerous biological applications. In this context, water- and protic solvent-soluble NHC-coordinated ruthenium catalysts were targeted in an attempt to overcome the relatively low stability and activity of the early bis(phosphine) water-soluble catalysts.<sup>37–39,250</sup> In fact, the first report of olefin metathesis utilizing NHC-coordinated complexes in protic media involved the use of conventional **3** and **5** (Figures 66 and 8, respectively), which were shown to effect the RCM and, to a lesser extent, CM of model substrates in MeOH, as well as in MeOH–water and DMF–water mixtures.<sup>251</sup>

Two kinds of functionalities have been employed thus far to solubilize the desired NHC-bearing (pre)catalysts in water: (i) poly(ethylene glycol) (PEG) chains (**406** and **407**, Figure 79);<sup>40,41</sup> and (ii) quaternary ammonium groups (**408–411**, Figure 79).<sup>43,99,168,252,253</sup> As can be seen in Figure 79, these solubilizing moieties have been attached: (i) to the NHC ligand, as in **406–407**; (ii) through the benzylidene, as in **408–410**; or (iii) via the anionic ligand, as in **411**. In particular, **406** efficiently initiates the ROMP of strained cyclic olefins in both water and methanol.<sup>40b</sup> In the former case, the presence of 1 equiv of HCl, relative to **406**, is necessary in order to protonate the dissociated tricyclohexylphosphine, thereby inhibiting its reassociation to the ruthenium center and preventing catalyst decomposition by base. Phosphine dissociation in water was proposed to be disfavored due to the energetic cost of solvating two neutral molecules. Catalyst **406**, which remains in solution throughout the entire metathesis reaction in water or MeOH, was also found to catalyze the RCM of benchmark dienes in MeOH. With the intention of avoiding the incorporation of the PEG–carbamoyl–benzyl moiety, which was suggested to reduce the stability of **406**, the PEG group (number average molecular weight  $\approx$  2600) has been alternatively appended on the backbone of the NHC ligand (**407**).<sup>41</sup> Indeed, water-soluble complex **407**, which is also soluble in common organic solvents such as dichloromethane and toluene, exerts improved stability and activity in water, compared to both **406** and all previously reported water-



**Figure 79.** Ruthenium metathesis catalysts **406–411** for use in water and protic solvents.

soluble bis(phosphine) catalysts. Thus, **407** efficiently carried out the ROMP of norbornene derivatives, the unprecedented RCM of a series of water-soluble  $\alpha,\omega$ -dienes, and the self-CM of *cis*-2-butene-1,4-diol. In an analogous fashion, complexes **255** and **256** (Figures 54 and 55, respectively), bearing PEG- and phosphorylcholine-substituted pyridine ligands, were more recently shown to initiate the ROMP of a PEG-containing oxanorbornene monomer under a variety of conditions.<sup>168</sup>

Further studies have furnished small-molecule catalysts **408** and **409**,<sup>252</sup> as well as **410**<sup>253</sup> and **411**<sup>43</sup> (Figure 79). In brief, **408** and **409** efficiently mediate a series of ROMP and RCM transformations in water,<sup>252</sup> whereas **410** performs RCM and CM reactions in water (only for X = I), alcohols, and homogeneous alcohol–water mixtures, even in the presence of air.<sup>253</sup> In micellar solutions, **410** acts both as an initiator and a surfactant promoting RCM and CM under heterogeneous aqueous conditions. Complex **411** also proved to be an efficient RCM catalyst in alcohols and homogeneous alcohol–water mixtures in air.<sup>43</sup> Complex **73** (Figure 16) can be transformed into its moderately water-soluble bisprotonated analogue by the addition of 2 equiv of HCl.<sup>99</sup> Unfortunately though, this bisprotonated complex suffers from a high decomposition rate, owing to the hydrolysis of the NHC–ruthenium bond.

Olefin metathesis in water can also be carried out by occluding existing homogeneous ruthenium catalysts in a hydrophobic matrix of polydimethylsiloxane and then using the resulting polydimethylsiloxane slabs in heterogeneous reactions.<sup>42,254</sup> For a more detailed discussion of heterogeneous olefin metathesis, refer to section 10. Finally, note that Raines and co-workers successfully utilized conventional



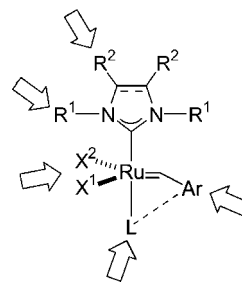
NHC-coordinated catalysts **3** and **5** (Figures 66 and 8, respectively) in RCM and CM reactions in homogeneous water/organic mixtures, achieving high conversions for a variety of substrates.<sup>255</sup>

### 10. Removal of Ruthenium Impurities from Metathesis Products and Ruthenium Recycling Strategies

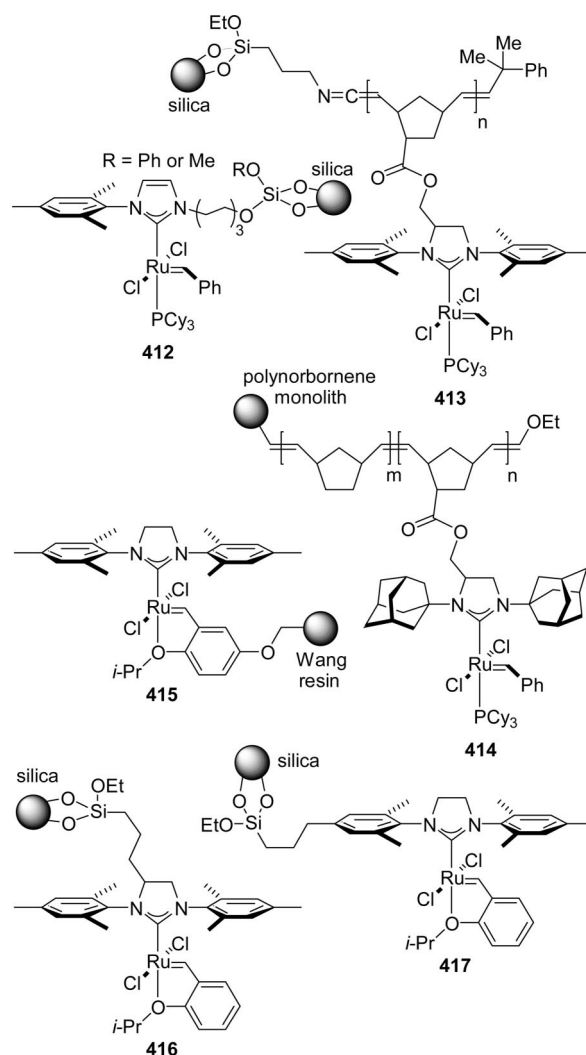
Despite the widespread use of ruthenium-catalyzed metathesis, removal of ruthenium byproducts at the end of the reaction is still rather challenging. In addition to pharmaceutical chemistry applications, where the acceptable ruthenium content is <10 ppm in the final compound, efficient purification of olefin metathesis products is also highly important in the case of polymeric materials, especially when these are to be used in electronics and other technologically advanced applications. Of equal importance is the unsuccessful exclusion of ruthenium impurities during the production of fine chemicals, which invokes the danger of undesired side-reactions in subsequent steps. Another closely related and very significant issue, from both an environmental and an economic point of view, is catalyst recycling and regeneration.

The most common strategies that have been thus far employed to address these problems are based on ruthenium catalyst tagging with (i) inorganic materials (e.g., silica gel); (ii) insoluble polymers; (iii) ionic liquid functionalities; (iv) perfluorinated hydrocarbons; or (v) soluble polymers or small-molecule functionalities. Ideally, these modified catalysts can be easily recovered from reaction mixtures by filtration (supports i and ii above) or by extracting the catalyst into the ionic liquid or fluorous phase (functionalities iii and iv, respectively), resulting in reduced ruthenium impurities. Another procedure involves precipitation controlled on demand, or purification via a chromatographic procedure (approach v). As illustrated in Figure 80, attachment of NHC-coordinated ruthenium catalysts with the above-mentioned functionalities can be achieved through the NHC nonlabile ligand (positions R<sup>1</sup> or R<sup>2</sup>), anionic ligand(s) X<sup>1</sup> and/or X<sup>2</sup>, the benzylidene moiety (Ar), or phosphine- or pyridine-based labile ligand(s) L. Besides affecting recycling along with easier and more efficient purification, immobilizing the catalytic complex onto a solid support has also been proposed to improve catalyst stability and prevent the undesirable bimolecular decomposition pathways, by inhibiting intermolecular catalyst–catalyst interactions via a phenomenon known as site isolation.<sup>256</sup> In view of the fact that this research field has been very well described in a series of recent review articles,<sup>257</sup> herein we only briefly discuss some representative examples.<sup>258</sup>

Catalysts of the types shown in Figure 81 (**412–417**)<sup>102,259–262</sup> are immobilized onto solid insoluble supports and are utilized in heterogeneous catalysis. Thus, **412** was prepared by immobilizing the precursor alcohol adduct on commercial silica gel, which was pretreated with MeSiCl<sub>3</sub> or PhSiCl<sub>3</sub> in order to install the necessary chlorosilane anchoring functionalities on its surface. **412** effects the RCM of a series of  $\alpha,\omega$ -dienes and could be reused up to three times; however, it was proved to exert lower catalytic activity compared to its homogeneous analogue.<sup>102</sup> **413**, immobilized onto non-porous silica with a 0.5 wt % ruthenium loading, also shows modest RCM activity in slurry-type reactions.<sup>259</sup> On the other hand, catalyst **414**, prepared with a loading of 1.4 wt %, efficiently promotes both ROMP and RCM transformations, while ruthenium contamination of the products was found to be as low as 70 ppm.<sup>260</sup> Silica-supported catalysts **416** and **417** were shown to competently catalyze a variety of model RCM and CM reactions.<sup>261</sup> **416** and **417** can be efficiently recycled multiple times and, most importantly, do not leach ruthenium, as revealed by inductively coupled plasma–mass spectrometry (ICP-MS) analysis of filtered reaction solutions (ruthenium contamination of filtrate < 5 ppb). **415** also could be recycled up to five times with no significant loss of activity in the CM of a series of highly electron-deficient alkenes;<sup>262</sup> other ruthenium isopropoxy-

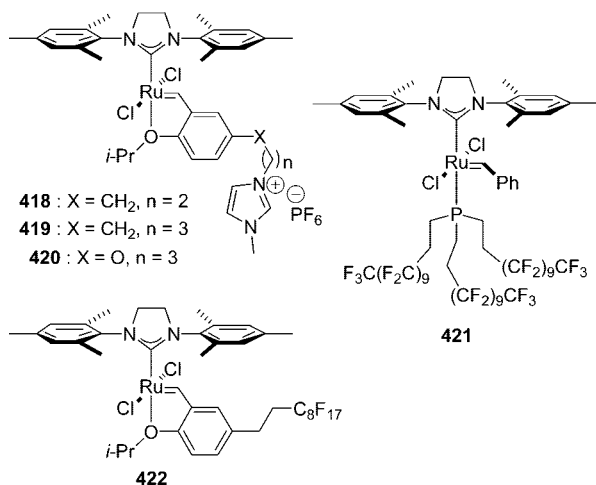


**Figure 80.** Variable positions for NHC-coordinated ruthenium catalysts tagging. The dashed line between Ar and L indicates that the coordinating ligand L may or may not be connected to the alkylidene.



**Figure 81.** Representative NHC-coordinated heterogeneous ruthenium catalysts **412–417**.

efficiently promotes both ROMP and RCM transformations, while ruthenium contamination of the products was found to be as low as 70 ppm.<sup>260</sup> Silica-supported catalysts **416** and **417** were shown to competently catalyze a variety of model RCM and CM reactions.<sup>261</sup> **416** and **417** can be efficiently recycled multiple times and, most importantly, do not leach ruthenium, as revealed by inductively coupled plasma–mass spectrometry (ICP-MS) analysis of filtered reaction solutions (ruthenium contamination of filtrate < 5 ppb). **415** also could be recycled up to five times with no significant loss of activity in the CM of a series of highly electron-deficient alkenes;<sup>262</sup> other ruthenium isopropoxy-

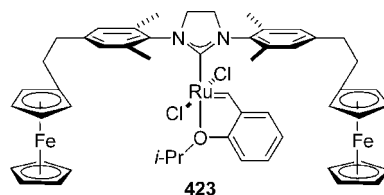


**Figure 82.** Examples of ionic-tagged and fluoruous-tagged ruthenium catalysts **418**–**422**.

benzylidenes, supported on monolithic silica discs, were reportedly reused in 20 cycles.<sup>263</sup> Note that in the case of “boomerang-type” catalysts resembling **415** (i.e., anchored through the benzylidene ligand), the active species are homogeneous. Nevertheless, it is proposed that a large fraction of these catalytically active ruthenium species are recaptured during metathesis, forming the more stable chelating isopropoxybenzylidenes, whereas complexes that decompose remain in solution.

The use of ionic liquids as alternative solvents provides many potential advantages over their conventional counterparts. These advantages include their high chemical and thermal stability, extremely low vapor pressure, insolubility or immiscibility with either aqueous or organic reaction media, and good ability to solvate both polar and nonpolar species. In this context, specially designed catalysts incorporating an ionic moiety into their structure, such as **198**,<sup>147a</sup> **410**,<sup>253</sup> or **418**–**420**<sup>264–268</sup> in Figures 45, 79, and 82, respectively, have been exploited in ruthenium-catalyzed biphasic (i.e., organic solvent/ionic liquid) olefin metathesis reactions, aiming at the recovery and reusability of the catalyst. In brief, **198**<sup>147a</sup> and **410**<sup>253</sup> efficiently promote olefin metathesis in organic solvents, aqueous media, and ionic liquids, leading to levels of ruthenium contamination in the products as low as 25 and 12 ppm, respectively, after a simple filtration through silica gel; however, they both display poor recyclability, and their activity is significantly reduced in the second cycle. On the contrary, complexes **419**<sup>265,266</sup> and **420**<sup>267b</sup> are very efficient RCM catalysts and display relatively high recyclability (i.e., they can be reused up to 8 and 17 times, respectively, with no significant loss of activity). Furthermore, **419** affords low ruthenium contamination levels in the ring-closed products (1–22 ppm).

As noted above, attempts to eliminate ruthenium contamination have been carried out by utilizing ruthenium complexes bearing fluoruous tags, either via filtration through a short pad of fluoruous-phase silica gel or by fluoruous-phase extraction. For example, complex **421** (Figure 82) was found to be efficient in the RCM of benchmark  $\alpha,\omega$ -dienes under both monophasic (CH<sub>2</sub>Cl<sub>2</sub>) and biphasic (CH<sub>2</sub>Cl<sub>2</sub>/fluoruous solvent mixtures) conditions; the rate acceleration observed in the latter case was proposed to arise from phase transfer of the dissociated fluoruous phosphine.<sup>269</sup> Moreover, **421** could be recycled up to three times with no significant loss of activity, by extracting the reaction mixtures with perflu-

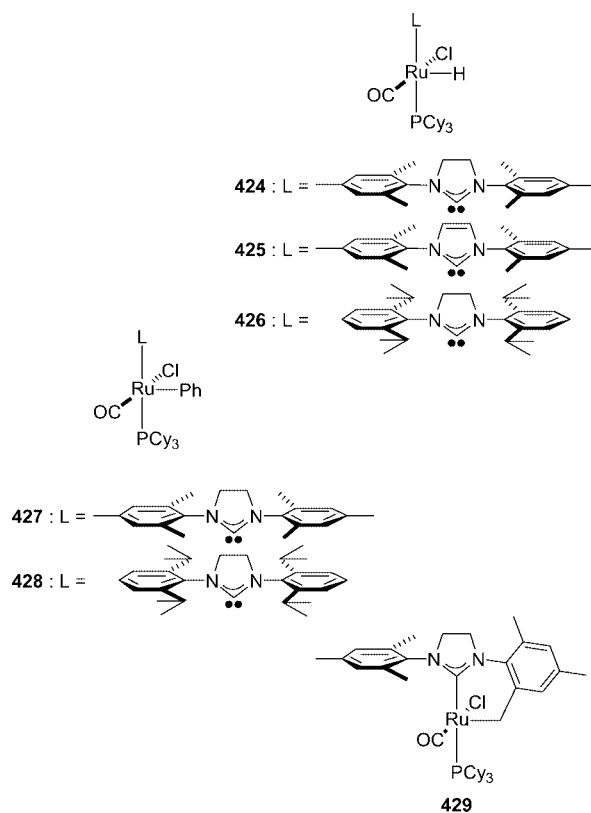


**Figure 83.** Ruthenium-based catalyst **423** bearing two ferrocenyl moieties.

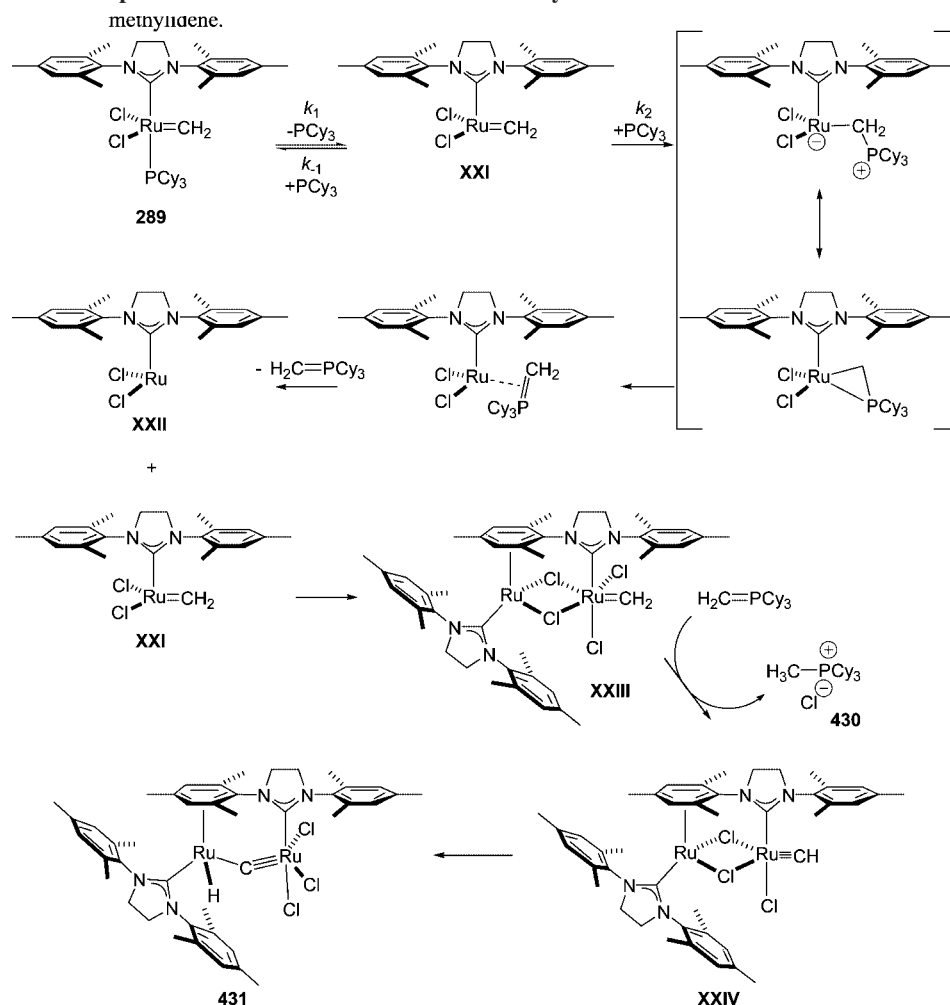
ro(methylcyclohexane). Fluoruous-tagged complex **422** (Figure 82) was also shown to be highly active in RCM and CM transformations of terminal olefins.<sup>270</sup> Removal of ruthenium residues from the metathesized products was achieved either by fluoruous-phase extraction or by filtration through fluoruous-phase silica gel, resulting in ruthenium contamination levels as low as 500 ppm.

An alternative, on-demand purification and recycling strategy, employing the redox-switchable ferrocenyl moieties in complex **423** (Figure 83), was published by Süßner and Plenio in 2005.<sup>271</sup> In particular, after utilizing soluble catalyst **423** to catalyze the RCM of *N,N*-diallyl tosylamine, they were able to in situ oxidize its two ferrocenyl moieties, causing its precipitation and separation from the reaction products; precipitated and washed **423** could then be easily redissolved by reduction. By repeating the same protocol, **423** could efficiently perform up to three consecutive metathesis-redox cycles.

Ruthenium contamination levels as low as 41 ppm were achieved by simply extracting the RCM reaction mixtures carried out by **407** (Figure 79) with water.<sup>272</sup> Furthermore, treatment of the ring-closed products with activated carbon after aqueous extraction led to ruthenium levels below 0.04 ppm (ICP-MS). Other published strategies, attempting to address the difficulties in removing ruthenium residues



**Figure 84.** Ruthenium-based metathesis catalysts degradation adducts **424**–**429**.

Scheme 12. Proposed Decomposition Mechanism for Ruthenium Methylidene **289**

coming from homogeneous metathesis catalysts, include (i) purification of the products on silica gel along with treatment with activated carbon (ruthenium contamination levels as low as 60 ppm);<sup>273</sup> (ii) use of ruthenium scavengers, such as dimethyl sulfoxide,<sup>274</sup> Ph<sub>3</sub>P=O,<sup>274</sup> or lead tetraacetate,<sup>275</sup> in combination with column chromatography (residual ruthenium levels as low as 240 ppm); (iii) treatment of the metathesized products with amine-modified silica (ruthenium contamination less than 2000 ppm);<sup>276</sup> and (iv) treatment of the metathesis product(s) mixture with isocyanide CNCH<sub>2</sub>CO<sub>2</sub>K (residual ruthenium as low as 120 ppm)<sup>277</sup> or tris(hydroxymethyl)phosphine.<sup>278</sup>

### 11. Decomposition Studies

Understanding the decomposition pathways of existing ruthenium-based metathesis catalysts is crucial for the development of new, more efficient catalysts, by rationally designing and utilizing adjusted ligand environments that reduce reactions that result in alkylidene loss. Along these lines, hydridocarbonyl chlorides **424–426** and phenylcarbonyl chlorides **427** and **428** (Figure 84), formed in basic alcoholic solutions upon prolonged heating of the corresponding benzylidenes, comprise the first reported family of heterocyclic carbene-coordinated ruthenium catalyst degradation adducts.<sup>53,279,280</sup> Note that **424** is also formed upon prolonged heating of parent complex **3** (Figure 66) in the presence of oxygen-containing substrates such as ethyl vinyl ether,<sup>53</sup> and **427** can also be produced by the reaction

of solid **3** with oxygen in 29% isolable yield.<sup>279</sup> Complexes **424–428** are derived through alcohol decarbonylation, although the exact mechanism of this process is still unknown. Moreover, while many of these complexes are highly efficient hydrogenation- and olefin isomerization<sup>87</sup> catalysts, they usually do not impose significant problems on olefin metathesis reactions carried out in alcoholic solvents, due to the high temperatures and prolonged reaction times needed for their production.<sup>279,280</sup> Structurally similar species **429** (Figure 84), encompassing an H<sub>2</sub>IMes ligand that has undergone C–H bond activation on one of its *ortho*-methyl groups, is formed when **3** is prepared under a moderately rigorous inert atmosphere.<sup>53</sup> However, it should be noted that none of the above decomposition adducts (**424–429**) are formed from typical metathesis conditions employing aprotic solvents (e.g., dichloromethane, benzene, or toluene), and consequently, their generation cannot be considered universal.

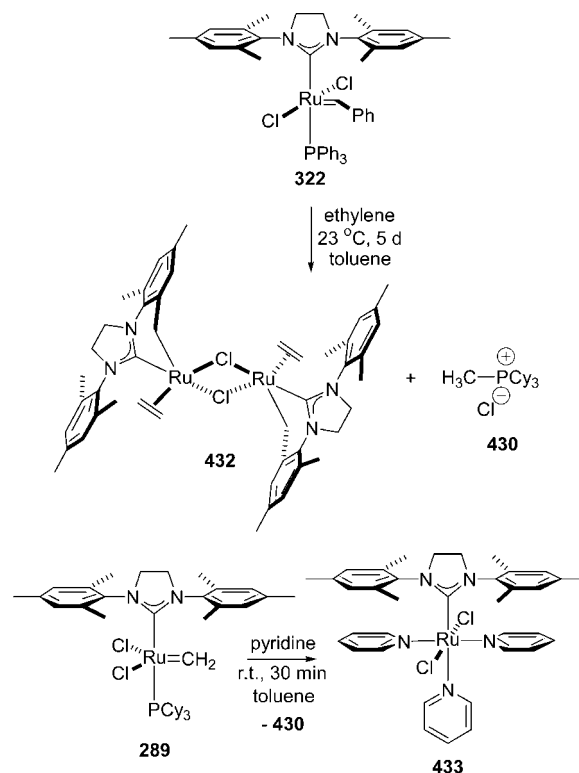
On the contrary, by taking into consideration that ruthenium methylidenes such as **289** (Scheme 12) are common intermediates in most metathesis reactions, studying their decomposition was expected to shed some light on ruthenium catalyst degradation in general. Initial investigations revealed that **289** decomposes rapidly ( $t_{1/2} = 5$  h 40 min) compared to the parent benzylidene complex **3** (Figure 66), via a unimolecular pathway, despite exhibiting very low initiation rates.<sup>24,281</sup> While decomposition of **3** was found to be inhibited by adding free phosphines, this was certainly not

the case with **289**. Subsequent studies led to the isolation of the first well-characterized decomposition products of **289**, namely, **430** and **431** (Scheme 12).<sup>282</sup> As shown by X-ray crystallographic analysis, dinuclear ruthenium hydride **431** bears a bridging carbide between the two ruthenium centers (Ru1 and Ru2), whereas the complete loss of phosphine ligands is accompanied by  $\eta^6$ -binding of Ru2 to one of the mesityl rings in the NHC on Ru1. The proposed mechanism for the formation of methyltricyclohexylphosphonium chloride (**430**) and binuclear complex **431** is illustrated in Scheme 12. Decomposition of **289** commences by nucleophilic attack of dissociated tricyclohexylphosphine on the methylidene moiety of **XXI**. Next, the 12-electron species **XXII**, formed upon elimination of phosphonium ylide  $\text{CH}_2=\text{PCy}_3$ , binds one of the mesityl rings of **XXI** to afford **XXIII**. Terminal alkylidyne species **XXIV**, along with **430**, are then generated through HCl abstraction by  $\text{CH}_2=\text{PCy}_3$ . In the final step, insertion into the alkylidyne C–H bond in **XXIV** with concomitant migration of the two chlorides leads to the formation of **431**, isolated as an orange–yellow crystalline solid in 46% yield. It is important to emphasize that complex **431** was found to catalyze alkene isomerization under metathesis conditions, suggesting that the above-described decomposition route of methylidene **289**, and accordingly (pre)catalyst **3**, could be responsible for competing unwanted alkene isomerization reactions during olefin metathesis transformations carried out by **3**.

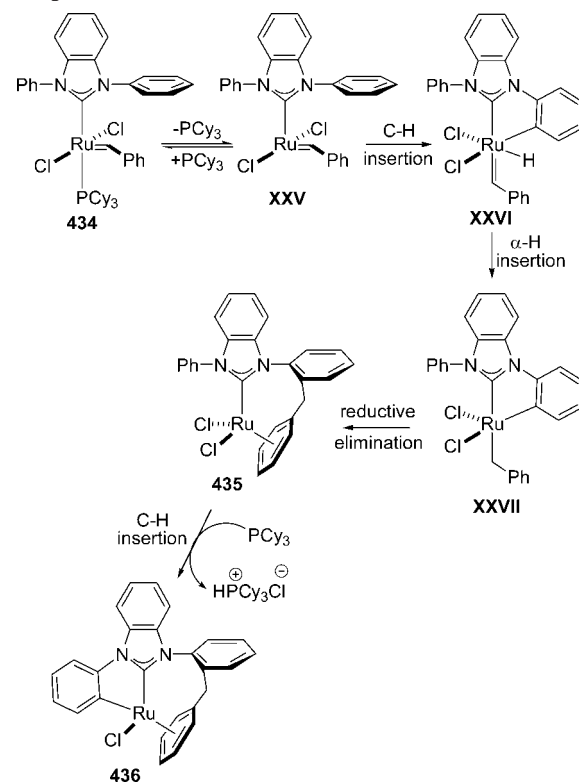
Expanding this decomposition study, to include other heteroleptic (phosphine–NHC) model ruthenium methylidenes, confirmed the assumption of phosphine attack on the methylidene carbon along the major decomposition pathway.<sup>95</sup> This was also found to be the case in decomposition experiments performed in the presence of ethylene as a model olefin substrate. Thus, after five days at room temperature, in a toluene solution under an atmosphere of ethylene, complex **322** (Scheme 13) was found to quantitatively afford methyltricyclohexylphosphonium chloride **430** along with binuclear complex **432** (in about 70% yield). With the exception of the necessary *ortho*-methyl C–H bond activation step of the NHC ligands, the proposed mechanistic pathway for the generation of **432** was essentially the same as for complex **431**. Finally, tris(pyridine) decomposition adduct **433** (Scheme 13) was isolated in 29% yield during attempts to prepare the corresponding bis(pyridine) ruthenium methylidene.

In related studies, *N*-phenyl-substituted NHC-coordinated ruthenium complexes were shown to also be prone to C–H bond activation.<sup>94</sup> In particular, when complex **434** (Scheme 14) was heated in benzene at 60 °C for 3 days, decomposition adduct **435** precipitated in 58% yield, together with traces (<2%) of **436** (Scheme 14). When **434** was heated in dichloromethane at 40 °C, the isolated yields of **435** and **436** after 12 h were 24% and 38%, respectively. The structures of both **435** and **436** were elucidated by X-ray crystallographic analysis, and the mechanism proposed to rationalize their generation is illustrated in Scheme 14. Intermediate **XXVI**, formed by the oxidative addition of an *ortho* C–H bond of one of the *N*-phenyl NHC substituents to the ruthenium center, undergoes hydride insertion at the  $\alpha$ -carbon atom of the benzylidene to afford **XXVII**. This is followed by reductive elimination between the metalated phenyl carbon atom of the NHC and the  $\alpha$ -carbon atom of benzylidene to yield complex **435**. Decomposition adduct

**Scheme 13. Decomposition of Ruthenium Complexes 289 and 322**



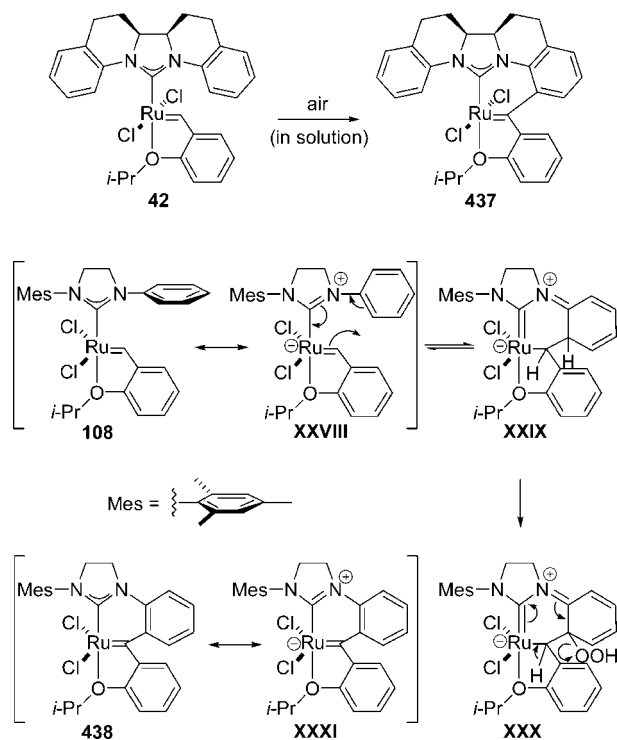
**Scheme 14. Proposed Mechanistic Pathway for the Decomposition of 434**



**436** is finally generated via a second C–H insertion and  $\text{PCy}_3$ -mediated elimination of HCl.

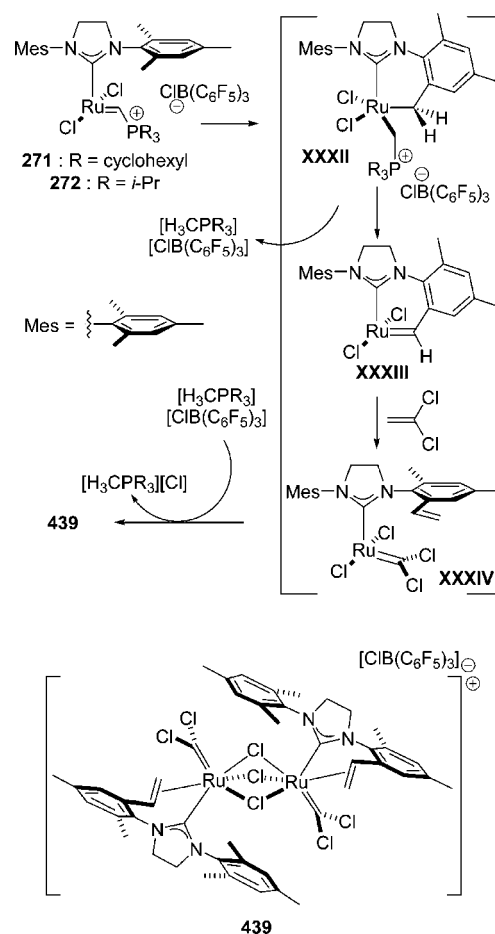
NHC-coordinated alkoxybenzylidene complexes lacking *ortho* substituents on the *N*-aryl groups of the NHCs show a high decomposition tendency via *ortho* C–H bond activation. Hence, in 2007, Blechert and co-workers reported the



**Scheme 15. Decomposition of Ruthenium Complexes 42 and 108**

isolation of oxidative degradation products **437** and **438**, derived from solutions of complexes **42** and **108**, respectively, in the presence of oxygen (Scheme 15).<sup>92</sup> As expected, **437** and **438** were found to be completely metathesis inactive. The proposed mechanistic pathway for the formation of **438** (Scheme 15) begins with a pericyclic cyclization reaction of valence structure **XXVIII** leading to **XXIX**. Reaction with oxygen (**XXX**) followed by elimination and rearomatization (**XXXI**) affords the final insertion product **438**. As also mentioned in section 3.1, this deactivation route, involving *ortho* C–H bond activation of *N*-phenyl groups in NHC-coordinated ruthenium complexes, can be shut off by placing bulky substituents on the backbone of the NHC, thereby restricting the intramolecular rotation of the *N*-aryl groups that brings the *ortho*-aryl C–H bonds closer to the ruthenium center.<sup>96</sup>

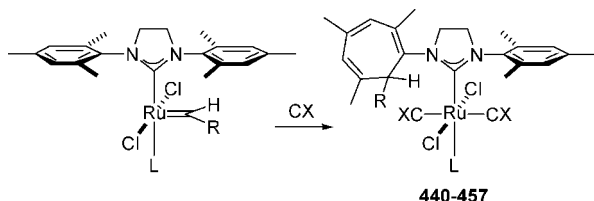
In 2008, Piers and co-workers published a detailed work on the thermal decomposition of 14-electron phosphonium alkylidene species **271** and **272** (Scheme 16).<sup>283</sup> During their studies, in which they utilized 1,1-dichloroethylene as a trapping agent, the formation of cationic trichloride-bridged dimer **439** (Scheme 16) was observed in 40–45% NMR yield, along with methylphosphonium chloride  $[\text{H}_3\text{CPR}_3]^+\text{Cl}^-$ . As can be seen in Scheme 16, **439** contains a dichloromethylidene and a vinyl-modified NHC ligand at each ruthenium center. The mechanism proposed to account for all findings (characterization of decomposition adducts as well as kinetic isotope effects and deuterium-labeling studies) includes the C–H bond activation of an *ortho*-methyl group of one of the *N*-mesityl substituents (**XXXII**), followed by elimination of the methylphosphonium species (isolated) to yield the cyclometalated ruthenium benzylidene **XXXIII**. Intermediate species **XXXIV**, formed after the CM reaction of highly reactive **XXXIII** with 1,1-dichloroethylene, eventually undergoes loss of a chloride anion and dimerization to afford the final degradation product **439**.

**Scheme 16. Proposed Decomposition Mechanism for Complexes 271 and 272**

$\text{H}_2\text{IMes}$ -coordinated ruthenium complexes bearing phosphine ligands have been also found to undergo carbon monoxide- and aryl isocyanide-promoted alkylidene insertion into the aryl substituent of their  $\text{H}_2\text{IMes}$  ligand.<sup>277,284,285</sup> In fact, catalyst degradation adducts of this kind (**440**–**455**, Scheme 17) were initially observed during attempts to develop a rapidly quenching procedure for metathesis reactions by blocking any available coordination sites with carbon monoxide. Aryl isocyanides promote the same insertion reaction for isopropoxybenzylidene-coordinated  $\text{H}_2\text{IMes}$  ruthenium complexes, but only after initial displacement of the coordinated ether by a phosphine (**456**, **457**, Scheme 17).<sup>285</sup> Ruthenium complexes **440**–**457** were reported to form through carbon monoxide or aryl isocyanide coordination-triggered carbene cyclopropanation of the closest “double bond” of the mesityl ring, followed by electrocyclic ring-opening of the resulting cyclopropane derivative to afford the final cycloheptatriene.<sup>284,285</sup> As discussed in section 10, this isocyanide-promoted degradation route has also been utilized as a “cleanup” procedure for metathesis transformations.<sup>277</sup> Finally, it should be noted that a number of theoretical calculations have dealt with the decomposition of ruthenium olefin metathesis catalysts.<sup>286</sup> For example, on the basis of a series of DFT calculations, van Rensburg and co-workers have suggested a substrate-induced decomposition mechanism involving a  $\beta$ -hydride transfer from a ruthenacyclobutane intermediate.<sup>286a,b</sup>

To summarize, the most important decomposition modes of NHC-coordinated catalyst precursors and intermediates include (i) degradation with primary alcohols, producing

### Scheme 17. Carbon Monoxide- or Aryl Isocyanide-Promoted Transformation of H<sub>2</sub>IMes-Substituted Ruthenium Alkylidenes



insertion adduct	R	L	CX
440	Ph	PCy <sub>3</sub>	CO
441	H	PCy <sub>3</sub>	CO
442	Me	PCy <sub>3</sub>	CO
443	CH=CHMe <sub>2</sub>	PCy <sub>3</sub>	CO
444	Ph	PCy <sub>3</sub>	4-CiC <sub>6</sub> H <sub>4</sub> NC
445	H	PCy <sub>3</sub>	4-CiC <sub>6</sub> H <sub>4</sub> NC
446	Me	PCy <sub>3</sub>	4-CiC <sub>6</sub> H <sub>4</sub> NC
447	4-NO <sub>2</sub> -C <sub>6</sub> H <sub>4</sub> O	PPh <sub>3</sub>	CO
448	Ph	PMe <sub>3</sub>	CO
449	Ph	PBu <sub>3</sub>	CO
450	Ph	PPh <sub>3</sub>	CO
451	Ph	P(O <i>i</i> -Pr) <sub>3</sub>	CO
452	Ph	PBu <sub>3</sub>	4-CiC <sub>6</sub> H <sub>4</sub> NC
453	Ph	PPh <sub>3</sub>	4-CiC <sub>6</sub> H <sub>4</sub> NC
454	Ph	PMe <sub>3</sub>	4-CiC <sub>6</sub> H <sub>4</sub> NC
455	Ph	P(O <i>i</i> -Pr) <sub>3</sub>	4-CiC <sub>6</sub> H <sub>4</sub> NC
456	2-(O <i>i</i> -Pr)-C <sub>6</sub> H <sub>4</sub>	PCy <sub>3</sub>	4-CiC <sub>6</sub> H <sub>4</sub> NC
457	2-(O <i>i</i> -Pr)-C <sub>6</sub> H <sub>4</sub>	PPh <sub>3</sub>	4-CiC <sub>6</sub> H <sub>4</sub> NC

ruthenium hydrido carbonyls; (ii) insertion of ruthenium into the C–H bond of the methyl groups of the H<sub>2</sub>IMes ligand; (iii) carbon monoxide- or aryl isocyanide-promoted benzylidene or methylidene insertion into one of the aryl substituents of their NHC ligand; (iv) nucleophilic attack of a dissociated phosphine molecule on the methylidene carbon of ruthenium methylidenes, forming the corresponding carbide-bridged dimers; and (v) *ortho* C–H bond activation of one of the *N*-aryl NHC substituents in ruthenium complexes lacking *ortho* substituents on the *N*-aryl groups of the NHCs.

## 12. Conclusions and Perspectives

As discussed above, nearly 400 ruthenium heterocyclic carbene-coordinated olefin metathesis catalysts have been prepared. They offer a wide array of structures and activities that will benefit specific applications such as aqueous and asymmetric reactions. In spite of all these structures, it is pleasing to recognize that, for most applications, a few structures will provide excellent results. The *N*-mesityl and *N*-tolyl NHC-coordinated complexes bearing chelating alkoxylbenzylidene ligands provide an excellent starting point for most applications. It also appears as though the mechanisms of all the complexes involve the formation of a 14-electron species that adds an olefin to initiate the reaction. The general reactivity can be understood in terms of the effect of a ligand on the initiation formation of the 14-electron species and the turnover of the olefin complex. Given the increasing rate at which new catalysts are now appearing, we look forward to further surprises and control mechanisms.

## 13. Acknowledgments

The authors are grateful for financial support provided by the National Science Foundation, the National Institutes of

Health, and the 6th European Community Framework Programme.

## 14. References

- (1) (a) Anderson, A. W.; Merckling, N. G. (Du Pont de Nemours & Co.) U.S. Patent 2,721,189, 1955. Also see: (b) Truett, W. L.; Johnson, D. R.; Robinson, I. M.; Montague, B. A. *J. Am. Chem. Soc.* **1960**, *82*, 2337.
- (2) The term “disproportionation”, used by Banks and Bailey, actually refers to the overall process of olefin metathesis and olefin isomerization: Banks, R. L.; Bailey, G. C. *Ind. Eng. Chem., Prod. Res. Dev.* **1964**, *3*, 170.
- (3) (a) Calderon, N.; Chem, H. Y.; Scott, K. W. *Tetrahedron Lett.* **1967**, *34*, 3327. (b) Calderon, N. *Acc. Chem. Res.* **1972**, *5*, 127.
- (4) Ivin, K. J.; Mol, J. C. *Olefin Metathesis and Metathesis Polymerization*; Academic Press: San Diego, CA, 1997.
- (5) Grubbs, R. H. *Handbook of Metathesis*; Wiley-VCH: Weinheim, Germany, 2003.
- (6) For the 2005 Nobel Prize in Chemistry Lectures, see: (a) Chauvin, Y. *Angew. Chem., Int. Ed.* **2006**, *45*, 3740. (b) Schrock, R. R. *Angew. Chem., Int. Ed.* **2006**, *45*, 3748. (c) Grubbs, R. H. *Angew. Chem., Int. Ed.* **2006**, *45*, 3760.
- (7) (a) Hérisson, J.-L.; Chauvin, Y. *Makromol. Chem.* **1971**, *141*, 161.
- (8) For a series of mechanistic studies that followed the hypothesis of the metallacyclobutane mechanism, see: (a) Katz, T. J.; McGinnis, J. J. *J. Am. Chem. Soc.* **1975**, *97*, 1592. (b) Grubbs, R. H.; Burk, P. L.; Carr, D. D. *J. Am. Chem. Soc.* **1975**, *97*, 3265. (c) Katz, T. J.; Rothchild, R. J. *J. Am. Chem. Soc.* **1976**, *98*, 2519. (d) Grubbs, R. H.; Carr, D. D.; Hoppin, C.; Burk, P. L. *J. Am. Chem. Soc.* **1976**, *98*, 3478. (e) Katz, T. J.; McGinnis, J. J. *J. Am. Chem. Soc.* **1977**, *99*, 1903. Also see ref 5 and (f) Leconte, M.; Basset, J.-M.; Quignard, F.; Larroche, C. Mechanistic Aspects of the Olefin Metathesis Reaction. In *Reactions of Coordinated Ligands*; Braterman, P. S., Ed.; Plenum: New York, 1986; Vol. 1, pp 371–420.
- (9) Slugovc, C. *Macromol. Rapid Commun.* **2004**, *25*, 1283.
- (10) Wiberg, K. B. *Angew. Chem., Int. Ed. Engl.* **1986**, *25*, 312.
- (11) Tebbe, F. N.; Parshall, G. W.; Reddy, G. S. *J. Am. Chem. Soc.* **1978**, *100*, 3611.
- (12) (a) Schrock, R. R. *J. Am. Chem. Soc.* **1975**, *97*, 6577. (b) Wood, C. D.; McLain, S. J.; Schrock, R. R. *J. Am. Chem. Soc.* **1979**, *101*, 3210. (c) Rocklage, S. M.; Fellmann, J. D.; Rupprecht, G. A.; Messerle, L. W.; Schrock, R. R. *J. Am. Chem. Soc.* **1981**, *103*, 1440. (d) Wallace, K. C.; Liu, A. H.; Dewan, J. C.; Schrock, R. R. *J. Am. Chem. Soc.* **1988**, *110*, 4964.
- (13) (a) Katz, D. J.; Lee, S. J.; Acton, S. *Tetrahedron Lett.* **1976**, *47*, 4247. (b) Kress, J.; Wesolek, M.; Osborn, J. A. *J. Chem. Soc., Chem. Commun.* **1982**, 514. (c) Katz, T. J.; Sivavec, T. M. *J. Am. Chem. Soc.* **1985**, *107*, 737. (d) Quignard, F.; Leconte, M.; Basset, J.-M. *J. Chem. Soc., Chem. Commun.* **1985**, 1816. (e) Kress, J.; Aguero, A.; Osborn, J. A. *J. Mol. Catal.* **1986**, *36*, 1. (f) Schaverien, C. J.; Dewan, J. C.; Schrock, R. R. *J. Am. Chem. Soc.* **1986**, *108*, 2771. (g) Kress, J.; Osborn, J. A.; Greene, R. M. E.; Ivin, K. J.; Rooney, J. J. *J. Am. Chem. Soc.* **1987**, *109*, 899. (h) Schrock, R. R.; DePue, R. T.; Feldman, J.; Schaverien, C. J.; Dewan, J. C.; Liu, A. H. *J. Am. Chem. Soc.* **1988**, *110*, 1423.
- (14) (a) Schrock, R. R.; Murdzek, J. S.; Bazan, G. C.; Robbins, J.; DiMare, M.; O'Regan, M. B. *J. Am. Chem. Soc.* **1990**, *112*, 3875. (b) Bazan, G. C.; Khosravi, E.; Schrock, R. R.; Feast, W. J.; Gibson, V. C.; O'Regan, M. B.; Thomas, J. K.; Davis, W. M. *J. Am. Chem. Soc.* **1990**, *112*, 8378. (c) Bazan, G. C.; Oskam, J. H.; Cho, H.-N.; Park, L. Y.; Schrock, R. R. *J. Am. Chem. Soc.* **1991**, *113*, 6899. (d) Aeilts, S. L.; Cefalo, D. R.; Bonitatebus, P. J., Jr.; Houser, J. H.; Hoveyda, A. H.; Schrock, R. R. *Angew. Chem., Int. Ed.* **2001**, *40*, 1452.
- (15) Armstrong, S. K. *J. Chem. Soc., Perkin Trans. 1* **1998**, 371.
- (16) Trnka, T. M.; Grubbs, R. H. *Acc. Chem. Res.* **2001**, *34*, 18.
- (17) Grubbs, R. H. *Tetrahedron* **2004**, *60*, 7117.
- (18) (a) Michelotti, F. W.; Keaveney, W. P. *J. Polym. Sci.* **1965**, *A3*, 895. (b) Rinehart, R. E.; Smith, H. P. *Polym. Lett.* **1965**, *3*, 1049.
- (19) (a) Novak, B. M.; Grubbs, R. H. *J. Am. Chem. Soc.* **1988**, *110*, 960. (b) Novak, B. M.; Grubbs, R. H. *J. Am. Chem. Soc.* **1988**, *110*, 7542.
- (20) (a) France, M. B.; Paciello, R. A.; Grubbs, R. H. *Macromolecules* **1993**, *26*, 4739. (b) France, M. B.; Grubbs, R. H.; McGrath, D. V.; Paciello, R. A. *Macromolecules* **1993**, *26*, 4742.
- (21) Nguyen, S. T.; Johnson, L. K.; Grubbs, R. H.; Ziller, J. W. *J. Am. Chem. Soc.* **1992**, *114*, 3974.
- (22) (a) Schwab, P.; France, M. B.; Ziller, J. W.; Grubbs, R. H. *Angew. Chem., Int. Ed. Engl.* **1995**, *34*, 2039. (b) Schwab, P.; Grubbs, R. H.; Ziller, J. W. *J. Am. Chem. Soc.* **1996**, *118*, 100. Ruthenium-based metathesis catalysts (L<sub>2</sub>X<sub>2</sub>Ru=CHR) are usually divided into two families: the first- and the second-generation ones. In the first-generation catalysts, both neutral ligands (L) are phosphines, while

- in the second-generation ones, one of the neutral ligands is a heterocyclic carbene.
- (23) Scholl, M.; Ding, S.; Lee, C. W.; Grubbs, R. H. *Org. Lett.* **1999**, *1*, 953.
- (24) Sanford, M. S.; Love, J. A.; Grubbs, R. H. *J. Am. Chem. Soc.* **2001**, *123*, 6543.
- (25) Kingsbury, J. S.; Harrity, J. P. A.; Bonitatebus, P. J., Jr.; Hoveyda, A. H. *J. Am. Chem. Soc.* **1999**, *121*, 791.
- (26) Garber, S. B.; Kingsbury, J. S.; Gray, B. L.; Hoveyda, A. H. *J. Am. Chem. Soc.* **2000**, *122*, 8168.
- (27) Gessler, S.; Randl, S.; Blechert, S. *Tetrahedron Lett.* **2000**, *41*, 9973.
- (28) Review articles on the applications of olefin metathesis include the following: (a) Grubbs, R. H.; Miller, S. J.; Fu, G. C. *Acc. Chem. Res.* **1995**, *28*, 446. (b) Schuster, M.; Blechert, S. *Angew. Chem., Int. Ed. Engl.* **1997**, *36*, 2037. (c) Grubbs, R. H.; Chang, S. *Tetrahedron* **1998**, *54*, 4413. (d) Armstrong, S. K. *J. Chem. Soc., Perkin Trans. 1* **1998**, 371. (e) Ivin, K. J. *J. Mol. Catal. A: Chem.* **1998**, *133*, 1. (f) Buchmeiser, M. R. *Chem. Rev.* **2000**, *100*, 1565. (g) Fürstner, A. *Angew. Chem., Int. Ed.* **2000**, *39*, 3012. (h) Connon, S. J.; Blechert, S. *Angew. Chem., Int. Ed.* **2003**, *42*, 1900. (i) Schrock, R. R.; Hoveyda, A. H. *Angew. Chem., Int. Ed.* **2003**, *42*, 4592. (j) Donohoe, T. J.; Orr, A. J.; Bingham, M. *Angew. Chem., Int. Ed.* **2006**, *45*, 2664. (k) Binder, J. B.; Raines, R. T. *Curr. Opin. Struct. Biol.* **2008**, *12*, 767.
- (29) Seiders, T. J.; Ward, D. W.; Grubbs, R. H. *Org. Lett.* **2001**, *3*, 3225.
- (30) van Veldhuizen, J. J.; Garber, S. B.; Kingsbury, J. S.; Hoveyda, A. H. *J. Am. Chem. Soc.* **2002**, *124*, 4954.
- (31) van Veldhuizen, J. J.; Gillingham, D. G.; Garber, S. B.; Kataoka, O.; Hoveyda, A. H. *J. Am. Chem. Soc.* **2003**, *125*, 12502.
- (32) Gillingham, D. G.; Kataoka, O.; Garber, S. B.; Hoveyda, A. H. *J. Am. Chem. Soc.* **2004**, *126*, 12288.
- (33) van Veldhuizen, J. J.; Campbell, J. E.; Giudici, R. E.; Hoveyda, A. H. *J. Am. Chem. Soc.* **2005**, *127*, 6877.
- (34) Funk, T. W.; Berlin, J. M.; Grubbs, R. H. *J. Am. Chem. Soc.* **2006**, *128*, 1840.
- (35) Berlin, J. M.; Goldberg, J. M.; Grubbs, R. H. *Angew. Chem., Int. Ed.* **2006**, *45*, 7591.
- (36) Giudici, R. E.; Hoveyda, A. H. *J. Am. Chem. Soc.* **2007**, *129*, 3824.
- (37) Lynn, D. M.; Mohr, B.; Grubbs, R. H.; Henling, L. M.; Day, M. W. *J. Am. Chem. Soc.* **2000**, *122*, 6601.
- (38) Lynn, D. M.; Grubbs, R. H. *J. Am. Chem. Soc.* **2001**, *123*, 3187.
- (39) Rölle, T.; Grubbs, R. H. *Chem. Commun.* **2002**, 1070.
- (40) (a) Varray, S.; Lazaro, R.; Martinez, J.; Lamaty, F. *Organometallics* **2003**, *22*, 2426. (b) Gallivan, J. P.; Jordan, J. P.; Grubbs, R. H. *Tetrahedron Lett.* **2005**, *46*, 2577.
- (41) Hong, S. H.; Grubbs, R. H. *J. Am. Chem. Soc.* **2006**, *128*, 3508.
- (42) Mwangi, M. T.; Runge, M. B.; Bowden, N. B. *J. Am. Chem. Soc.* **2006**, *128*, 14434.
- (43) Binder, J. B.; Guzei, I. A.; Raines, R. T. *Adv. Synth. Catal.* **2007**, *349*, 395.
- (44) Berlin, J. M.; Campbell, K.; Ritter, T.; Funk, T. W.; Chlenov, A.; Grubbs, R. H. *Org. Lett.* **2007**, *9*, 1339.
- (45) Stewart, I. C.; Ung, T.; Pletnev, A. A.; Berlin, J. M.; Grubbs, R. H.; Schrodi, Y. *Org. Lett.* **2007**, *9*, 1589.
- (46) (a) Öfele, K. J. *Organomet. Chem.* **1968**, *12*, 42. (b) Wanzlick, H. W.; Schönherr, H. J. *Angew. Chem., Int. Ed. Engl.* **1968**, *7*, 141.
- (47) (a) Cardin, D. J.; Cetinkaya, B.; Lappert, M. F. *Chem. Rev.* **1972**, *72*, 545. (b) Cardin, D. J.; Doyle, M. J.; Lappert, M. F. *J. Chem. Soc., Chem. Commun.* **1972**, 927.
- (48) (a) Arduengo, A. J., III; Harlow, R. J.; Kline, M. *J. Am. Chem. Soc.* **1991**, *113*, 361. (b) Arduengo, A. J., III; Kline, M.; Calabrese, J. C.; Davidson, F. *J. Am. Chem. Soc.* **1991**, *113*, 9704. Note that the first stable carbenes were isolated by Bertrand and co-workers. (c) Igau, A.; Grutzmacher, H.; Baceiredo, A.; Bertrand, G. *J. Am. Chem. Soc.* **1988**, *110*, 6463. (d) Igau, A.; Baceiredo, A.; Trinquier, G.; Bertrand, G. *Angew. Chem., Int. Ed. Engl.* **1989**, *28*, 621. For two excellent review articles on stable carbenes, see (e) Bourissou, D.; Guerret, O.; Gabbai, F. P.; Bertrand, G. *Chem. Rev.* **2000**, *100*, 39. (f) Canac, Y.; Soleilhavoup, M.; Conejero, F.; Bertrand, G. *J. Organomet. Chem.* **2004**, *689*, 3857.
- (49) Representative review articles: (a) Herrmann, W. A.; Köcher, C. *Angew. Chem., Int. Ed. Engl.* **1997**, *36*, 2162. (b) Herrmann, W. A. *Angew. Chem., Int. Ed.* **2002**, *41*, 1290. (c) Perry, M. C.; Burgess, K. *Tetrahedron: Asymmetry* **2003**, *14*, 951. (d) Hahn, F. E. *Angew. Chem., Int. Ed.* **2006**, *45*, 1348. (e) Kantchev, E. A. B.; O'Brien, C. J.; Organ, M. G. *Angew. Chem., Int. Ed.* **2007**, *46*, 2768. In addition: *Coordination Chemistry Reviews* has devoted a special issue on the organometallic chemistry of NHCs: **2007**, *251* (5–6), 595–896. *Chemical Reviews* has also devoted a special issue on carbenes: **2009**, *109* (8), 3209–3884. *European Journal of Inorganic Chemistry* has devoted a special issue on *N*-heterocyclic carbene complexes: **2009**, (13), 1663–2007.
- (50) Representative review articles: (a) Enders, D.; Balensiefer, T. *Acc. Chem. Res.* **2004**, *37*, 534. (b) Nair, V.; Bindu, S.; Sreekumar, V. *Angew. Chem., Int. Ed.* **2004**, *43*, 5130. (c) Marion, N.; Diez-González, S.; Nolan, S. P. *Angew. Chem., Int. Ed.* **2007**, *46*, 2988.
- (51) (a) Cardin, D. J.; Cetinkaya, B.; Lappert, M. F. *Chem. Rev.* **1972**, *72*, 545. (b) Hu, X.; Castro-Rodriguez, I.; Olsen, K.; Meyer, K. *Organometallics* **2004**, *23*, 755. (c) Süßner, M.; Plenio, H. *Chem. Commun.* **2005**, 5417. (d) Cavallo, L.; Correa, A.; Costabile, C.; Jacobsen, H. *J. Organomet. Chem.* **2005**, *690*, 5407. (e) Jacobsen, H.; Correa, A.; Costabile, C.; Cavallo, L. *J. Organomet. Chem.* **2006**, *691*, 4350.
- (52) (a) Herrmann, W. A. *Synthetic Methods of Organometallic and Inorganic Chemistry*; Georg Thieme Verlag: Stuttgart, New York, 1995. (b) Herrmann, W. A.; Köcher, C.; Goossen, L. J.; Artus, G. R. *Chem.—Eur. J.* **1996**, *2*, 1627. (c) Arduengo, A. J., III; Krafczyk, R.; Schmutzler, R.; Craig, H. A.; Goerlich, J. R.; Marshall, W. J.; Unverzagt, M. *Tetrahedron* **1999**, *55*, 14523. (d) Weskamp, T.; Böhm, V. P. W.; Herrmann, W. A. *J. Organomet. Chem.* **2000**, *600*, 12. (e) Enders, D.; Gielen, H. J. *Organomet. Chem.* **2001**, *617*–618, 70. (f) Altenhoff, G.; Goddard, R.; Lehmann, C.; Glorius, F. *J. Am. Chem. Soc.* **2004**, *126*, 15195.
- (53) Trnka, T. M.; Morgan, J. P.; Sanford, M. S.; Wilhelm, T. E.; Scholl, M.; Choi, T. L.; Ding, S. D.; Day, M. W.; Grubbs, R. H. *J. Am. Chem. Soc.* **2003**, *125*, 2546.
- (54) Upon prolonged heating ruthenium–chloride complexes in the presence of *KOt*-Bu, substitution of the chlorides by *tert*-butoxide occurs: Sanford, M. S.; Henling, L. M.; Day, M. W.; Grubbs, R. H. *Angew. Chem., Int. Ed.* **2000**, *39*, 3451. This side-product can be avoided by using hexafluoro-*tert*-butoxide instead (ref 23).
- (55) (a) Nyse, G. W.; Csihony, S.; Waymouth, R. M.; Hedrick, J. L. *Chem.—Eur. J.* **2004**, *10*, 4073. (b) Voutchkova, A. M.; Appelhans, L. N.; Chianese, A. R.; Crabtree, R. H. *J. Am. Chem. Soc.* **2005**, *127*, 17624. (c) Tudose, A.; Delaude, L.; Andre, B.; Demonceau, A. *Tetrahedron Lett.* **2006**, *47*, 8529. (d) Voutchkova, A. M.; Feliz, M.; Clot, E.; Eisenstein, O.; Crabtree, R. H. *J. Am. Chem. Soc.* **2007**, *129*, 12834.
- (56) (a) Wang, H. M. J.; Lin, I. J. B. *Organometallics* **1998**, *17*, 972. (b) Lin, I. J. B.; Vasam, C. S. *Comments Inorg. Chem.* **2004**, *25*, 75. (c) de Frémont, P.; Scott, N. M.; Stevens, E. D.; Rammial, T.; Lightbody, O. C.; Macdonald, C. L. B.; Clyburne, J. A. C.; Abernethy, C. D.; Nolan, S. P. *Organometallics* **2005**, *24*, 6301. (d) Garrison, J. C.; Youngs, W. J. *Chem. Rev.* **2005**, *105*, 3978. (e) Yu, X. Y.; Patrick, P. O.; James, B. R. *Organometallics* **2006**, *25*, 2359.
- (57) Review articles on NHC-coordinated ruthenium complexes: (a) Jafarpour, L.; Nolan, S. P. *J. Organomet. Chem.* **2001**, *617*–618, 17. (b) Dragutan, I.; Dragutan, V.; Delaude, L.; Demonceau, A. *Arcivoc* **2005**, *x*, 206. (c) Despagne-Ayoub, E.; Ritter, T. *Top. Organomet. Chem.* **2007**, *21*, 193. (d) Schrodi, Y.; Pederson, R. L. *Aldrichim. Acta* **2007**, *40*, 45. (e) Colacino, E.; Martinez, J.; Lamaty, F. *Coord. Chem. Rev.* **2007**, *251*, 726. (f) Dragutan, V.; Dragutan, I.; Delaude, L.; Demonceau, A. *Coord. Chem. Rev.* **2007**, *251*, 765. (g) Samojłowicz, C.; Bieniek, M.; Grela, K. *Chem. Rev.* **2009**, *109*, 3708. Also see (h) Deshmukh, P. H.; Blechert, S. *Dalton Trans.* **2007**, 2479.
- (58) Weskamp, T.; Schattenmann, W. C.; Spiegler, M.; Herrmann, W. A. *Angew. Chem., Int. Ed.* **1998**, *37*, 2490.
- (59) Weskamp, T.; Kohl, F. J.; Hieringer, W.; Gleich, D.; Herrmann, W. A. *Angew. Chem., Int. Ed.* **1999**, *38*, 2416.
- (60) Scholl, M.; Trnka, T. M.; Morgan, J. P.; Grubbs, R. H. *Tetrahedron Lett.* **1999**, *40*, 2247.
- (61) Huang, J.; Stevens, E. D.; Nolan, S. P.; Petersen, J. L. *J. Am. Chem. Soc.* **1999**, *121*, 2674.
- (62) For an improved preparation protocol of complex **14a**, see: Jafarpour, L.; Nolan, S. P. *Organometallics* **2000**, *19*, 2055.
- (63) Weskamp, T.; Kohl, F. J.; Herrmann, W. A. *J. Organomet. Chem.* **1999**, *582*, 362.
- (64) Huang, J.; Schanz, H. J.; Stevens, E. D.; Nolan, S. P. *Organometallics* **1999**, *18*, 5375.
- (65) More recent studies of the carbonyl stretching frequencies in NHC-containing transition-metal complexes imply that saturated NHCs are marginally less electron-donating than their unsaturated analogues. Moreover, calorimetric studies suggest relatively small differences in the donor capacities between saturated and unsaturated NHCs. For a recent review article on the stereochemical and electronic properties of NHCs, see: Diez-Gonzalez, S.; Nolan, S. P. *Coord. Chem. Rev.* **2007**, *251*, 874.
- (66) (a) Chatterjee, A. K.; Morgan, J. P.; Scholl, M.; Grubbs, R. H. *J. Am. Chem. Soc.* **2000**, *122*, 3783. The performance of **3** in the CM of acrylate esters can be enhanced by the addition of *p*-cresol: (b) Forman, G. S.; Tooze, R. P. *J. Organomet. Chem.* **2005**, *690*, 5863.
- (67) For a study regarding the dependence of the RCM performance of **3** on solvent, see: Adjiman, C. S.; Clarke, A. J.; Cooper, G.; Taylor, P. C. *Chem. Commun.* **2008**, 2806.



- (68) Bielawski, C. W.; Grubbs, R. H. *Angew. Chem., Int. Ed.* **2000**, *39*, 2903.
- (69) Chatterjee, A. K.; Grubbs, R. H. *Org. Lett.* **1999**, *1*, 1751.
- (70) Jafarpour, L.; Hillier, A. C.; Nolan, S. P. *Organometallics* **2002**, *21*, 442.
- (71) Sanford, M. S.; Ulman, M.; Grubbs, R. H. *J. Am. Chem. Soc.* **2001**, *123*, 749.
- (72) Adlhart, C.; Chen, P. *Helv. Chim. Acta* **2003**, *86*, 941.
- (73) On the basis of element-specific X-ray spectroscopies and theoretical calculations, the increased initiation rate of the phosphine-coordinated catalysts was rationalized on the basis of a higher electron density on the metal center: (a) Getty, K.; Delgado-Jaime, M. U.; Kennepohl, P. *J. Am. Chem. Soc.* **2007**, *129*, 15774. Also see (b) Antonova, N. S.; Carbó, J. J.; Poblet, J. M. *Organometallics* **2009**, *28*, 4283.
- (74) Adlhart, C.; Chen, P. *Angew. Chem., Int. Ed.* **2002**, *41*, 4484.
- (75) Adlhart, C.; Chen, P. *J. Am. Chem. Soc.* **2004**, *126*, 3496.
- (76) Straub, B. F. *Angew. Chem., Int. Ed.* **2005**, *44*, 5974.
- (77) Tsipis, A. C.; Orpen, A. G.; Harvey, J. N. *Dalton Trans.* **2005**, 2849.
- (78) Zhao, Y.; Truhlar, D. G. *Org. Lett.* **2007**, *9*, 1967.
- (79) Kingsbury, J. S.; Hoveyda, A. H. *J. Am. Chem. Soc.* **2005**, *127*, 4510.
- (80) Jafarpour, L.; Stevens, E. D.; Nolan, S. P. *J. Organomet. Chem.* **2000**, *606*, 49.
- (81) Fürstner, A.; Ackermann, L.; Gabor, B.; Goddard, R.; Lehmann, C. W.; Mynott, R.; Stelzer, F.; Thiel, O. R. *Chem.—Eur. J.* **2001**, *7*, 3236.
- (82) Dinger, M. B.; Mol, J. C. *Adv. Synth. Catal.* **2002**, *344*, 671.
- (83) Courchay, F. C.; Sworen, J. C.; Wagener, K. B. *Macromolecules* **2003**, *36*, 8231.
- (84) Ritter, T.; Hejl, A.; Wenzel, A. G.; Funk, T. W.; Grubbs, R. H. *Organometallics* **2006**, *25*, 5740.
- (85) Weigl, K.; Köhler, K.; Dechert, S.; Meyer, F. *Organometallics* **2005**, *24*, 4049.
- (86) (a) Bai, C. X.; Lu, X. B.; He, R.; Zhang, W. Z.; Feng, X. J. *Org. Biomol. Chem.* **2005**, *3*, 4139. (b) Bai, C. X.; Zhang, W. Z.; He, R.; Lu, X. B.; Zhang, Z. Q. *Tetrahedron Lett.* **2005**, *46*, 7225. (c) Zhang, W. Z.; He, R.; Zhang, R. *Eur. J. Inorg. Chem.* **2007**, 5345.
- (87) Courchay, F. C.; Sworen, J. C.; Ghiviriga, I.; Abboud, K. A.; Wagener, K. B. *Organometallics* **2006**, *25*, 6074.
- (88) Ritter, T.; Day, M. W.; Grubbs, R. H. *J. Am. Chem. Soc.* **2006**, *128*, 11768.
- (89) Wakamatsu, H.; Blechert, S. *Angew. Chem., Int. Ed.* **2002**, *41*, 2403.
- (90) Stewart, I. C.; Douglas, C. J.; Grubbs, R. H. *Org. Lett.* **2008**, *10*, 441.
- (91) Stewart, I. C.; Benitez, D.; O'Leary, D. J.; Tkatchouk, E.; Day, M. W.; Goddard, W. A., III; Grubbs, R. H. *J. Am. Chem. Soc.* **2009**, *131*, 1931.
- (92) Vehlou, K.; Gessler, S.; Blechert, S. *Angew. Chem., Int. Ed.* **2007**, *46*, 8082.
- (93) Luan, X.; Mariz, R.; Gatti, M.; Costabile, C.; Poater, A.; Cavallo, L.; Linden, A.; Dorta, R. *J. Am. Chem. Soc.* **2008**, *130*, 6848.
- (94) Hong, S. H.; Chlenov, A.; Day, M. W.; Grubbs, R. H. *Angew. Chem., Int. Ed.* **2007**, *46*, 5148.
- (95) Hong, S. H.; Wenzel, A. G.; Salguero, T. T.; Day, M. W.; Grubbs, R. H. *J. Am. Chem. Soc.* **2007**, *129*, 7961.
- (96) Chung, C. K.; Grubbs, R. H. *Org. Lett.* **2008**, *10*, 2693.
- (97) Kuhn, K. M.; Bourg, J.-B.; Chung, C. K.; Virgil, S. C.; Grubbs, R. H. *J. Am. Chem. Soc.* **2009**, *131*, 5313.
- (98) Leuthäuffer, S.; Schmidts, V.; Thiele, C. M.; Plenio, H. *Chem.—Eur. J.* **2008**, *14*, 5465.
- (99) (a) Balof, S. L.; P'Pool, S. J.; Berger, N. J.; Valente, E. J.; Shiller, A. M.; Schanz, H. *J. Dalton Trans.* **2008**, 5791. (b) Balof, S. L.; Yu, B.; Lowe, A. B.; Ling, Y.; Zhang, Y.; Schanz, H. *J. Inorg. Chem.* **2009**, 1717.
- (100) Ledoux, N.; Linden, A.; Allaert, B.; Mierde, H. V.; Verpoort, F. *Adv. Synth. Catal.* **2007**, *349*, 1692.
- (101) Dinger, M. B.; Nieczypor, P.; Mol, J. C. *Organometallics* **2003**, *22*, 5291.
- (102) Prühs, S.; Lehmann, C. W.; Fürstner, A. *Organometallics* **2004**, *23*, 280.
- (103) Vehlou, K.; Maechling, S.; Blechert, S. *Organometallics* **2006**, *25*, 25.
- (104) Ledoux, N.; Allaert, B.; Pattyn, S.; Mierde, H. V.; Vercaemst, C.; Verpoort, F. *Chem.—Eur. J.* **2006**, *12*, 4654.
- (105) Ledoux, N.; Allaert, B.; Linden, A.; van der Voort, P.; Verpoort, F. *Organometallics* **2007**, *26*, 1052.
- (106) Vougioukalakis, G. C.; Grubbs, R. H. *Organometallics* **2007**, *26*, 2469.
- (107) Vougioukalakis, G. C.; Grubbs, R. H. *Chem.—Eur. J.* **2008**, *14*, 7545.
- (108) Chatterjee, A. K.; Choi, T. L.; Sanders, D. P.; Grubbs, R. H. *J. Am. Chem. Soc.* **2003**, *125*, 11360.
- (109) Hejl, A. H. Ph.D. Thesis, California Institute of Technology, Pasadena, CA, 2007.
- (110) For a review article on the use of chiral NHCs in transition-metal complexes, see: Snead, D. R.; Seo, H.; Hong, S. *Curr. Org. Chem.* **2008**, *12*, 1370.
- (111) Costabile, C.; Cavallo, L. *J. Am. Chem. Soc.* **2004**, *126*, 9592.
- (112) Fournier, P. A.; Collins, S. K. *Organometallics* **2007**, *26*, 2945.
- (113) (a) Fournier, P. A.; Savoie, J.; Stenne, B.; Bédard, M.; Grandbois, A.; Collins, S. K. *Chem.—Eur. J.* **2008**, *14*, 8690. (b) Grandbois, A.; Collins, S. K. *Chem.—Eur. J.* **2008**, *14*, 9323.
- (114) Vehlou, K.; Wang, D.; Buchmeiser, M. R.; Blechert, S. *Angew. Chem., Int. Ed.* **2008**, *47*, 2615.
- (115) Grisi, F.; Costabile, C.; Gallo, E.; Mariconda, A.; Tedesco, C.; Longo, P. *Organometallics* **2008**, *27*, 4649.
- (116) Hoveyda, A. H.; Gillingham, D. G.; van Veldhuizen, J. J.; Kataoka, O.; Garber, S. B.; Kingsbury, J. S.; Harrity, J. P. A. *Org. Biomol. Chem.* **2004**, *2*, 8.
- (117) For a comparative study of chiral molybdenum- and ruthenium-based metathesis catalysts, see: Cortez, G. A.; Baxter, C. A.; Schrock, R. R.; Hoveyda, A. H. *Org. Lett.* **2007**, *9*, 2871.
- (118) Yun, J.; Marinez, E. R.; Grubbs, R. H. *Organometallics* **2004**, *23*, 4172.
- (119) Yang, L.; Mayr, M.; Wurst, K.; Buchmeiser, M. R. *Chem.—Eur. J.* **2004**, *10*, 5761.
- (120) Despagnet-Ayoub, E.; Grubbs, R. H. *Organometallics* **2005**, *24*, 338.
- (121) (a) Anderson, D. R.; Lavallo, V.; O'Leary, D.; Bertrand, G.; Grubbs, R. H. *Angew. Chem., Int. Ed.* **2007**, *46*, 7262. Synthesis of cyclic (alkyl)(amino) carbenes. (b) Lavallo, J.; Canac, Y.; Praesang, C.; Donnadiou, B.; Bertrand, G. *Angew. Chem., Int. Ed.* **2005**, *44*, 5705. (c) Jazzar, R.; Dewhurst, R. D.; Bourg, J.-B.; Donnadiou, B.; Canac, Y.; Bertrand, G. *Angew. Chem., Int. Ed.* **2007**, *46*, 2899. (d) Jazzar, R.; Bourg, J.-B.; Dewhurst, R. D.; Donnadiou, B.; Bertrand, G. *J. Org. Chem.* **2007**, *72*, 3492.
- (122) Anderson, D. R.; Ung, T.; Mkrtumyan, G.; Bertrand, G.; Grubbs, R. H.; Schrodi, Y. *Organometallics* **2008**, *27*, 563.
- (123) Vougioukalakis, G. C.; Grubbs, R. H. *J. Am. Chem. Soc.* **2008**, *130*, 2234.
- (124) Tzur, E.; Ben-Asuly, A.; Diesendruck, C. E.; Goldberg, I.; Lemcoff, N. G. *Angew. Chem., Int. Ed.* **2008**, *47*, 6422.
- (125) (a) Liu, S. T.; Reddy, K. R. *Chem. Soc. Rev.* **1999**, *28*, 315. (b) Simms, R. W.; Drewitt, M. J.; Baird, M. C. *Organometallics* **2002**, *21*, 2958. (c) Titcomb, L. R.; Caddick, S.; Cloke, F. G. N.; Wilson, D. J.; McKercher, D. *Chem. Commun.* **2001**, 1388.
- (126) Zhang, W.; Bai, C.; Lu, X.; He, R. *J. Organomet. Chem.* **2007**, *692*, 3563.
- (127) Frenzel, U.; Weskamp, T.; Kohl, F. J.; Schattenmann, W. C.; Nuyken, O.; Herrmann, W. A. *J. Organomet. Chem.* **1999**, *586*, 263.
- (128) Ackermann, L.; Fürstner, A.; Weskamp, T.; Kohl, F. J.; Herrmann, W. A. *Tetrahedron Lett.* **1999**, *40*, 4787.
- (129) Sanford, M. S.; Love, J. A.; Grubbs, R. H. *Organometallics* **2001**, *20*, 5314.
- (130) Conrad, J. C.; Yap, G. P. A.; Fogg, D. E. *Organometallics* **2003**, *22*, 1986.
- (131) Marshall, C.; Ward, M. F.; Harrison, W. T. A. *J. Organomet. Chem.* **2005**, *690*, 3970.
- (132) Wright, J. A.; Danopoulos, A. A.; Motherwell, W. B.; Carroll, R. J.; Ellwood, S. *J. Organomet. Chem.* **2006**, *691*, 5204.
- (133) Wakamatsu, H.; Blechert, S. *Angew. Chem., Int. Ed.* **2002**, *41*, 794.
- (134) Dunne, A. M.; Mix, S.; Blechert, S. *Tetrahedron Lett.* **2003**, *44*, 2733.
- (135) Zaja, M.; Connon, S. J.; Dunne, A. M.; Rivard, M.; Buschmann, N.; Jiricek, J.; Blechert, S. *Tetrahedron* **2003**, *59*, 6545.
- (136) Maechling, S.; Zaja, M.; Blechert, S. *Adv. Synth. Catal.* **2005**, *347*, 1413.
- (137) Grela, K.; Harutyunyan, S.; Michrowska, A. *Angew. Chem., Int. Ed.* **2002**, *41*, 4038.
- (138) Grela, K.; Kim, M. *Eur. J. Org. Chem.* **2003**, 963.
- (139) Michrowska, A.; Bujok, R.; Harutyunyan, S.; Sashuk, V.; Dolgonos, G.; Grela, K. *J. Am. Chem. Soc.* **2004**, *126*, 9318.
- (140) Bujok, R.; Bieniek, M.; Masnyk, M.; Michrowska, A.; Sarosiek, A.; Stepowska, H.; Arlt, D.; Grela, K. *J. Org. Chem.* **2004**, *69*, 6894.
- (141) Bieniek, M.; Michrowska, A.; Gułajski, Ł.; Grela, K. *Organometallics* **2007**, *26*, 1096.
- (142) Gułajski, Ł.; Michrowska, A.; Bujok, R.; Grela, K. *J. Mol. Catal. A: Chem.* **2006**, *254*, 118.
- (143) Ettari, R.; Micale, N. *J. Organomet. Chem.* **2007**, *692*, 3574.
- (144) Bieniek, M.; Bujok, R.; Cabaj, M.; Lugan, N.; Lavigne, G.; Arlt, D.; Grela, K. *J. Am. Chem. Soc.* **2006**, *128*, 13652.
- (145) Gawin, R.; Makal, A.; Woźniak, K.; Mauduit, M.; Grela, K. *Angew. Chem., Int. Ed.* **2007**, *46*, 7206.
- (146) Bieniek, M.; Bujok, R.; Stepowska, H.; Jacobi, A.; Hagenkötter, R.; Arlt, D.; Jarzemska, K.; Makal, A.; Woźniak, K.; Grela, K. *J. Organomet. Chem.* **2006**, *691*, 5289.
- (147) (a) Rix, D.; Clavier, H.; Coutard, Y.; Gułajski, Ł.; Grela, K.; Mauduit, M. *J. Organomet. Chem.* **2006**, *691*, 5397. For some representative articles regarding the utilization of neutral NHC-coordinated ruthenium



- nium complexes in ionic liquid solvents, see (b) Buijsman, R. C.; van Vuuren, E.; Sterrenburg, J. G. *Org. Lett.* **2001**, *3*, 3785. (c) Mayo, K. G.; Nearhoof, E. H.; Kiddle, J. J. *Org. Lett.* **2002**, *4*, 1567. (d) Ding, X.; Lv, X.; Hui, B.; Chen, Z.; Xiao, M.; Guo, B.; Tang, W. *Tetrahedron Lett.* **2006**, *47*, 2921. (e) Williams, D. B. G.; Ajam, M.; Ranwell, A. *Organometallics* **2006**, *25*, 3088.
- (148) Barbasiewicz, M.; Bieniek, M.; Michrowska, A.; Szadkowska, A.; Makal, A.; Woźniak, K.; Grela, K. *Adv. Synth. Catal.* **2007**, *349*, 193.
- (149) Rix, D.; Caijo, F.; Laurent, I.; Boeda, F.; Clavier, H.; Nolan, S. P.; Mauduit, M. *J. Org. Chem.* **2008**, *73*, 4225.
- (150) Barbasiewicz, M.; Szadkowska, A.; Makal, A.; Jarzemska, K.; Woźniak, K.; Grela, K. *Chem.—Eur. J.* **2008**, *14*, 9330.
- (151) Fürstner, A.; Thiel, O. R.; Lehmann, C. *Organometallics* **2002**, *21*, 331.
- (152) Slugovc, C.; Perner, B.; Stelzer, F.; Mereiter, K. *Organometallics* **2004**, *23*, 3622.
- (153) Ben-Asuly, A.; Tzur, E.; Diesendruck, C. E.; Sigalov, M.; Goldberg, I.; Lemcoff, N. G. *Organometallics* **2008**, *27*, 811.
- (154) Kost, T.; Sigalov, M.; Goldberg, I.; Ben-Asuly, A.; Lemcoff, N. G. *J. Organomet. Chem.* **2008**, *693*, 2200.
- (155) Szadkowska, A.; Makal, A.; Woźniak, K.; Kadyrov, R.; Grela, K. *Organometallics* **2009**, *28*, 2693.
- (156) Love, J. A.; Sanford, M. S.; Day, M. W.; Grubbs, R. H. *J. Am. Chem. Soc.* **2003**, *125*, 10103.
- (157) Love, J. A.; Morgan, J. P.; Trnka, T. M.; Grubbs, R. H. *Angew. Chem., Int. Ed.* **2002**, *41*, 4035.
- (158) Choi, T. L.; Grubbs, R. H. *Angew. Chem., Int. Ed.* **2003**, *42*, 1743.
- (159) Wang, D.; Yang, L.; Decker, U.; Findeisen, M.; Buchmeiser, M. R. *Macromol. Rapid Commun.* **2005**, *26*, 1757.
- (160) Ung, T.; Hejl, A.; Grubbs, R. H.; Schrodri, Y. *Organometallics* **2004**, *23*, 5399.
- (161) For a recent review article on latent olefin metathesis catalysts bearing chelating alkylidene ligands, see: Szadkowska, A.; Grela, K. *Curr. Org. Chem.* **2008**, *12*, 1631.
- (162) Lehman, S. E.; Wagener, K. B.; Akvan, S. *J. Polym. Sci., Part A: Polym. Chem.* **2005**, *43*, 6134.
- (163) Lehman, S. E.; Wagener, K. B. *Organometallics* **2005**, *24*, 1477.
- (164) (a) Monsaert, S.; Drozdak, R.; Dragutan, V.; Dragutan, I.; Verpoort, F. *Eur. J. Inorg. Chem.* **2008**, 432. (b) Monsaert, S.; de Canck, E.; Drozdak, R.; van der Voort, P.; Verpoort, F.; Martins, J. C.; Hendrickx, P. M. S. *Eur. J. Org. Chem.* **2009**, 655.
- (165) Burtscher, D.; Lexer, C.; Mereiter, K.; Winde, R.; Karch, R.; Slugovc, C. *J. Polym. Sci., Part A: Polym. Chem.* **2008**, *46*, 4630.
- (166) de Frémont, P.; Clavier, H.; Montebault, V.; Fontaine, L.; Nolan, S. P. *J. Mol. Catal. A: Chem.* **2008**, *283*, 108.
- (167) Mennecke, K.; Grela, K.; Kunz, U.; Kirschning, A. *Synlett* **2005**, *19*, 2948.
- (168) Samanta, D.; Kratz, K.; Zhang, X.; Emrick, T. *Macromolecules* **2008**, *41*, 530.
- (169) Barbasiewicz, M.; Szadkowska, A.; Bujok, R.; Grela, K. *Organometallics* **2006**, *25*, 3599.
- (170) Gstrein, X.; Burtscher, D.; Szadkowska, A.; Barbasiewicz, M.; Stelzer, F.; Grela, K.; Slugovc, C. *J. Polym. Sci., Part A: Polym. Chem.* **2007**, *45*, 3494.
- (171) Slugovc, C.; Burtscher, D.; Stelzer, F.; Mereiter, K. *Organometallics* **2005**, *24*, 2255.
- (172) Hejl, A.; Day, M. W.; Grubbs, R. H. *Organometallics* **2006**, *25*, 6149.
- (173) Romero, P. E.; Piers, W. E.; McDonald, R. *Angew. Chem., Int. Ed.* **2004**, *43*, 6161.
- (174) Wenzel, A.; Grubbs, R. H. *J. Am. Chem. Soc.* **2006**, *128*, 16048.
- (175) van der Eide, E. F.; Romero, P. E.; Piers, W. E. *J. Am. Chem. Soc.* **2008**, *130*, 4485.
- (176) Romero, P. E.; Piers, W. E. *J. Am. Chem. Soc.* **2005**, *127*, 5032.
- (177) Romero, P. E.; Piers, W. E. *J. Am. Chem. Soc.* **2007**, *129*, 1698.
- (178) The same structure has been also computationally predicted. For example, see ref 75.
- (179) Tallarico, J. A.; Bonitatebus, P. J., Jr.; Snapper, M. L. *J. Am. Chem. Soc.* **1997**, *119*, 7157.
- (180) Trnka, T. M.; Day, M. W.; Grubbs, R. H. *Organometallics* **2001**, *20*, 3845.
- (181) (a) Anderson, D. R.; Hickstein, D. D.; O'Leary, D.; Grubbs, R. H. *J. Am. Chem. Soc.* **2006**, *128*, 8386. (b) Anderson, D. R.; O'Leary, D.; Grubbs, R. H. *Chem.—Eur. J.* **2008**, *14*, 7536.
- (182) Jafarpour, L.; Schanz, H. J.; Stevens, E. D.; Nolan, S. P. *Organometallics* **1999**, *18*, 5416.
- (183) For a recent review article on ruthenium indenylidene complexes, see: Boeda, F.; Clavier, H.; Nolan, S. P. *Chem. Commun.* **2008**, 2726.
- (184) Fürstner, A.; Thiel, O. R.; Ackermann, L.; Schanz, H. J.; Nolan, S. P. *J. Org. Chem.* **2000**, *65*, 2204.
- (185) Clavier, H.; Nolan, S. P. *Chem.—Eur. J.* **2007**, *13*, 8029.
- (186) Boeda, F.; Bantreil, X.; Clavier, H.; Nolan, S. P. *Adv. Synth. Catal.* **2008**, *350*, 2959.
- (187) Randl, S.; Gessler, S.; Wakamatsu, H.; Blechert, S. *Synlett* **2001**, 430.
- (188) Clavier, H.; Urbina-Blanco, C. A.; Nolan, S. P. *Organometallics* **2009**, *28*, 2848.
- (189) Williams, J. E.; Harner, M. J.; Sponsler, M. B. *Organometallics* **2005**, *24*, 2013. Ruthenium alkylidenes **272–274** were also prepared starting from their bis(3-bromopyridine) analogues.
- (190) Katayama, H.; Urushima, H.; Nishioka, T.; Wada, C.; Nagao, M.; Ozawa, F. *Angew. Chem., Int. Ed.* **2000**, *39*, 4513.
- (191) Louie, J.; Grubbs, R. H. *Organometallics* **2002**, *21*, 2153.
- (192) Schanz, H. J.; Jafarpour, L.; Stevens, E. D.; Nolan, S. P. *Organometallics* **1999**, *18*, 5187.
- (193) Opstal, T.; Verpoort, F. *J. Mol. Catal. A: Chem.* **2003**, *200*, 49.
- (194) For some representative examples, see: (a) Chao, W. C.; Weinreb, S. M. *Org. Lett.* **2003**, *5*, 2505. (b) Salim, S. S.; Bellingham, R. K.; Satcharoen, V.; Brown, R. C. *Org. Lett.* **2003**, *5*, 3403. (c) de Matteis, V.; van Delft, F. L.; de Gelder, R.; Tiebes, J.; Rutjes, F. *Tetrahedron Lett.* **2004**, *45*, 959.
- (195) Trnka, T. M.; Day, M. W.; Grubbs, R. H. *Angew. Chem., Int. Ed.* **2001**, *40*, 3441.
- (196) Macnaughtan, M. L.; Johnson, M. J. A.; Kampf, J. W. *Organometallics* **2007**, *26*, 780.
- (197) Macnaughtan, M. L.; Johnson, M. J. A.; Kampf, J. W. *J. Am. Chem. Soc.* **2007**, *129*, 7708.
- (198) Bielawski, C. W.; Benitez, D.; Grubbs, R. H. *Science* **2002**, *297*, 2041.
- (199) Bielawski, C. W.; Benitez, D.; Grubbs, R. H. *J. Am. Chem. Soc.* **2003**, *125*, 8424.
- (200) Boydston, A. J.; Xia, Y.; Kornfield, J. A.; Gorodetskaya, I. A.; Grubbs, R. H. *J. Am. Chem. Soc.* **2008**, *130*, 12775.
- (201) Occhipinti, G.; Björsvik, H. R.; Törnroos, K. W.; Fürstner, A.; Jensen, V. R. *Organometallics* **2007**, *26*, 4383.
- (202) Yun, S. Y.; Kim, M.; Lee, D.; Wink, D. J. *J. Am. Chem. Soc.* **2009**, *131*, 24.
- (203) Bolton, S. L.; Williams, J. E.; Sponsler, M. B. *Organometallics* **2007**, *26*, 2485. The ruthenium propylidene analogue of **301** was also prepared.
- (204) Review articles on the steric properties of phosphines: (a) Tolman, C. A. *Chem. Rev.* **1977**, *77*, 313. (b) Brown, T. L.; Lee, K. J. *Coord. Chem. Rev.* **1993**, *128*, 89. For a recent review article on the computational description of phosphorus ligands and the metal–phosphorus bond, see: (c) Fey, N.; Orpen, A. G.; Harvey, J. N. *Coord. Chem. Rev.* **2009**, *253*, 704.
- (205) Zhang, W.; Liu, P.; Jin, K.; He, R. *J. Mol. Catal. A: Chem.* **2007**, *275*, 194.
- (206) For a recent, related theoretical study, see: Straub, B. F. *Adv. Synth. Catal.* **2007**, *349*, 204.
- (207) Conrad, J. C.; Amoroso, D.; Czechura, P.; Yap, G. P. A.; Fogg, D. E. *Organometallics* **2003**, *22*, 3634.
- (208) Conrad, J. C.; Parnas, H. H.; Snelgrove, J. L.; Fogg, D. E. *J. Am. Chem. Soc.* **2005**, *127*, 11882.
- (209) Monfete, S.; Fogg, D. E. *Organometallics* **2006**, *25*, 1940.
- (210) (a) Conrad, J. C.; Snelgrove, J. L.; Eelman, M. D.; Hall, S.; Fogg, D. E. *J. Mol. Catal. A: Chem.* **2006**, *254*, 105. (b) Conrad, J. C.; Fogg, D. E. *Curr. Org. Chem.* **2006**, *10*, 185.
- (211) Denk, K.; Fridgen, J.; Herrmann, W. A. *Adv. Synth. Catal.* **2002**, *344*, 666.
- (212) Jordaam, M.; Vosloo, H. C. M. *Adv. Synth. Catal.* **2007**, *349*, 184.
- (213) de Clercq, B.; Verpoort, F. *Tetrahedron Lett.* **2002**, *43*, 9101.
- (214) de Clercq, B.; Verpoort, F. *J. Organomet. Chem.* **2003**, *672*, 11.
- (215) Review articles on ruthenium-based complexes bearing bidentate Schiff base ligands: (a) Drozdak, R.; Allaert, B.; Ledoux, N.; Dragutan, I.; Dragutan, V.; Verpoort, F. *Adv. Synth. Catal.* **2005**, *347*, 1721. (b) Drozdak, R.; Ledoux, N.; Allaert, B.; Dragutan, I.; Dragutan, V.; Verpoort, F. *Cent. Eur. J. Chem.* **2005**, *3*, 404. (c) Drozdak, R.; Allaert, B.; Ledoux, N.; Dragutan, I.; Dragutan, V.; Verpoort, F. *Coord. Chem. Rev.* **2005**, *249*, 3055. (d) Ding, F.; Sun, Y. G.; Monsaert, S.; Drozdak, R.; Dragutan, I.; Dragutan, V.; Verpoort, F. *Curr. Org. Synth.* **2008**, *5*, 291.
- (216) Allaert, B.; Dieltiens, N.; Ledoux, N.; Vercaemst, C.; van der Voort, P.; Stevens, C. V.; Linden, A.; Verpoort, F. *J. Mol. Catal. A: Chem.* **2006**, *260*, 221.
- (217) (a) Ledoux, N.; Allaert, B.; Schaubroeck, D.; Monsaert, S.; Drozdak, R.; van der Voort, P.; Verpoort, F. *J. Organomet. Chem.* **2006**, *691*, 5482. (b) Monsaert, S.; Drozdak, R.; Verpoort, F. *Chem. Today* **2008**, *26*, 93.
- (218) Opstal, T.; Verpoort, F. *Angew. Chem., Int. Ed.* **2003**, *42*, 2876.
- (219) Hahn, F. E.; Paas, M.; Fröhlich, R. *J. Organomet. Chem.* **2005**, *690*, 5816.
- (220) Samec, J. S. M.; Grubbs, R. H. *Chem.—Eur. J.* **2008**, *14*, 2686.
- (221) Krause, J. O.; Nuyken, O.; Wurst, K.; Buchmeiser, M. R. *Chem.—Eur. J.* **2004**, *10*, 777.

- (222) Halbach, T. S.; Mix, S.; Fisher, D.; Maechling, S.; Krause, J. O.; Sievers, C.; Blechert, S.; Nuyken, O.; Buchmeiser, M. R. *J. Org. Chem.* **2005**, *70*, 4687.
- (223) Vehlou, K.; Maechling, S.; Köhler, K.; Blechert, S. *Tetrahedron Lett.* **2006**, *47*, 8617.
- (224) Vehlou, K.; Maechling, S.; Köhler, K.; Blechert, S. *J. Organomet. Chem.* **2006**, *691*, 5267.
- (225) Tanaka, K.; Böhm, V. P. W.; Chadwick, D.; Roeper, M.; Braddock, D. C. *Organometallics* **2006**, *25*, 5696.
- (226) Braddock, D. C.; Tanaka, K.; Chadwick, D.; Böhm, V. P. W.; Roeper, M. *Tetrahedron Lett.* **2007**, *48*, 5301.
- (227) Zhang, Y.; Wang, D.; Lönnecke, P.; Scherzer, T.; Buchmeiser, M. R. *Macromol. Symp.* **2006**, *236*, 30.
- (228) Buchmeiser, M. R.; Wang, D.; Zhang, Y.; Naumov, S.; Wurst, K. *Eur. J. Inorg. Chem.* **2007**, 3988.
- (229) Wang, D.; Wurst, K.; Knolle, W.; Decker, U.; Prager, L.; Naumov, S.; Buchmeiser, M. R. *Angew. Chem., Int. Ed.* **2008**, *47*, 3267.
- (230) For a recent review article on  $\eta^6$ -arene ruthenium complexes, see: Therrien, B. *Coord. Chem. Rev.* **2009**, *253*, 493.
- (231) Jafarpour, L.; Huang, J.; Stevens, E. D.; Nolan, S. P. *Organometallics* **1999**, *18*, 3760.
- (232) Lo, C.; Cariou, R.; Fischmeister, C.; Dixneuf, P. H. *Adv. Synth. Catal.* **2007**, *349*, 546.
- (233) Sauvage, X.; Borguet, Y.; Noels, A. F.; Delaude, L.; Demonceau, A. *Adv. Synth. Catal.* **2007**, *349*, 255.
- (234) Delaude, L.; Demonceau, A.; Noels, A. F. *Chem. Commun.* **2001**, 986.
- (235) Ledoux, N.; Allaert, B.; Verpoort, F. *Eur. J. Inorg. Chem.* **2007**, 5578.
- (236) An alternative method for the in situ generation of some of these NHC ligands has been also reported: Tudose, A.; Demonceau, A.; Delaude, L. *J. Organomet. Chem.* **2006**, *691*, 5356.
- (237) Delaude, L.; Spzya, M.; Demonceau, A.; Noels, A. F. *Adv. Synth. Catal.* **2002**, *344*, 749.
- (238) Delaude, L.; Demonceau, A.; Noels, A. F. *Curr. Org. Chem.* **2006**, *10*, 203.
- (239) Maj, A. M.; Delaude, L.; Demonceau, A.; Noels, A. F. *J. Organomet. Chem.* **2007**, *692*, 3048.
- (240) (a) Hitchcock, P. B.; Lappert, M. F.; Pye, P. L.; Thomas, S. *J. Chem. Soc., Dalton Trans.* **1979**, 1929. (b) Simal, F.; Jan, D.; Delaude, L.; Demonceau, A.; Spirlet, M. R.; Noels, A. F. *Can. J. Chem.* **2001**, *79*, 529.
- (241) Sémeril, D.; Cléran, M.; Bruneau, C.; Dixneuf, P. H. *Adv. Synth. Catal.* **2001**, *343*, 184.
- (242) Ackermann, L.; Bruneau, C.; Dixneuf, P. H. *Synlett* **2001**, 3, 397.
- (243) Sémeril, D.; Bruneau, C.; Dixneuf, P. H. *Helv. Chim. Acta* **2001**, *84*, 3335.
- (244) Sémeril, D.; Bruneau, C.; Dixneuf, P. H. *Adv. Synth. Catal.* **2002**, *344*, 585.
- (245) Castarlenas, R.; Alaoui-Abdallaoui, I.; Sémeril, D.; Mernari, B.; Guesmi, S.; Dixneuf, P. H. *New J. Chem.* **2003**, *27*, 6.
- (246) Cetinkaya, B.; Demir, S.; Özdemir, I.; Toupet, L.; Sémeril, D.; Bruneau, C.; Dixneuf, P. H. *New J. Chem.* **2001**, *25*, 519.
- (247) Cetinkaya, B.; Demir, S.; Özdemir, I.; Toupet, L.; Sémeril, D.; Bruneau, C.; Dixneuf, P. H. *Chem.—Eur. J.* **2003**, *9*, 2323.
- (248) Özdemir, I.; Demir, S.; Cetinkaya, B.; Toupet, L.; Castarlenas, R.; Fischmeister, C.; Dixneuf, P. H. *Eur. J. Inorg. Chem.* **2007**, 2862.
- (249) Castarlenas, R.; Vovard, C.; Fischmeister, C.; Dixneuf, P. H. *J. Am. Chem. Soc.* **2006**, *128*, 4079.
- (250) For two recent review articles on aqueous olefin metathesis, see: (a) Burtscher, D.; Grela, K. *Angew. Chem., Int. Ed.* **2009**, *48*, 442. (b) Zaman, S.; Curnow, O. J.; Abell, A. D. *Aust. J. Chem.* **2009**, *62*, 91.
- (251) Connon, S. J.; Rivard, M.; Zaja, M.; Blechert, S. *Adv. Synth. Catal.* **2003**, *345*, 572.
- (252) Jordan, J. P.; Grubbs, R. H. *Angew. Chem., Int. Ed.* **2007**, *46*, 5152.
- (253) (a) Michrowska, A.; Gułajski, Ł.; Kaczmarek, Z.; Mennecke, K.; Kirschning, A.; Grela, K. *Green Chem.* **2006**, *8*, 685. (b) Michrowska, A.; Gułajski, Ł.; Grela, K. *Chem. Today* **2006**, *24*, 19. (c) Gułajski, Ł.; Michrowska, A.; Naroznik, J.; Kaczmarek, Z.; Rupnicki, L.; Grela, K. *ChemSusChem* **2008**, *1*, 103.
- (254) Runge, M. B.; Mwangi, M. T.; Bowden, N. B. *J. Organomet. Chem.* **2006**, *691*, 5278.
- (255) Binder, J. B.; Blank, J. J.; Raines, R. T. *Org. Lett.* **2007**, *9*, 4885.
- (256) (a) Collman, J. P.; Belmont, J. A.; Brauman, J. J. *J. Am. Chem. Soc.* **1983**, *105*, 7288. (b) Drago, R. S.; Pribich, D. C. *Inorg. Chem.* **1985**, *24*, 1983. (c) Tollner, K.; Popovity-Biro, R.; Lahav, M.; Milstein, D. *Science* **1997**, *278*, 2100. (d) Annis, D. A.; Jacobsen, E. N. *J. Am. Chem. Soc.* **1999**, *121*, 4147.
- (257) (a) Buchmeiser, M. R. *New J. Chem.* **2004**, *28*, 549. (b) Sommer, W. J.; Weck, M. *Coord. Chem. Rev.* **2007**, *251*, 860. (c) Clavier, H.; Grela, K.; Kirschning, A.; Mauduit, M.; Nolan, S. P. *Angew. Chem., Int. Ed.* **2007**, *46*, 6786. (d) Copéret, C.; Basset, J.-M. *Adv. Synth. Catal.* **2007**, *349*, 78. (e) Šebesta, R.; Kmentová, I.; Toma, S. *Green Chem.* **2008**, *10*, 484. (f) Śledź, P.; Mauduit, M.; Grela, K. *Chem. Soc. Rev.* **2008**, *37*, 2433. (g) Buchmeiser, M. R. *Chem. Rev.* **2009**, *109*, 303.
- (258) For some recent representative studies, see: (a) Rix, D.; Caijo, F.; Laurent, I.; Gułajski, Ł.; Grela, K.; Mauduit, M. *Chem. Commun.* **2007**, 3771. (b) van Berlo, B.; Houthoofd, K.; Sels, B. F.; Jacobs, P. A. *Adv. Synth. Catal.* **2008**, *350*, 1949. (c) Chen, S.-W.; Kim, J. H.; Shin, H.; Lee, S.-G. *Org. Biomol. Chem.* **2008**, *6*, 2676. (d) Lim, J.; Lee, S. S.; Ying, J. Y. *Chem. Commun.* **2008**, 4312. (e) Elias, X.; Pleixats, R.; Man, M. W. C. *Tetrahedron* **2008**, *64*, 6770. (f) Clavier, H.; Nolan, S. P.; Mauduit, M. *Organometallics* **2008**, *27*, 2287. (g) Wakamatsu, H.; Saito, Y.; Masubuchi, M.; Fujita, R. *Synlett* **2008**, *12*, 1805. (h) Consorti, C. S.; Aydos, G. L. P.; Ebeling, G.; Dupont, J. *Org. Lett.* **2008**, *10*, 237. (i) Keraani, A.; Renouard, D.; Fischmeister, C.; Bruneau, C.; Rabiller-Baudry, M. *ChemSusChem* **2008**, *1*, 927. (j) Schoeps, D.; Buhr, K.; Dijkstra, M.; Ebert, K.; Plenio, H. *Chem.—Eur. J.* **2009**, *15*, 2960. (k) Kim, J. H.; Park, B. Y.; Chen, S.-W.; Li, S.-G. *Eur. J. Org. Chem.* **2009**, 2239. (l) Chen, S.-W.; Kim, J. H.; Ryu, K. Y.; Lee, W.-W.; Hong, J.; Lee, S.-G. *Tetrahedron* **2009**, *65*, 3397.
- (259) Mayr, M.; Buchmeiser, M. R.; Wurst, K. *Adv. Synth. Catal.* **2002**, *344*, 712.
- (260) Mayr, M.; Mayr, B.; Buchmeiser, M. R. *Angew. Chem., Int. Ed.* **2001**, *40*, 3839.
- (261) Allen, D. P.; van Wingerden, M. M.; Grubbs, R. H. *Org. Lett.* **2009**, *11*, 1261.
- (262) Randl, S.; Buschmann, N.; Connon, S. J.; Blechert, S. *Synlett* **2001**, *10*, 1547.
- (263) Kingsbury, J. S.; Garber, S. B.; Giftos, J. M.; Gray, B. L.; Okamoto, M. M.; Farrer, R. A.; Fourkas, J. T.; Hoveyda, A. H. *Angew. Chem., Int. Ed.* **2001**, *40*, 4251.
- (264) Audic, N.; Clavier, H.; Mauduit, M.; Guillemin, J. C. *J. Am. Chem. Soc.* **2003**, *125*, 9248.
- (265) Clavier, H.; Audic, N.; Mauduit, M.; Guillemin, J. C. *Chem. Commun.* **2004**, 2282.
- (266) Clavier, H.; Audic, N.; Mauduit, M.; Guillemin, J. C. *J. Organomet. Chem.* **2005**, *690*, 3585.
- (267) (a) Yao, Q.; Zhang, Y. *Angew. Chem., Int. Ed.* **2003**, *42*, 3395. (b) Yao, Q.; Sheets, M. J. *Organomet. Chem.* **2005**, *690*, 3577.
- (268) For another type of ionic liquid functionality attached to the benzylidene ligand, see: Thurier, C.; Fischmeister, C.; Bruneau, C.; Olivier-Bourbigou, H.; Dixneuf, P. H. *J. Mol. Catal. A: Chem.* **2007**, *268*, 126.
- (269) (a) Corrêa da Costa, R.; Gladysz, J. A. *Chem. Commun.* **2006**, 2619. (b) Corrêa da Costa, R.; Gladysz, J. A. *Adv. Synth. Catal.* **2007**, *349*, 243.
- (270) Matsugi, M.; Curran, D. P. *J. Org. Chem.* **2005**, *70*, 1636.
- (271) Süßner, M.; Plenio, H. *Angew. Chem., Int. Ed.* **2005**, *44*, 6885.
- (272) Hong, S. H.; Grubbs, R. H. *Org. Lett.* **2007**, *9*, 1955.
- (273) Cho, J. H.; Kim, B. M. *Org. Lett.* **2003**, *5*, 531.
- (274) Ahn, Y. M.; Yang, K. L.; Georg, G. I. *Org. Lett.* **2001**, *3*, 1411.
- (275) Mendez-Andino, J.; Paquette, L. A. *Org. Lett.* **2000**, *2*, 1263.
- (276) McEleney, K.; Allen, D. P.; Holliday, A. E.; Crudden, C. M. *Org. Lett.* **2006**, *8*, 2663.
- (277) Galan, B. R.; Kalbarczyk, K. P.; Szczepankiewicz, S.; Keister, J. B.; Diver, S. T. *Org. Lett.* **2007**, *9*, 1203.
- (278) Ferguson, M. L.; O'Leary, D. J.; Grubbs, R. H. *Org. Synth.* **2003**, *80*, 85.
- (279) Dinger, M. B.; Mol, J. C. *Eur. J. Inorg. Chem.* **2003**, 2827.
- (280) Banti, D.; Mol, J. C. *J. Organomet. Chem.* **2004**, *689*, 3113.
- (281) Ulman, M.; Grubbs, R. H. *J. Org. Chem.* **1999**, *64*, 7202.
- (282) Hong, S. H.; Day, M. W.; Grubbs, R. H. *J. Am. Chem. Soc.* **2004**, *126*, 7414.
- (283) Leitao, E. M.; Dubberley, S. R.; Piers, W. E.; Wu, Q.; McDonald, R. *Chem.—Eur. J.* **2008**, *14*, 11565.
- (284) Galan, B. R.; Gembicky, M.; Dominica, P. M.; Keister, J. B.; Diver, S. T. *J. Am. Chem. Soc.* **2005**, *127*, 15702.
- (285) Galan, B. R.; Pitak, M.; Gembicky, M.; Keister, J. B.; Diver, S. T. *J. Am. Chem. Soc.* **2009**, *131*, 6822.
- (286) For some representative examples, see: (a) van Rensburg, W. J.; Steynberg, P. J.; Meyer, W. H.; Kirk, M. M.; Forman, G. S. *J. Am. Chem. Soc.* **2004**, *126*, 14332. (b) van Rensburg, W. J.; Steynberg, P. J.; Kirk, M. M.; Meyer, W. H.; Forman, G. S. *J. Organomet. Chem.* **2006**, *691*, 5312. (c) Mathew, J.; Koga, N.; Suresh, C. H. *Organometallics* **2008**, *27*, 4666.